Characterisation of HIV-1 Envelope features of breakthrough infections from the CAPRISA 004 Microbicide Trial

By

Sherazaan Dineo Ismail

ISMSHE006

SUBMITTED TO THE UNIVERSITY OF CAPE TOWN

In fulfilment of the requirements for the degree

MSc (Med) in Medical Virology

Department of Pathology

Faculty of Health Sciences

UNIVERSITY OF CAPE TOWN

University of Cape Town

Date of submission:	25th May 2016
Supervisor:	Prof Carolyn Williamson
Co-Supervisor:	Dr Philippe Selhorst

The copyright of this thesis vests in the author. No quotation from it or information derived from it is to be published without full acknowledgement of the source. The thesis is to be used for private study or non-commercial research purposes only.

Published by the University of Cape Town (UCT) in terms of the non-exclusive license granted to UCT by the author.

University of Cape Town

Table of Contents

Acknowledgements

Firstly and foremost, none of this would have been possible without the immeasurable grace of my Creator. I am and always will be in awe of You.

I would like to express my thanks to Professor Carolyn Williamson, my supervisor; whose support and encouragement has helped me grow over the years that I have been in been a part of her group. I would like to express my gratitude to Dr Philippe Selhorst who has been my co-supervisor for the duration of my Masters research. I thank you both for your patience and willingness to teach. I would like to express my thanks to Dr Melissa-Rose Abrahams who always goes over and above what is asked of her to help whenever needed (you are a superhero); to Ruwayhida Thebus for time spent in the lab; to Cecelia Rademeyer, Jinny Marais, Dr Denis Chopera and Dr Andile Nofemela for technical advice. I'd also like to thank the women of the Centre for the AIDS Programme of Research (CAPRISA) 004 cohort, Dr Quarraisha Abdool Karim, Dr Salim Abdool Karim, and all of the CAPRISA 004 study team.

I would like to thank the following organisations for funding, either as student support or project funding: CAPRISA, the National Research Foundation (NRF), the Poliomyelitis Research Foundation (PRF) and the Clinical Infectious Diseases Research Initiative (CIDRI).

Finally, I'd like to thank my family and friends, all of who have contributed to who I am today. I am so grateful for all of you. To Clementene, Cheleka, Eduardo and Dieter for keeping me sane and being true friends. To Wesley, thank you for your love and your belief in me. To my parents, Desiree and Salim, you supported and encouraged me to live my best life, and my grandmother, Elizabeth Freda Kyzer, for your endless words of wisdom. And importantly, thank you to my siblings, Carmen and Zunaid, whom I love with all of me. Thank you for being my partners in crime. This is for you guys.

"For I know the plan I have for you", declares the Lord, "Plans to prosper you and not to harm you, plans to give you hope and a future" –Jeremiah 29:11

Declaration and TurnItIn Originality Report

I, Sherazaan Dineo Ismail, hereby declare that the work on which this dissertation is based is my original work (except where acknowledgements indicate otherwise) and that neither the whole work nor any part of it has been, is being, or is to be submitted for another degree in this or any other university.

I empower the university to reproduce for the purpose of research either the whole or any portion of the contents in any manner whatsoever.

Signature: Signed by candidate
Signature Removed

Date: 15th May 2016

Abstract

The CAPRISA 004 trial demonstrated the safety and a 39% efficacy of a 1% tenofovir (TFV) gel for the prevention of HIV-1 acquisition in young African women. It was subsequently shown that women assigned to the TFV arm who became infected had higher viral loads, slower anti-HIV-1 antibody avidity maturation, and higher Gag-specific IFN-γ+ CD4+ T cell responses; although replication capacity, as measured by Gag-Pro recombinant viruses, did not differ between arms. We thus aimed to investigate if there were differences in Envelope function, or TFV susceptibility, which may be selected for during transmission in those who became infected despite being assigned to the TFV arm.

Viruses from 39 out of 48 recently HIV-1 infected individuals from the trial (matched on time post-infection and the presence of protective HLAs) were isolated. Isolate *env* genes were sequenced using a single genome amplification approach and were compared to plasma sequences from the same time-point. To evaluate phenotypic characteristics of *env*, inhibition assays were performed using the following inhibitors: tenofovir, maraviroc, T20, PSC-RANTES and anti-CD4 antibody clone SK3. In addition, *env*s for 19 participants were cloned and used to generate pseudoviruses which were evaluated for entry efficiency.

Viral isolates were identical or very similar to viruses in circulation *in vivo*; however had a lower diversity, indicating that they were representative of *in vivo* virus but did not reflect the entire quasispecies in plasma. The TFV arm viruses were not more resistant to TFV than those in the placebo arm. A comparison of variable loop characteristics, distance to a consensus representative of viruses circulating in the region, and sensitivity to inhibitors or entry efficiencies of the viruses, also found no difference in genotypic nor phenotypic properties between study arms. When assessing the impact of viral phenotype on markers of disease progression, it was found that sensitivity to inhibitors did not contribute to VL or $CD4^+$ count in this cohort. To evaluate envelope in isolation of the rest of the genome, pseudoviruses were generated from 11 participants. We found that PSV entry efficiency did not correlate with VL at isolation, 3 months post-infection and set-point, or with $CD4^+$ counts at set-point. However, pseudovirus inhibitor sensitivities were significantly different to those of isolates for the inhibitors T20, anti-CD4 antibody SK3 and PSC-RANTES.

Overall, the isolate *env* genotypic and phenotypic characteristics investigated in this study did not differ between trial arms. Interestingly, pseudoviruses showed significant differences in their sensitivity to entry inhibitors when compared to their corresponding isolate, highlighting the importance of caution when interpreting data from *in vitro* studies, and motivates for further evaluation of *in vitro* models.

Abbreviations

^{o}C	Degree(s) Celsius
µ	Micro
AIDS	Acquired immunodeficiency syndrome
ART	Antiretroviral therapy
ARV	Antiretroviral
CAPRISA	Centre for the AIDS Programme of Research in South Africa
CCR5	Chemokine receptor 5
CD4	Cluster of division 4
CI	Confidence interval
CO_2	Carbon dioxide
CT	Cytoplasmic tail
CXCR4	C-X-C chemokine receptor 4
DEAE	Diethylaminoethyl
dH_2O	Distilled water
ddH_2O	Distilled, de-ionized water
DMEM	Dulbecco's modified Eagle medium
DMSO	Dimethyl sulphoxide
DNA	Deoxyribonucleic acid
E. coli	*Escherichia coli*
EDTA	Ethylenediamine tetra-acetic acid
EFV	Efavirenz
ELISA	Enzyme-linked immunosorbent assay
env	Viral gene encoding the Envelope protein
Env	Viral envelope protein
FBS	Foetal bovine serum
FTC	Emtricitabine
g	Gram(s)
gag	Viral gene encoding the capsid, matrix and nucleoproteins
Gag p24	Viral capsid protein (see also "p24")
GM	Growth medium
Gp160	160kDa Envelope glycoprotein

Gp120	120kDa Envelope glycoprotein
Gp41	41kDa Envelope glycoprotein
h	Hour(s)
HCl	Hydrochloric acid
HEK	Human embryonic kidney
HIV	Human Immunodeficiency Virus
HLA	Huma leukocyte antigen
HR	Heptad repeat
HRP	Horseradish peroxidase
IDU	Injection drug users
IMC	Infectious molecular clone
IQR	Interquartile range
kb	Kilobases
kDa	Kilodaltons
L	Litre
LB	Luria-Bertani broth
LLP	Lentiviral lytic peptide
LTR	Long terminal repeat
m	Milli
M	Molar
MA	Viral matrix protein encoded by *gag*
$MgCL_2$	Magnesium chloride
min	minute(s)
MSM	Men who have sex with men
MVC	Maraviroc
n	Nano
NaCl	Sodium chloride
nef	Viral gene encoding Nef protein
Nef	Negative Factor
p24	Viral capsid protein (see also “Gag p24”)
PBMC	Peripheral blood mononuclear cell
PBS	Phosphate buffered saline
PCR	Polymerase Chain Reaction

PEP	Post-exposure prophylaxis
pH	Power of Hydrogen
PHA	Phytohemagglutinin
PLB	Placebo
PrEP	Pre-exposure prophylaxis
PSV	Pseudovirus
RLU	Relative light units
RNA	Ribonucleic acid
rpm	revolutions per minute
s	second(s)
SGA	Single genome amplification
SIV	Simian immunodeficiency virus
STI	Sexually transmitted infection
T20	Enfurvitide
TBS	Tris-buffered Saline
TCID	Tissue culture infectious dose
TDF	Tenofovir disoproxil fumarate
TFV	Tenofovir
Tris	2-amino-2-(hydroxymethyl)-1,3-propandiol
T/F	Transmitted-Founder
T_m	Melting temperature
USA	United States of America
UV	Ultraviolet
V	Volt(s)
VL	Viral load

List of Tables and Figures

1. Literature Review

1.1 Introduction

Human Immunodeficiency Virus (HIV-1), the causative agent of Acquired Immune Deficiency Syndrome (AIDS), has claimed more than 39 million lives since it was first described in 1981 (1). In 2013, 2.1 million new infections globally brought the total number of people living with HIV-1 worldwide to 35 million. Of these people infected with HIV-1, the majority live in Sub-Saharan Africa which contributes to almost 70% of new infections. Women disproportionately carry the burden of HIV-1 infection in most regions in the world. It is estimated that in sub-Saharan Africa, three to six times as many young women are infected than young men (1). Many socioeconomic factors play a part in this disease burden disparity; most notably, cultural attitudes towards sex (2, 3), gender inequality (4), intergenerational sex (5), concurrent sexual partners (6), gender-based violence (7), poor education, poverty and unemployment (8); all of which increase vulnerability to HIV-1 infection. Aside from the socioeconomic factors, women have been found to more biologically susceptible to infection with heterosexual transmission of HIV-1 from male to female being up to eight-fold as efficient as from female to male (9–12). Factors which have been identified as contributing to the higher efficiency of heterosexual transmission of HIV-1 from male to female include:

i. The female genital mucosa has a large surface area through which transmission of HIV-1 can occur (9);
ii. The epithelial barrier of the endocervix and uterus is only a single layer of cells thick and has been shown to be more susceptible to the transmission of HIV-1 (13, 14);
iii. The vaginal mucosa is susceptible to hormonal changes which occur during the menstrual cycle and when hormonal contraceptives are used (15–18). More specifically, thinning of the epithelial lining and decreased cervical mucous resulting in a reduced barrier to infection;
iv. Intercourse can lead to micro-abrasions which lower the barrier to infection.
v. There is a higher likelihood of genital ulcer disease and undiagnosed sexually transmitted infection (STIs) in women as well as bacterial vaginosis which men do not experience (15, 18, 19).
vi. A high availability of target cells in the vagina due to genital tract inflammation (16, 20, 21)

HIV-1 was discovered during a time when major breakthroughs were being made in the field of vaccinology and it was thought that a vaccine would be available within a few years. However, 35 years later, we are still without an effective vaccine. Current management of the global burden of disease promotes safer sex practices such as abstinence, condom use and limiting the number of sexual partners, voluntary counselling, voluntary and frequent testing, antiretroviral therapy (ART), treatment of STIs, and male circumcision [reviewed in (22)]. The last decade has seen an expansion of biomedical interventions including pre- and post-exposure prophylaxis (PrEP and PEP, respectively); as well as microbicides (detailed in section 1.5). Microbicides are of particular relevance to women, providing them control over their protection from acquiring HIV; especially important in situations where condom-use cannot be negotiated.

This chapter will review HIV-1 transmission, the biomedical intervention trials including the CAPRISA 004 1% Tenofovir microbicide gel (the first successful clinical trial to demonstrate protection by a microbicide). Finally the focus of this thesis will be how HIV phenotype affects transmission and disease progression, outlining why HIV-1 *envelope* (*env*) is a gene of interest.

1.2 HIV-1 transmission and disease progression

The HIV-1 transmission bottleneck

During heterosexual transmission of HIV-1, only a subset of viruses from the diverse quasispecies within the donor will be transmitted and will establish productive infection (23–27). In approximately 80% of cases this transmission bottleneck results in a single virus initiating clinical infection, known as the transmitted/founder (T/F) virus.

Intravenous and intrarectal dose-challenge studies in Indian Rhesus macaques resulted in a genetic bottleneck similar to that seen in humans and HIV-1. Simian Immunodeficiency Virus (SIV) challenge studies in monkeys have thus been used as a model system to aid in investigating HIV-1 transmission in humans. In macaques, intravenous inoculation or high dose challenges delivered mucosally resulted in a larger proportion of multi-variant virus infections. In humans, studies have found a higher multiplicity of infection in injection drug users (IDU), men who have sex with men (MSM) and heterosexual transmission in the presence of high genital inflammation, where 60% (28), 36% (29), and 57% (30) of infections were due to multiple variants, respectively. Susceptibility to multivariant HIV-1 infection can increase in cases such as in penile-anal transmission (where there is a higher availability of target cells) [reviewed in (31)] and transmission coinciding with genital disease and inflammation (15, 18–21). Moreover, cases in

which HIV-1 circumvents the mucosal barrier altogether may also lead to multivariant transmissions as seen in some IDU studies (28), although this was not seen in all studies (32). Together, this data suggests that the mucosal barrier is largely responsible for the genetic bottleneck and that multivariant transmission is associated with modes of transmission where the risk of HIV-1 acquisition is increased.

Disease progression and viral load

Viral load (VL) is the number of copies of HIV-1 RNA per millilitre of blood and it fluctuates along the course of HIV-1 infection (33, 34), which is characterised by a period of acute infection followed by chronic infection. During acute infection, the VL reaches a peak, after which the VL declines due to viral suppression by the host immune responses. After acute infection (~3 months post-infection), the chronic phase of infection sets in, which is characterised by clinical latency and stable VL over time, termed "set-point". The VL measurement at set-point is most reliably measured around 12 months post-infection and is used as a predictor of disease progression (35, 36) since set-point VL has been positively correlated with time to AIDS-defining illness or $CD4^+$ T cell count below a certain critical value (currently 350 cells per microliter of blood) (37). Some virological factors have been shown to affect disease progression as well, for instance, multi-variant infections. Multi-variant infections have been correlated with higher VL at set-point and faster disease progression (30). These factors are thus clinically important to study.

1.3 Evidence for selection at the mucosal barrier

The fact that there is a bottleneck raises the question of whether transmission represents a stochastic event in which each donor virus has an equal but very low chance of making it across, or whether the bottleneck represents a selection event where viral variants that have biological properties favourable to establishing new infections are favoured. For HIV-1 infection to become established, the transmitted variant must be present in the mucosa at the site of transmission, must be able to cross the mucosal barrier to make contact with target cells in the recipient efficiently establish a local focus of infection and, finally, systemic infection. While a large part of transmission may be based on chance, there are a number of factors pointing to an element of selection during transmission.

Studies showing that transmitted viruses share common phenotypes, and that they differ from viruses present during chronic infection, suggests that there is selection occurring at the time of

transmission. A study using infectious molecular clones (IMCs) showed that transmitted variants are more infectious and have 1.9-fold more Envelope glycoprotein (Env) on their surfaces per virus particle than viruses from chronic infection. Transmitted viruses also share the common phenotype of CCR5 co-receptor usage (23, 38–43), and subtype A and C, but not subtype B, have been found to have more compact *env*s (i.e. shorter variable loop regions and fewer N-linked glycosylation sites) (24, 44–46). While one study found that T/F viruses were more resistant to the antiviral cytokine interferon alpha (subtype B viruses) (47) than viruses from chronic infection, a more recent study was unable to reproduce this finding (48).

Serodiscordant couples (where one partner is HIV-1 infected and the other is not) and transmission pairs (when the seronegative partner in a serodiscordant pair becomes HIV-1 infected) allow for the study of donor and recipient viruses, and offer insight into which factors, both viral and immunological, affect transmission. In transmission pairs, where donor viruses were compared to early viruses in the recipient, transmitted variants were shown to be more sensitive to neutralization by the donor serum (49). Furthermore, Carlson *et al.* observed the favoured transmission of variants with amino acid identities closer to the cohort consensus than what chronic viruses were in the donor (50). Since consensus sequences represent viruses which are 'fitter' within a given environment (in the case of transmission, viruses which have favourable characteristics that allow them to be transmitted more easily), this suggests that transmitted viruses have a greater replicative fitness than viruses from chronic infection. Moreover, participants with a higher risk of transmission showed a reduction in this selection bias for consensus-like amino acids. For example, there was a weaker bias for transmission of consensus amino acids during transmission to women than to men, but men with inflammation or genital ulcers show a similar selection bias to that of women. Also by studying transmission pairs, Boeras *et al.* showed that the transmitted variant is not the predominant variant in the genital tract (51); indicating that there is selection of a more favourably transmissible variant.

The basis of selection during mucosal infection is complex with many factors contributing to the establishment of clinical infection; such as the target cell population at the mucosa and the level of inflammation present at the time of infection. From these studies, it is evident that several properties of HIV-1 Env glycoprotein are implicated in selective transmission, making it a suitable candidate for investigation as a factor that may increase the chances of infection by certain viral variants over others.

1.4 The importance of Envelope in the transmission of HIV-1

Cell-free virus transmission

The Env glycoprotein of HIV-1 is responsible for attachment of virions to target cells, fusion of the viral and host cell membranes and entry of the viral capsid into the cell (52). The *env* gene encodes gp160 which consists of a signal peptide, gp120 and gp41, subsequently cleaved by the host endoproteases (53–55) in the Golgi into gp120 and gp41. This occurs as the proteins are exported to the cell surface prior to viral assembly at the cell membrane and budding. It is important to note that cleavage of Env into gp120 and gp41 is not required for Env export onto the cell surface (55). On budding and mature virions, fully processed Env spikes occur as Env trimers on the virion surface. Each trimer consists of the gp120 non-covalently attached to gp41 (56, 57). Gp41 is embedded in the viral membrane and provides anchorage of Env to the virion surface. To initiate the entry process, gp120 binds to the CD4 receptor on target cells which causes a conformational change in the Env complex, allowing for co-receptor engagement. After CD4 and co-receptor binding, the N-terminal domain of gp41 (membrane fusion peptide) penetrates the cell membrane after which the two heptad repeat regions, HR1 and HR2, interact (fold back on each other) and form a hairpin structure. This results in fusion of the viral and cell membranes, and subsequently, the viral capsid is released into the cell.

Cell-associated virus transmission

In contrast to cell-free transmission, which relies on stochastic interaction between cell surface receptors and free-floating virions in the extracellular space, cell-to-cell transmission (fig. 3) takes advantage of the biological need for direct contact between immune cells as a means of communication. While the mechanisms of cell-to-cell spread are poorly understood, it has been shown to be more efficient than cell-free transmission and has long been proposed as an important determinant in viral dissemination (58–60). Cell-to-cell transmission depends on the interaction of receptors in donor- and target cell membranes and the subsequent formation of a virological synapse (VS) across which viruses traverse (61–67). Infected cells have been shown to transfer virus particles across a VS to T cells at a high multiplicity of infection (60, 68–70).

It has been shown in tissue culture models that high-multiplicity of infection resulting from cell-to-cell contact increases the probability that a virus may escape drug inhibition. This can occur if the number of infecting viral particles exceeds the effective drug concentration within the cell (71, 72). It is a particular effective strategy of replication in the face of Tenofovir (TFV), which is an intracellular drug. In the case of the drug being present prior to infection, sub-optimal levels

of TFV within immune cells in the mucosa could have been overcome by this mode of transmission. Some groups have shown that cell-to-cell spread allows for efficient replication of the virus in the face of neutralizing antibody immune responses (60, 68, 72–74). However there is contradicting evidence that this method of spread is not a mechanism to evade antibodies or other entry inhibitors (63).

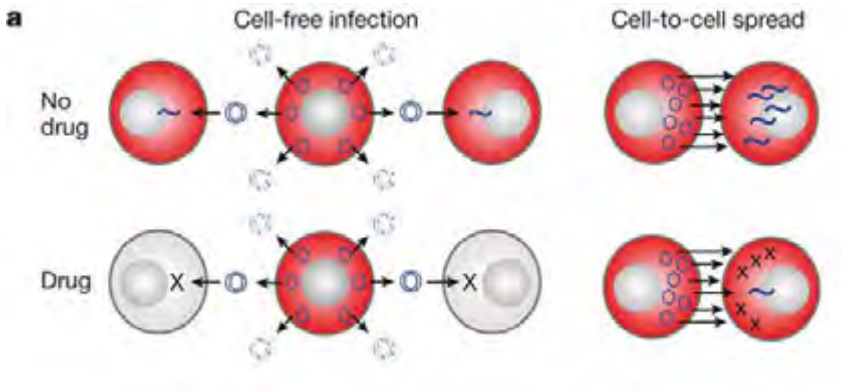

Figure 1.1. Cell-to-cell spread facilitates multiple infections per cell. One mechanism by which HIV can overcome intracellular drug concentrations is by cell to cell spread. Infected cells are represented in red; uninfected cells in grey; blue hexagons represent viruses (encircled blue hexagon= cell-free virus); crosses represent a viral integration event blocked by a drug molecule; wavelets represent provirus (productive infection) and dotted circles outside of cells represent non-functional virions and those that do not go on to infect new cells. Taken from Sigal *et al*. 2011. (71).

Env is a key component in cell-to-cell transmission as it mediates the initial contact of infected cells (which have gp120 exposed on their surfaces) to uninfected target cells, and the formation of a VS (61). Thus, Env engagement with cell surface receptors and co-receptors is essential for efficient transmission and dissemination and preventing this from occurring could be an effective way to prevent the establishment of infection.

Target cell tropism

HIV-1 most commonly makes use of one of two co-receptors to enter target cells: C-C chemokine receptor type 5 (CCR5) and C-X-C chemokine receptor 4 (CXCR4). CCR5 is commonly found on macrophages, dendritic cells, activated T-lymphocytes and, to a lesser extent, monocytes (in which case the virus is R5-tropic), while CXCR4 is found on T-lymphocytes, thymocytes and immune precursor cells (making the virus X4-tropic). Binding of Env trimers to the CD4 receptor via the V1/V2 loop of Gp120 causes a conformational change in Env which, in turn, repositions the V1/V2, and the V3 loops. The Env trimer then binds the chemokine receptors on the target cell surface [reviewed in (75)]. The V3 region of gp120, has been implicated as a determinant of co-receptor usage and can be used as a predictor of cell tropism (76, 77).

1.5 Antiretroviral therapy and prevention

The different classes of anti-retroviral therapy (ART) are able to block or inhibit essential steps of the HIV-1 replication cycle (Table I) thereby decreasing HIV-1 VL to below levels of detection, and slowing down disease progression. Although historically ART refers to these drugs used individually or with one other drug to treat HIV-1 infection, the current standard of care is combination, multi-drug therapy also known as Highly Active ART (HAART). HAART employs the use of three or more drugs from at least two different drug classes in combination. In South Africa, the current first line regimen consists of Tenofovir Disoproxil Fumarate (TDF), emtricitabine (FTC), and efavirenz (EFV) in combination. Combination therapy has the added benefit of deferring the emergence of drug resistance by blocking multiple steps of the HIV-1 replication cycle simultaneously; ensuring that variants with resistance to one of the drugs are still not able to replicate.

Table 1.1. Antiretroviral drug classes and the steps of the viral life cycle acted on*

Step of HIV-1 replication cycle inhibited	**ARV drug class**	**Abbreviation**	**Example of drug in class (WHO abbreviation)**	**Used in treatment in South Africa?**
Entry	Fusion inhibitors	FIs	Enfurvitide (T20)	No
	Co-receptor inhibitors	CRIs	Maraviroc (MVC)	3rd line
Reverse transcription	Nucleoside reverse transcriptase inhibitors	NRTIs	Tenofovir (TFV) disoproxil fumarate (TDF)	1st line and after
	Non-nucleoside reverse transcriptase inhibitors	NNRTIs	Efavirenz (EFV)	1st line and after
Integration	Integrase inhibitors	INIs	Raltegravir (RAL)	3rd line
Virion assembly and maturation	Protease inhibitors	PIs	Lopinavir/ritonavir (LPV/r)	2nd line and after

*This table was modified from the table provided on the AIDS info website, National Institutes of Health, USA (78) and the Scientific Electronic Online Library South Africa .

A meta-analysis of ten studies showed that transmission correlated directly with VL in ART-naïve, serodiscordant couples (79) indicating that VL is a determinant of transmission. This finding formed the basis of the treatment as prevention (TasP) strategy where ART is used by infected

individuals to prevent them from transmitting HIV-1. Thus, in HIV-1 infected patients on ART, successful treatment leads to a reduction in their plasma VL, an increased CD4 count over time and also reduces the risk of transmission. TasP has been shown to be effective in both serodiscordant couples (9, 80–85) and from mother to child during childbirth and breastfeeding (86–88) if the infected individual's VL is suppressed below 50 copies/mL.

ART has also been found to have prophylactic efficacy when administered to uninfected individuals either directly after an exposure event (post-exposure prophylaxis or PEP) or before an expected exposure event (pre-exposure prophylaxis or PrEP). PrEP can be administered in a number of ways, including oral doses of ARVs and as topical microbicides. Numerous efficacy trials have been conducted using both oral, topical and injectable PrEP as a means of preventing HIV-1 acquisition. Of these, the pre-exposure prophylaxis initiative (iPrEx) trial (89), Partners PrEP (90) and TDF2 (91) studies resulted in a high degree of protection ranging from 44- to 75% in MSM (89) and heterosexual (90, 91) serodiscordant couples, respectively. Adherence is a major challenge in PrEP and is thought to account for the failure of some. Lack of protection due to lack of adherence was evident for example in the FEM-PrEP (daily oral PrEP) and MTN 003 (VOICE; daily oral and vaginal PrEP) trials which were discontinued early due to lack of evidence for protection against HIV-1 acquisition in women (92, 93). A summary of the successful efficacy trials, dosing regimens, and efficacy in high adherers is summarised in table 1.2. In order to overcome problems with adherence, trials investigating Cabotegravir, a long-acting integrase inhibitor, are currently underway (94).

Table 1.2. A summary of successful placebo-controlled PrEP and microbicide trials and their efficacy

Trial name	Drug & dosing regimen	Cohort	Overall efficacy	Efficacy by adherence	Adherence measurement
iPrEX (89)	Daily oral FTC/TDF	MSM & transgender women	44%	High (>90%): 73%	Self-reported pill use
Partners PrEP (90)	Daily oral TDF or FTC/TDF	Heterosexual HIV-1 serodiscordant couples	66% and 73%, respectively	Adherence was high throughout the study	Pill counts of returned medication
TDF2 (91)	Daily oral FTC/TDF	Young heterosexual men and women	63%	Adherence was high throughout the study	Pill counts of returned medication
CAPRISA 004 (95)	Pericoital dosing of 1% TFV gel	Young women	39%	High: 54%	Returned applicators and self-reported gel use
ASPIRE (96)	Monthly dapivirine vaginal ring	Heterosexual women	27%	High in women >21 y/o: 56%	Drug levels in blood and residual drug in ring
The Ring Study*	Monthly dapivirine vaginal ring	Heterosexual women	31%	High in women >21 y/o: 37%	Drug levels in blood and residual drug in ring

* CROI, Boston, MA, USA. February, 2016.

These studies provided evidence that ART, when taken correctly, has the potential to affect transmission at the individual level and also, possibly, the course of HIV-1 incidence at the population level (97, 98). Reducing the rate of infection in women is essential to changing the current trajectory of the HIV-1 epidemic in Africa. Microbicides in particular may be of benefit for use by women in order to take control over their own protection. Microbicides are a topical form of PrEP and can be made into a number of formulations (such as gels, sponges or rings) to contain either compounds with broad antiviral activity or HIV-specific ARVs. These can be inserted into the vagina or rectum in order to prevent transmission of HIV-1 (or other STIs depending on the formulation). Efficacy trials have shown that those microbicides containing compounds with non-specific antiviral activity (such as PRO2000, SDS and nonoxylin-9) have been ineffective at preventing acquisition of HIV-1 (99, 100). On the contrary, some of these non-HIV-1 specific microbicides lead to damage of the mucosa (101) and recruitment of HIV-1 target cells (102) resulting in increased rates of transmission.

However, microbicide trials with HIV-specific ARVs have yielded some success (see table 1.2). The first of these tested a microbicide containing Tenofovir (TFV). TFV is an adenosine nucleotide analogue that terminates DNA strand synthesis by the viral reverse transcriptase enzyme because it does not have a 5' phosphate for the next incoming base to react with. Hence, no phosphodiester bond can be formed and the process of reverse transcription is disrupted. This makes it potent against retroviruses (103, 104). The CAPRISA 004 microbicide trial was the first to demonstrate the success of a vaginal microbicide in preventing the acquisition of HIV-1 and also herpes simplex virus type 2 (HSV-2) (95, 105). In sub-Saharan Africa, up to 80% of sexually active women and 50% of sexually active men are infected with HSV-2, which is the most common cause of genital ulcer disease and which, in turn, can increase the risk of HIV-1 acquisition.

One advantage of microbicide use over oral PrEP is that uninfected individuals are only exposed to the ARVs at the mucosal sites of transmission and hence they have higher levels of the drug at the site of infection, while experiencing fewer adverse systemic effects associated with their use.

It is essential that drug levels (systemic or in the mucosa) are maintained at optimal levels in order to achieve protection. This was supported by observations from the CAPRISA 004 (see section 1.6) and FACTS 001 cohorts (106–108), where the degree of protection was linked to adherence of participants to the treatment regimen. There is a necessity to identify dosing and counselling strategies which would encourage participants to adhere to treatment regimens so that effectiveness of treatments can be accurately determined.

Non-adherence to treatment regimens has also been found to be associated with resistance of the virus to ARVs (109). Resistance to TFV is associated with mutations in the reverse transcriptase (*rt*) gene which has been shown to confer viral resistance in cell culture (110, 111) and in patients on ART (109). The most common of these mutations is the K65R point mutation which occurs in 23-65% of people failing first-line ART containing TFV in South Africa (112–115). In addition to the emergence of resistance due to drug exposure (116), these resistance mutations are able to be transmitted and confer viral resistance in recipients who become infected with these viruses (117). Selection of TFV-resistant T/F viruses, which may occur due to the presence of the drug at mucosal sites, or the development of resistance by breakthrough viruses during the establishment of local infection while drug concentrations are suboptimal would pose a threat to the efficacy of TFV-based microbicides. Thus far, however, no transmitted resistance due to the use of TFV-based microbicides has been observed (95, 118). Hence, microbicides represent a step forward in the advancement of prevention methods.

1.6 The CAPRISA 004 1% tenofovir gel Microbicide Trial

The Centre for the AIDS Programme of Research in South Africa (CAPRISA) conducted a phase IIb randomised, placebo (PLB)-controlled trial testing the safety and effectiveness of a 1% tenofovir gel formulation in women from rural and urban areas in Kwa-Zulu Natal, South Africa (95). A total of 889 females between the ages of 18 and 40 years and who were sexually active were requested to use one dose of the microbicide gel 12h **b**efore sexual intercourse and one dose as soon as possible within 12h **a**fter with no more than **t**wo doses in a **24**h period (**BAT24**). The study provided the first evidence that coitally-linked dosing of the microbicide gel lead to a reduction in the acquisition of HIV-1 (fig. 1.2). Overall, there was a 39% reduction in acquisition in women from the TFV arm (5.6 infections per 100 women-years compared to 9.1 infections per 100 women-years in the PLB arm) and a 54% lower chance of acquiring the virus when adherence to the treatment regimen was high. A phase III study for the licensure of 1% Tenofovir gel (FACTS 001) showed that treatment had no overall protective effect but that the effectiveness of TFV gel was highest in high adherers who reported use of the gel in greater than 72% of sex acts (only 20% of the cohort) (108). Of those with self-reported high adherence, detectable TFV in their cervicovaginal lavages correlated significantly with protection from HIV-1 acquisition.

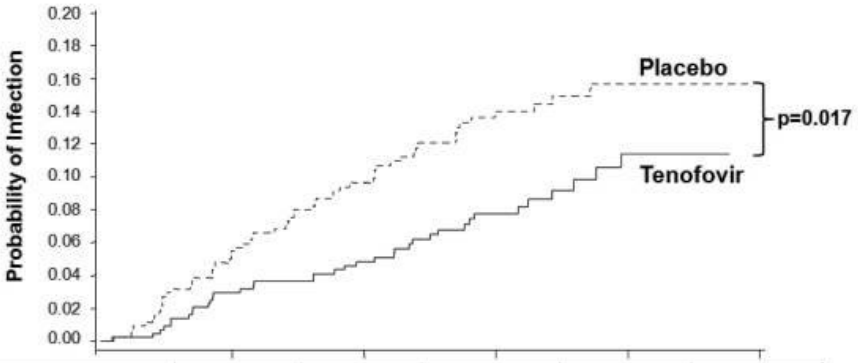

Months of follow-up	6	12	18	24	30
Cumulative HIV endpoints	37	65	88	97	98
Cumulative women-years	432	833	1143	1305	1341
HIV incidence rates (Tenofovir vs Placebo)	6.0 vs 11.2	5.2 vs 10.5	5.3 vs 10.2	5.6 vs 10.2	5.6 vs 9.1
Effectiveness (p-value)	**47% (0.064)**	**50% (0.007)**	**47% (0.004)**	**40% (0.013)**	**39% (0.017)**

Figure 1.2. Probability of infection over time by trial arm in the CAPRISA 004 trial. Figure taken from Karim *et al.* 2010. (95).

A follow up of the women in the CAPRISA 004 cohort showed that, in participants who became infected despite the use of TFV, VLs were significantly higher at one year post infection when compared to participants of the PLB arm (HIV-1 VL log 4.30 versus 3.72 copies/ml; p=0.02) (119). The VLs of participants followed this trend throughout the first two years of infection. Interestingly, participants from both arms had similar disease progression as measured by time to plasma $CD4^+$ T cell counts <350 cells/μL.

1.7 Explaining the sub-optimal efficacy of tenofovir gel

The characterisation of breakthrough infections reported in this study formed part of the Tenofovir gel Research for Advancing Prevention Science (TRAPS) Program, which was established to address questions that stemmed from the CAPRISA 004 Trial; including why only a 39% reduction in HIV-1 acquisition was observed in the drug arm of the trial.

One hypothesis was that pre-infection inflammation and immune activation resulted in target cells being readily-available for infection at the site of transmission, thereby reducing the effectiveness of 1% TFV gel. Naranbhai *et al.* (2012) found that participants who became infected while on the trial, regardless of the trial arm, expressed a unique pattern of innate proinflammatory and T cell homeostatic cytokines as well as higher proportions of activated NK cells in their blood plasma before infection (120). Similarly, Masson *et al.* (2015) have shown that higher levels of genital inflammation correlated with an increased risk of HIV-1 acquisition in these women, regardless of trial arm (21). The study found that raised levels of proinflammatory cytokines were persistent for about a year prior to infection. While the reason for this persistent inflammation remains unclear, elevated levels of inflammation at the genital mucosa and overall systemic innate immune activation contributed to the risk of acquiring HIV-1 in this cohort. However, since neither genital inflammation, nor innate immune activation were found to be different between trial arms, this cannot explain the suboptimal efficacy of TFV gel.

Adherence to the treatment regimen is a large contributing factor to the efficacy of all treatment and prevention methods and contributes to the transmission of resistant variants (see section 1.5). However, the high adherence group in the TFV arm of CAPRISA 004 still had suboptimal protection from infection (54%). Therefore, low adherence only partially explains the sub-optimal efficacy of the 1% TFV gel. In addition, no resistance was detected in CAPRISA 004 participants (95, 118) indicating that breakthrough infections were not the result of resistant viruses nor did breakthrough viruses develop resistance during early infection. This is consistent

with resistance screening in other TFV-based PrEP trials where no resistance to TFV was found (89–91, 112). These findings highlight the necessity of tweaking dosing strategies to confer optimal protection and present the challenge of elucidating why viruses were still able to be transmitted to participants despite high adherence to treatment.

1.8 Viral characteristics can influence disease progression

In vivo, the replicative fitness of a virus will depend on the interplay between the host's immune system and viral characteristics, such as the virus' ability to enter different target cells, the efficiency of the entry process, the efficiency of integration of the viral genome; and, how rapidly the virus can replicate and disseminate once it has entered the target cell. Firstly, disease progression varies with the infecting subtype of HIV-1. Subtype D infection is associated with faster disease progression than subtype A independently of viral load (121, 122), while subtype C infection is associated with faster disease progression than subtype B (123). Furthermore, a switch in target cell tropism over the course of infection, from R5- to X4-tropic HIV-1, has been shown to be associated with disease progression to AIDS-defining illness (41, 124, 125).

In elite controllers (individuals who suppress their VL to below 50 RNA copies/mL of plasma in the absence of ART) whose viruses have attenuated Gag (126, 127), Pol (128), Env or Nef (129) protein function, progression to AIDS-defining illness is slow. This diminished protein function is due to selection pressure by effective CD8+ T-cell responses mounted by each individual's protective human leukocyte antigens (HLAs) as part of the adaptive immune response to HIV-1 during the natural course of infection. It has also been shown that these attenuated strains can remain attenuated in the absence of immune pressure when transmitted to individuals who lack these protective HLA genes, as evidenced by a lower VL and more favourable disease progression in these patients (130, 131). Furthermore, there is evidence that infection with viruses with reduced replication capacity was associated with subsequent elite control (127). *In vitro* replicative capacity has been found to be a determinant of VL in chronic infection (132) and the replication capacity of recombinant viruses containing Gag-Pro genes from acute infection was shown to correlate with VL set-point and CD4 T cell decline (133). In addition, the VLs in HIV-1 recipients in both early infection and at set-point can be predicted by donor VLs (134, 135). Together, this evidence suggests that viral characteristics can have a large impact on disease progression, and that some of these characteristics which are observed during acute or early infection are transmissible.

1.9 Explaining the viral load differences between tenofovir and placebo recipients

A higher VL at set-point was observed in those who became infected in the TFV arm. Infection with multiple variants has been correlated with a higher VL at set-point and faster disease progression (30, 136, 137) and hence could possibly have explained the increased VL. However, Valley-Omar and colleagues showed that the genetic bottleneck in breakthrough infections was not affected by the presence of TFV (138). In the TFV arm 77% of infections were the result of a single variant; similar to the 93% in the PLB arm (P=0.37) and 80% in other subtype C studies (27, 138). Therefore, alteration of the mucosal barrier allowing more than one viral variant to be transmitted was not likely to be the reason for the increase seen in the VL at set-point.

Laeyenndecker *et al.* (2015) evaluated the antibody response to HIV-1 infection in the CAPRISA 004 cohort and found that women who became infected while assigned to the TFV arm showed slower antibody avidity maturation to gp120 (139); that is, the combined strength of antibody binding due to multiple interaction between the antibody and antigen (140). This finding mirrors the delayed antibody avidity seen in rhesus macaques following infection despite oral TFV PrEP (141). Both studies showed no difference in antibody titre between the trial arms. Interestingly, the macaque studies showed lower peak viremia during acute infection (which was not seen in the CAPRISA 004 cohort at the time of seroconversion) and reduced systemic inflammation in animals receiving PrEP (141, 142). Whether delayed antibody avidity maturation may have led to higher VL at set-point in both macaque and human studies was not shown and remains unknown.

An alternative hypothesis is that TFV selects for viruses that replicate better in the mucosal environment, establishing a greater local focus of infection that can overcome the TFV barrier and subsequently spreading to the lymph nodes to establish systemic infection. As *in vitro* replication capacity has been shown to correlate with *in vivo* VL (127, 130, 132, 133, 143–145), HIV-1 Gag, Gag-Protease and Nef function were investigated as the possible underlying factors for an increased replicative capacity and VL (146). Increased Nef activity, for example, has been shown to downregulate CD4 (147) and major histocompatibility complex (MHC) class I (148). The replication capacity of Gag-Pro recombinants derived from T/F viruses from CAPRISA 004 participants correlates with set-point VL; an observation that was also made using T/F Gag recombinants from a cohort in Zambia (144). However, no significant differences were found in *in vitro* Gag-Pro mediated replication capacity or Nef function of T/F viruses between the microbicide or the PLB arm (146). Therefore, the question remains as to what may have caused

the increased VL at set-point; and, if the cause was due to characteristics of the transmitted viruses, which characteristics may have been the reason for the increased VL.

1.10 Study rationale

Several studies have shown a relationship between HIV-1 replication *ex vivo* and plasma VL (132, 143, 149, 150). In addition, the Env glycoprotein has been shown to be an important determinant of *ex vivo* viral replicative fitness (76). In this study we investigated whether the presence of TFV in target cells selected for viruses with a certain Env phenotype at the time of transmission. We hypothesize that an altered Env phenotype in TFV arm virions, compared to the Env phenotype of PLB arm virions, conferred a replicative advantage which allowed viruses to replicate to a higher VL at set-point. To do this we compared the Env properties of early breakthrough viruses from TFV recipients to early viruses from PLB recipients from the CAPRISA 004 microbicide trial.

1.11 Significance of this research

Microbicides need to block the transmission event and hence there is a need to identify the characteristics of the earliest viruses present in individuals who become infected despite the use of prophylaxis. Inferences can be drawn from early viruses about the transmitted viruse(s) that were able to overcome the barrier of protection and those that may lead to high VL later on during infection. In the CAPRISA 004 cohort, preliminary studies show that VLs in women who become infected while assigned to the TFV arm are higher than those assigned to the PLB arm. Research is needed to understand the underlying mechanisms associated with the increase in VL. In addition to informing the improvement of microbicides, information about acute-phase infection and transmitted viruses will also aid in vaccine design efforts (23, 151).

1.12 Aims and specific objectives

The aim of this study was to characterise the phenotypes of the viral Env proteins from early viruses from both the PLB and TFV arm of the CAPRISA 004 trial; and to determine whether there were differences in Env phenotypes that could explain the higher VL observed in TFV recipients.

Objectives:

1) **To isolate early viruses (<3 months post-infection) from participant plasma.**

Approach: CD44 microbeads were used to isolate viruses from infected plasma by magnetic separation. The resultant eluate, containing virus, was used to inoculate cultures of primary cells. Primary cells from three different donors were isolated and pooled and subsequently stimulated under three different conditions before being infected.

2) **To assess if the isolates were representative of viruses *in vivo.***

Hypothesis: Isolates are representative of viruses *in vivo*, with only minor changes represented in isolate *env* sequences as compared with *env* sequences derived from plasma viruses

Approach: Sequences of *env* genes from culture virus and *env* sequences derived from plasma viruses were compared to determine if HIV-1 *env* of the isolates was representative of viruses circulating *in vivo* for each participant, and determine if major changes were introduced during tissue culture.

3) **To determine whether differences in Env genotype exist between study arms by comparing *env* genotypic properties between TFV and PLB arms**

Hypothesis: Viruses isolated from the TFV arm have more genotypic characteristics favouring transmission and infection, such as fewer glycosylation sites, shorter variable loops and are less charged. In addition, TFV arm viruses are closer to a subtype C consensus of viruses circulating *in vivo*.

Approach: For each participant, the average number of glycosylation sites, variable loop length, and variable loop charge was compared between TFV and PLB arm isolates. The predicted sites of glycosylation, loop length and charge were determined using online prediction tools. In addition, a subtype C consensus *env* representing viruses circulating in the region was generated and the distance of isolate *env* sequences to the consensus was evaluated for each study arm.

4) **To determine whether differences in Env function exist between study arms by comparing Env phenotypic properties between TFV and PLB arms including susceptibility to TFV, entry inhibitor sensitivities, and entry efficiency**

Hypothesis: Viruses isolated from the TFV arm have more favourable phenotypic characteristics such as higher CD4 and CCR5 binding capacity, higher fusion capacity, and a lower CCR5 dependence.

Approach: Isolates were assessed in inhibition assays to evaluate Env sensitivity to entry inhibitors. Maraviroc, T20, PSC-RANTES, and an anti-CD4 antibody, clone SK3 were the entry inhibitors chosen. These inhibitors act at the level of CCR5 binding, fusion, and CD4 binding, respectively. In addition, Pseudoviruses (PSVs) were used in a virion-cell fusion assay to assess the entry efficiency of the isolates more directly. Using this system we could assess the contribution of Env to viral fitness and compare this between different viruses without the confounding effects of functional differences in other viral proteins.

5) **To evaluate whether Env phenotypic characteristics of the isolates are associated with predictors of disease progression**

Hypothesis: Participants infected with viruses that have higher CD4 and CCR5 binding capacity, higher fusion capacity, a lower CCR5 dependence, and higher entry efficiency will have a lower CD4 count at set-point and higher VLs.

Approach: Correlations of all phenotypic characteristics investigated (objective 4) with VL at isolation, 3 months post-infection and at set point, as well as CD4 count at set-point were performed.

6) **To compare the phenotypic characteristics of PSVs with the phenotypic characteristics of viral isolates.**

Approach: Inhibitor sensitivities to maraviroc, T20, PSC-RANTES and anti-CD4 antibody clone SK3 were compared between isolates and the PSVs generated using the majority *env* corresponding to the same participant. These were evaluated to determine if pseudoviruses exhibit different Env phenotypic properties to their corresponding isolate.

The findings of this study may provide insight into entry characteristics of early viruses that result in a higher VL at set-point.

2. Materials and Methods

2.1 Ethics statement

The CAPRISA 004 Microbicide trial was reviewed and approved by the University of KwaZulu-Natal's Biomedical Research Ethics Committee (REC), Family Health International's Protection of Human Subjects Committee and the South African Medicines Control Council (95). All participants of the study cohort provided informed consent for study participation. This sub-study, including laboratory protocols and the use of participant information, was reviewed and approved by the University of Cape Town's (UCT) Faculty of Health Sciences Human REC (HREC REF number 587/2014).

2.2 CAPRISA 004 participants and the TRAPS cohort

The samples and information used in this study were from the Tenofovir gel Research for Advancing Prevention Science (TRAPS) programme, Durban, South Africa. TRAPS was an ancillary study of CAPRISA004 where all consenting HIV-1 seroconverters were recruited, and followed up, as part of the CAPRISA 002 Acute Infection cohort. Participants were followed until antiretroviral therapy commencement under the South African Antiretroviral Treatment Guidelines at the time; that is, when $CD4^+$ T cell count fell below 350 cell/μL or at the presentation of AIDS-defining illness. As part of the CAPRISA 004 trial protocol (95), blood samples (serum, plasma and PBMCs) were collected weekly for the first month, fortnight up to three months, monthly from months three to 12 and then at quarterly visits thereafter until antiretroviral therapy initiation. VLs and $CD4^+$ T cell counts measured at each sampling event, as well as gel adherence data, were provided. In this study, VL at set-point was calculated as the average of three VL measurements around 12 months post-infection: the VL nearest the 12 month visit, and the measurements before, and after the 12 month visit. VLs that differed by $1\log_{10}$ were excluded from the average. CD4 count at set-point was determined using measurements from the same visits used in the VL set-point determination for each participant.

2.3 Sample selection for this study

This study made use of blood plasma samples and clinical information obtained from 48 women from TRAPS. Plasma samples from the earliest time-point available were obtained from CAPRISA.

Participants from the Tenofovir arm (n = 24) were matched to PLB arm controls (n = 24) based on the time post-infection that the plasma sample was obtained as well as protective human leukocyte antigens (HLAs) of the HIV-infected participant. Adherence was measured by the number of unused applicators returned and the number of self-reported sex acts since the last study visit (data provided by N. Garrett). TFV concentrations from cervicovaginal lavages were also measured as part of a previous study to determine whether participants had detectable levels of TFV in the vaginal mucosa (118).

2.4 Cells and cell maintenance

PBMC isolation

Heparinized whole blood was obtained from HIV-negative donors and peripheral blood mononuclear cells (PBMCs) were isolated using Ficoll-Paque™ density gradient centrifugation. 2mM ethylene-diamine-tetra-acetic-acid (EDTA) in phosphate buffered saline (EDTA-PBS) at pH 7.2 was prepared and refrigerated at 4°C. The PBS used in all protocols of this study did not contain any Calcium or Magnesium. Whole blood was diluted four-fold in EDTA-PBS at room temperature. 35mL of diluted whole blood was layered carefully over 15mL Ficoll-Paque™ reagent in a 50mL conical tube which was then centrifuged for 20 min at 900 x g and at 20°C in a swinging bucket centrifuge without brake. All centrifugation steps of this study were performed in an Eppendorf 5810R Centrifuge (Eppendorf, Hamburg, Germany) unless otherwise stated. A 10mL serological pipette was used to remove the mononuclear cell layer from the interphase of the Ficoll-Paque (bottom) and blood plasma (top) layers; being careful not to disturb the layers. This was transferred to a fresh 50mL tube, made up to 50mL with EDTA-PBS and centrifuged for 10 min at 900 x g at 20°C. In order to remove platelets from the mononuclear cells, the pellet was resuspended in 50mL EDTA-PBS and centrifuged for another 10 min at 900 x g after which the supernatant (containing platelets) was removed. This wash step was repeated to ensure removal of all platelets. Cells were diluted two-fold in Trypan Blue (Invitrogen, CA, USA) to a total volume of 20µL and subsequently counted using a Countess cell counter and counting chamber slides (both by Invitrogen).

$CD8^+$ T cell depletion of PBMCs & cell storage

$CD8^+$ T cells were depleted from unstimulated PBMCs to ensure that HIV replication was not inhibited by these cells during virus isolation (152). This was achieved by magnetic labelling of $CD8^+$ T cells using MACS CD8 MicroBeads (all MACS products were from Miltenyi Biotec, CA, USA) and subsequent depletion by column separation. Briefly, the freshly isolated PBMCs in EDTA-

DPBS were centrifuged (300 x g for 10 min at 20°C) and the pellet was resuspended in 80 µl MACS buffer + 20 µl CD8 MicroBeads per 1 x 10^7 cells after removal of the supernatant. This was mixed well and the suspension was incubated for 15 min at 4°C. Cold wash buffer was prepared by diluting bovine serum albumin (BSA) in EDTA-PBS to a final concentration of 0.5%v/v. A MACS magnetic column was placed in the magnetic field of a MACS Separator mounted on a MACS MultiStand. The columns were prepared by rinsing twice with 2mL volumes of buffer. The labelled PBMCs were then added to the columns which were subsequently washed three times with 3mL of buffer each time. Any $CD8^+$ cells were retained in the column. The cells in the effluent (desired cells) were counted using the Countess cell counter as described previously. Cells were pelleted by centrifugation (500 x g for 10 min) and resuspended to a final concentration between 2 x 10^7 and 5 x 10^7 cells/mL in foetal bovine serum (FBS) containing 10% dimethyl sulfoxide (DMSO). PBMCs were frozen in 1mL aliquots at -80°C for one hour in a freezing container to ensure a 1°C/min decrease in temperature and then placed in liquid nitrogen (-196°C) for long-term storage until needed.

Cell lines

The HEK293T cell line was obtained from the American Type Culture Collection (ATCC® CRL3216™) and is a human embryonic kidney cell line used for the production of proteins by transfection with plasmid DNA (153, 154). The TZM-bl cell line was obtained through the National Institute of Health (NIH) AIDS Reagent Program- Division of AIDS, NIAID, NIH from Dr John C. Kappes, Dr Xiaoyun Wu and Tranzyme Inc (155–159). It is a HeLa cell line expressing CD4 and CCR5 which allows for entry of HIV virions into the cell. The cells also have a firefly luciferase reporter gene under the control of the HIV-1 long terminal repeat (LTR). The viral Tat protein binds to the LTR to initiate transcription of viral proteins during the normal viral replication cycle. Hence, viral entry, reverse transcription, integration and expression of the viral Tat protein results in expression of the luciferase reporter. This reporter system allows for quantification of infectivity of viral isolates by measuring luminescence after the addition of a luciferase detection reagent (SteadyLite, Perkin Elmer, MA, USA) to the infected cells. SteadyLite reagent lyses the cells and contains D luciferin, the substrate acted on by firefly luciferase resulting in the production of oxyluciferin and photons of light (fig. 2.1).

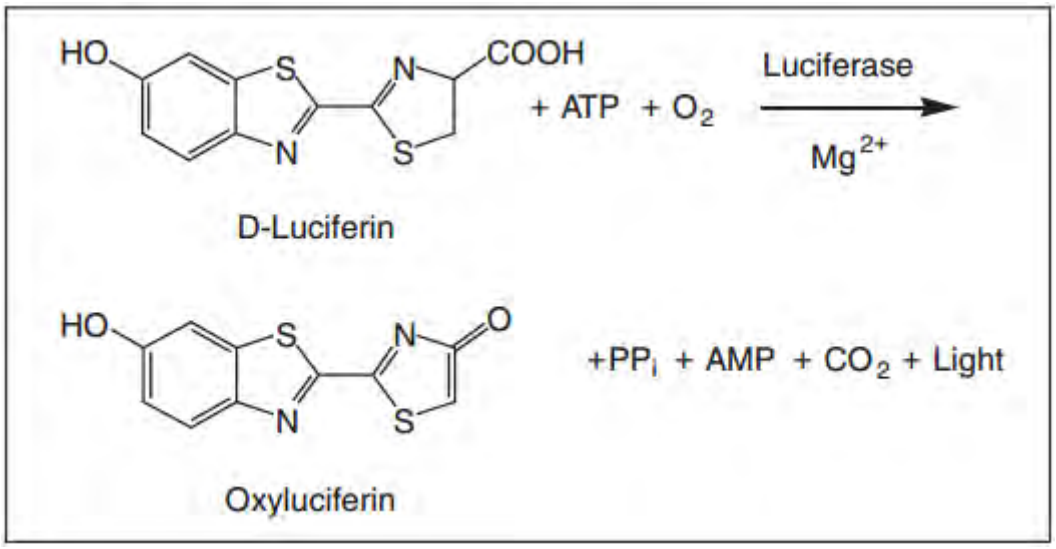

Figure 2.1. A schematic showing the SteadyLite reaction. Figure taken from the SteadyLite Plus High Sensitivity Luminescence Reporter Gene Assay System manual found at http://www.perkinelmer.com/CMSResources/Images/44-173606MAN-steadylite-plus.pdf.

Both cell lines were maintained in D10F growth medium (GM) which consists of Dulbecco's Modified Eagle Medium (DMEM) containing phenol red and supplemented with 50 μg/mL of gentamicin as well as 10% FBS. All cell culture incubation steps in this study were carried out in a humidified incubator at 37°C. Cells were grown in monolayers in T75 filter cap tissue culture flasks and were passaged every 2 to 4 days when they reached 70% to 80% confluency.

Passaging of HEK293T cells was carried out as follows: medium was removed and cells were washed with 5mL Dulbecco's Phosphate-Buffered Saline (DPBS) without Calcium or Magnesium to remove trypsin inhibitors. Thereafter, 5mL pre-warmed (37°C) 1X trypsin-EDTA (0.25% trypsin, 1mM EDTA) solution was added to the cells in order to cleave proteins that support cell adherence to the flask. Cells were incubated for one minute at room temperature after which 5mL pre-warmed D10F GM was used to inactivate the trypsin solution and wash the cells off the bottom of the flask. The cell suspension was transferred to a 15mL conical tube, centrifuged for 5 min at 900 x g and the pellet resuspended in 10mL D10F GM for counting. Cell counting was performed as described previously for PBMCs. Each new flask was seeded with 0.5 x 10^6 to 2 x 10^6 cells. TZM-bl cells were passaged in a similar manner with the following exceptions:

i. TZM-bl cells were incubated with 7 mL trypsin solution for up to five min at 37°C;
ii. 7 mL D10F GM was used to neutralize the trypsin solution after detachment of the cells.

2.5 Isolation of early viruses

PBMC stimulation

To minimize the effect of differences in donor PBMC susceptibility to HIV-1 infection on the efficiency of virus isolation (160), a 3x3 stimulation protocol was employed where PBMCs obtained from three different donors were stimulated under three different conditions (161, 132) to obtain a mix of PBMCs each time cells were added. Cell culture flasks were coated with OKT3 (BioLegend, CA, USA), which is an anti-CD3 monoclonal antibody, 24h before PBMC stimulation. OKT3 was diluted to a concentration of 10 µg/mL in DPBS and added to the flask which was incubated horizontally in a 37°C humidified incubator overnight. The total volume of OKT3-DPBS required to coat a T25 or T75 flask was 5mL or 10mL, respectively. Thereafter, the OKT3-DPBS was removed from the flask. $CD8^+$ depleted PBMCs from three buffy coat donors were thawed rapidly in a water bath set to 37°C. These were pooled, mixed well and diluted in RPMI 1640 supplemented with 10% FBS, 50 µg/mL gentamicin, 2mM L-glutamine and 200 U/mL IL-2 (IL-2/stimulation medium) to a concentration of 4×10^6 cells/mL. The pooled cells were split into three equal fractions; the first of which was added to the OKT3-coated flask. The remaining two fractions were added to two fresh flasks which were subsequently supplemented with phytohemagglutinin (PHA) to final concentrations of 0.5 µg/mL and 5 µg/mL, respectively (132, 161, 162). All three flasks were incubated in a humidified incubator for 72h; the PHA flasks incubated vertically and the OKT3 flask incubated horizontally. Over the incubation period roughly 50% of cells die; therefore, this was accounted for when determining the total number of PBMCs to stimulate prior to each application.

Virus isolation from plasma & infection of PBMCs

Viruses were isolated from participant plasma using the µMACS VitalVirus HIV Isolation Kit (Miltenyi Biotec). The principle involves positive selection of HIV by magnetically labelling virions which contain CD44, a mammalian cell surface marker, in their lipid envelopes (163). Subsequent addition of the magnetically labelled sample to a magnetic column captured the labelled viruses, which were later eluted from the column, while the remainder of the sample flowed through the column. Frozen plasma samples were thawed rapidly in a 37°C water bath and immediately centrifuged at 13 000 x g for 30s to remove large particles and cell debris. One millilitre of plasma (supernatant) was incubated with 250µL CD44 magnetic MicroBeads in a fresh tube at room temperature for 30 min. During incubation, PBMCs stimulated under the three different conditions described above, were pooled and counted as described previously using a Countess cell counter. The stimulated PBMCs were centrifuged at 900 x g for 10 min at room temperature and the cell pellet resuspended in IL-2 medium to a final concentration of 7×10^6

cells/mL. Cells were seeded at 0.7 x 10^6 cells per well in a 24-well plate (100 µL cell suspension per well). One µColumn per plasma sample was placed in the magnetic field of a µMACS Separator mounted on a MACS MultiStand. The column was prepared by adding 100 µL of equilibration buffer to the column followed by three washes with 100µL of virus wash buffer supplemented with 2% FBS. The magnetically labelled sample was then added to the column followed by four 200µL washes with the virus wash buffer. After removal of the columns from the magnetic separator, magnetically labelled virus was eluted directly into a single well of the 24-well plate using 350µL IL-2 medium and a syringe plunger. Plates were spinoculated for 60min at 1200 x g and at 25°C. Thereafter, plates were mixed gently and placed in a humidified 37°C incubator overnight.

Expansion & maintenance of infected cultures

The following day, 550µL fresh, pre-warmed IL-2 medium was added to each well up to a total of 1ml and the plates were placed back into the incubator. This was repeated 72h later at (day three) with 1mL IL-2 medium. On day seven, cultures were transferred to 6-well plates containing 2 x 10^6 stimulated PBMCs per well in 2mL medium; adding up to a final volume of 4mL. On day ten, these cultures were centrifuged at 900 x g and the resuspended in 10mL fresh, pre-warmed IL-2 medium and transferred to T25 culture flasks incubated vertically in a 37°C humidified incubator. Virus cultures were assayed for virus production by Gag p24 ELISA every seven days (see method described in section 2.6). On day 14, the infected PBMCs from intermediate and highly positive cultures were resuspended in 10mL fresh Il-2 medium and added to T75 culture flasks containing either 4- or 8 x 10^6 freshly stimulated PBMCs in 4 and 8mL IL-2 medium, respectively. PBMCs from Gag p24-negative cultures were resuspended in 10mL fresh Il-2 medium and transferred to T75 culture flasks containing 1 x 10^6 freshly stimulated PBMCs in 1mL IL-2 medium. Cultures were maintained in this way for 25-52 days with medium being refreshed as described every three days and cells being replenished as described every seven days.

Harvesting & storage of virus stocks

From day 18 onwards culture supernatants were harvested every three days and stored in 50mL conical tubes at -80°C. Aliquots of each culture were stored separately in order to perform p24 ELISAs as well as titration experiments in TZM-bl cells (see method described in section 2.7) after a single freeze-thaw cycle with all harvest days in the same experiment. The results of the p24 determination and viral titres were compared for all harvested supernatants and the harvest which had the highest titre in TZM-bl cells was thawed in a 37°C water bath and placed in long-term storage at -80°C in 500µL aliquots. For most cultures viral titres were highest at day 25.

2.6 Quantification of p24 antigen in viral isolate stocks

In-house ELISA

The Gag p24 content in viral culture supernatants was checked at regular intervals by enzyme-linked immunosorbent assay (ELISA). The protocol was developed in the Williamson laboratory (P. Selhorst, University of Cape Town, South Africa) and is based on a sandwich ELISA principle (fig. 2.2) in which a 96-well plate is coated with an anti-p24 capture antibody that will bind p24 antigen in the sample.

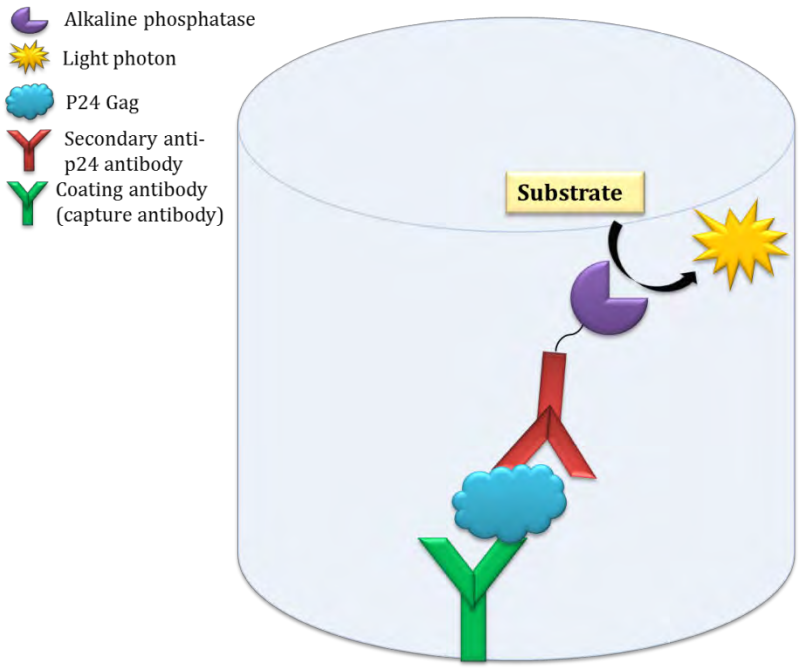

Figure 2.2. The sandwich ELISA principle used for quantifying the amount of p24 antigen in a sample. The figure depicts a single reaction taking place in a single well of a 96-well microtiter plate to which the coating antibody is bound with high affinity. In reality the entire surface of the well is covered with coating antibodies.

After washing, only the coating antibody and the bound p24 remain. Thereafter, a secondary anti-p24 antibody which is conjugated to alkaline phosphatase is added to the well and binds the p24 at a different epitope to the first antibody. After addition of the chemiluminescent substrate, alkaline phosphatase converts it to a product and light (fig. 2.3).

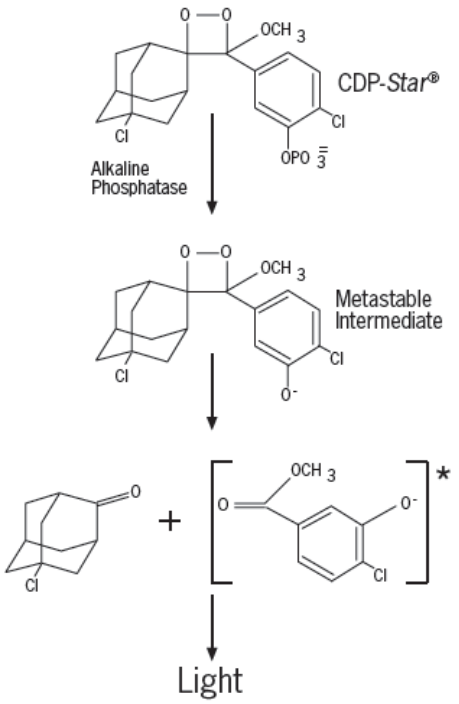

Figure 2.3. A schematic showing the action of alkaline phosphatase on the chemiluminescent substrate, Tropix® CDP-Star with Sapphire-II™. Figure taken from the Applied Biosystems Product Bulletin on Tropix® Chemiluminescent Substrate Formulations for OEM found at https://www3.appliedbiosystems.com/cms/groups/mcb_marketing/documents/generaldocuments/cms_047824.pdf.

Briefly, high-bind 96-well white, opaque microtiter plates (Corning® COSTAR®, NY, USA) were coated with 100 µL anti-HIV-1-Gag p24 antibody D7320 (sheep anti-HIV monoclonal) (Aalto Bio Reagents, Dublin, Ireland) which was diluted 1:600 in sodium bicarbonate (0.1M, pH 8.5) from stock concentration of 2mg/mL prior to coating. Plates were incubated overnight at room temperature and then washed 3 times with 1X TBS buffer (Appendix 1). The plates were then left to dry for 2h and stored at -20°C until needed.

Dilutions of culture supernatant were made for each culture; starting with neat supernatant. A 20 µL volume of a 5% solution of Empigen (Sigma-Aldrich, MO, USA) was pipetted into each well of the plate to which 80µL of viral culture supernatant was directly added in order to lyse virions and release p24. The p24 antigen standard was prepared by diluting recombinant HIV-1 Gag p24 (Aalto Bio Reagents) to a starting concentration of 12.5 ng/mL in cell culture medium. Thereafter, seven two-fold serial dilutions were made by diluting the p24 standard in the appropriate cell culture medium (the same one as in the samples). The Gag p24-standard dilutions were applied to the ELISA plate in duplicate with the eighth well in the dilution series containing cell culture medium only as the background control. Plates were incubated at room temperature for 2h and

then washed three times with 400µL of 1X TBS buffer. The secondary conjugate antibody (mouse anti-HIV monoclonal), alkaline phosphatase conjugate BC1071-AP (Aalto Bio Reagents), was diluted 1:12500 in 1X TBS containing 0.1% Tween-20 (Sigma-Aldrich) and 100 µL was applied to each well of the ELISA plate after the first wash. This was incubated for 1h at room temperature and then washed four times with 400µL of 1xTROPIX-0.1% Tween buffer CDP Star® substrate with Sapphire-II™ (Novex®, Life Technologies, CA, USA) was diluted 1:10 in 1X TROPIX buffer and 100 µL was added to each well of the ELISA plate after the second wash. After exactly 30 min incubation period with plates covered to ensure no exposure to light, luminometer readings were obtained (GLOMAX® 96-Mcroplate Luminometer using the Promega BrightGlo Protocol; Promega, WI, USA) as relative light units (RLU). The in-house ELISA was used in order to narrow down the dilution range required to quantify the amount of p24 and reduce the cost of performing the assay using a commercial ELISA kit, which provided more accurate p24 quantitation.

Commercial ELISA

The Gag p24 antigen content of each viral stock was confirmed by the commercially available PerkinElmer Alliance ELISA Kit (PerkinElmer) using the cell culture supernatant protocol. This kit provided accurate p24 quantification with reduced variation between experiments. The protocol follows a sandwich ELSA principle as described above. Briefly, the microplates were supplied pre-coated with a mouse monoclonal anti-p24 capture antibody which binds Gag p24 antigen. A viral lysis reagent (Triton X-100) was added to each well of a microplate. Dilutions of the virus stocks were added to each well and the plates were incubated at 37°C for 2h. Thereafter, plates were washed six times with the wash buffer supplied and a biotinylated polyclonal anti-HIV-1 p24 antibody was added to each of the sample wells. The plates were then incubated at 37°C for another hour and then washed six times with the same wash buffer. A Streptavidin-horseradish peroxidase (HRP) conjugate was added to the plate which was incubated at room temperature for 30 min. After a final six-wash step, ortho-phenyl-diamine-HCl (OPD) substrate was added to all wells and the plates were incubated at room temperature for 30 min in the dark.

OPD cleaved by HRP produces a yellow colour and the production of colour is directly proportional to the amount of p24 captured in each well. A stop solution was added after the final incubation period. Colour output was measured at 650nm and 490nm using an absorbance reader blanked on air. All plates were read within 15 min of stopping the reaction. In addition to sample dilution-containing wells, each plate had a substrate blank well and a standard curve loaded in duplicate. The substrate blank well did not undergo addition of lysis agent, sample or any antibody binding steps; but underwent all wash steps as well as addition of the substrate.

The standard curve was produced using the purified HIV-1 p24 supplied with the kit which was diluted to a 100pg/mL starting dilution and then serially diluted seven times by a factor of two.

2.7 Titration of isolate stocks

The relative titre for each stock of viral isolates was determined using a 50% Tissue Culture Infectious Dose ($TCID_{50}$) assay. The assay is based on infection of TZM-bl cells at various dilutions of virus stock to ascertain the concentration at which 50% of replicate wells result in 'positive' detection of infection. Infection is measured by luminescence after the addition of a firefly luciferase substrate to the cells. TZM-bl cells were seeded in a 96-well tissue culture-treated microtiter plate at a density of 1×10^4 cells per well in a final volume of 100µL of D10F GM with DEAE-dextran added at a final concentration of 40 ug/mL. DEAE-dextran is a polycation that increases cell-free virus infection by stabilizing virion adsorption to the cell membrane allowing for enhanced viral entry (164). Three-fold serial dilutions of the isolate stocks were made and 100µL of each dilution was to six replicate wells. Six background control wells were included per plate; by adding 100µL D10F GM instead of virus dilution to the cells. Outer wells of the plate were filled with 200 µL sterile water to decrease evaporation. After a 48h incubation period at 37°C, 120 µL of supernatant was removed from each well and replaced with 75µL SteadyLite reagent (PerkinElmer). Plates were incubated for 10 minutes at room temperature in the dark. The contents of each well were mixed and 100µL was transferred to an opaque white 96-well microtiter plate. Luminometer readings were obtained as described in section 2.6. Wells with RLUs greater than 2.5 times the average background value (average RLU from all negative control wells) were considered positive. Viral titres were calculated using the Reed and Muench method (165) and expressed as infectious units per mL.

2.8 Amplification and sequencing of viral *envelope* genes

RNA extraction & cDNA synthesis

One 500µL aliquot of each culture supernatant was thawed in a 37°C water bath and a 1:100 dilution in DPBS was made for each. HIV-1 RNA extractions were carried out on 200µL of the diluted supernatant using the Roche MagNA Pure Compact System and Roche MagNA Pure Compact RNA Isolation kit (Roche, Basel, Switzerland). RNA was eluted in 50µL final volume of elution buffer; 25µL of which was reverse transcribed into cDNA on the same day to avoid degradation of the sample during storage and freeze-thaw cycles. Reverse transcription was

carried out using a SuperScript™ III Reverse Transcriptase (RT) System (Invitrogen) with oligo(dT) as a primer. The final concentration of reagents in each reaction were as follows: 0.4mM dNTPs, 2μM oligo(dT), 1X Superscript buffer, 5mM DTT, 2 Units (U)/μL RNAseOUT (Ribonuclease inhibitor), 10U/μL SuperScript III™ reverse transcriptase and ddH_2O to a final volume of 50μL. These were set up as two separate master mixes. The RNA along with the dNTPs and oligo(dT), the first master mix, were added to 0.2mL PCR tubes and placed on a heating block set to 65°C for 5 min. Thereafter, the mix was put on ice for 1 min and the remainder of the reagents, in a second master mix, were added to each tube. The reaction was run on a thermocycler at 45°C for 2h and then 75°C for 15min to inactivate the RT enzyme. Thereafter, 2U RNAseH was added to each tube after which tubes were incubated for another 20 min at 37°C to digest the RNA template. cDNA was stored at -80°C until needed.

Single genome amplification (SGA) & sequencing

cDNA was thawed and serially diluted in molecular grade water (Sigma-Aldrich) in order to obtain less than 50% positive amplification reactions at which, theoretically, each positive reaction would have been amplified from a single copy of HIV-1 cDNA 69% of the time (166). Where possible, this was decreased to less than 30% positive in which case each reaction would have been amplified from a single cDNA copy more than 80% of the time. The SGA method was adapted by Salazar-Gonzalez *et al*. in order to reduce recombination and Tat-induced error when amplifying *env* from HIV-1 cDNA (27, 151). For amplification of *env*, a nested PCR was performed in which two rounds of PCR yield the desired product; the second round primers being nested within the first. Briefly, 1μL cDNA of a particular dilution was added to eight replicate wells of a 96-well PCR plate for first-round synthesis using OFM19 (5'-GCACTCAAGGCAAGCTTTATTGAGGCTTA-3') and VIF1 (5'-GGGTTTATTACAGGGACAGCAGAG-3') forward and reverse primers. Similarly, 1μL of first-round PCR product was added to corresponding wells of a second 96-well PCR plate for synthesis of the final product using EnvA (5'-GGCTTAGGCATCTCCTATGGCAGGAAGAA-3') and EnvN (5'-CTGCCAATCAGGGAAGTAGCCTTGTGT-3') forward and reverse primers. The concentrations of reagents (Invitrogen) in each reaction were as follows: 1X High Fidelity Buffer, 2mM magnesium sulfate ($MgSO_4$), 0.2mM of each dNTP, 0.2μM of each primer, 0.025 U/μL Platinum® *Taq* DNA Polymerase High Fidelity enzyme and ddH_2O to a final volume of 19μL. The first round PCR was carried out under the following cycling conditions: 94°C for 2 min, then 35 cycles of 94°C for 15s, 55°C for 30s and 68°C for 4min, followed by a final elongation at 68°C for 20min. The second round PCR was performed under the same conditions but for 45 cycles. Post-PCR clean-up and sequencing of the second-round product was carried out through the Central Analytical Facilities at the University of Stellenbosch using the ABI 3000 Genetic Analyzer (Applied Biosystems, CA,

USA) and BigDye terminator reagents. Twelve gp160 primers (Appendix 2) spanning the length of *env* were used.

Sequence analysis

Sequences for each *env* gene for each participant were compiled using Sequencher (v5.2.4) and aligned and visualized using BioEdit (v7.1.11) and AliView (v1.18) (167). MACSE (168) was used for all codon alignment. Sequences containing more than three 'double peaks' in the chromatogram, indicating the presence of more than one template during the amplification, were excluded. Those with one or two 'double peaks' were included. *env* sequences were compared to SGAs from plasma and derived transmitted/founder *env* sequences generated internally (Z. Valley-Omar, C. Rademeyer, R. Thebus & M. Logan, personal communication). Those SGAs generated in this study with deletions larger than 50 nucleotides compared with the plasma consensus were also excluded. Differences in both nucleotide and translated (using BioEdit) amino acid sequences were visualized using the Highlighter tool on the Los Alamos website (www.hiv.lanl.gov) as well as by neighbor-joining trees compiles using MEGA 6 (169). Pairwise DNA and amino acid distances between sequences were computed using MEGA 6. For this comparison, a consensus was generated using sequences from CAPRISA 002 participants who were recruited from the same population and same geographical region as CAPRISA 004 participants. A total of 592 *env* SGAs were aligned in MACSE and used to generate a consensus sequence in BioEdit. Variable loop length, charge and glycosylation prediction was performed using the Variable Region Characteristics tool and NX[ST] glycosylation sites were visualized along the *env* sequence with the N-glycosite tool (170), both on the Los Alamos website. For those infections that were not previously classified as single or multivariant transmissions, full-length plasma *env* sequences were used to predict multiplicity of infection using the Poisson-fitter tool (171) on the Los Alamos website, the phylogenetic trees, and highlighter plots generated.

2.9 Cloning of isolate *envelope* genes

An *env* SGA which was representative of the majority variant identified in the screened isolate sequences was selected for cloning. Where only one isolate sequence was obtained, that variant was cloned. Where two isolate sequences were obtained for the participant, the sequence which had the fewest number of nucleotide changes to the derived transmitted/founder sequence of the plasma sequences was selected for cloning. Second-round bulk amplification of the selected first round PCR products was performed in four replicates. The cycling conditions and reagents were

identical to the second round amplification described in section 2.8; however, a different forward primer was used to introduce the 5' CACC tag required for directional cloning; that is, EnvA-Rx (5'-CACCGGCTTAGGCATCTCCTATAGCAGGAAGAA-3'). The four replicate reactions were pooled and purified using the Qiagen MinElute PCR Purification kit (Qiagen, Venlo, Netherlands). The size and integrity of the resultant product was confirmed as ~3kb by gel electrophoresis through a 1% agarose gel. The following was mixed and loaded into each well: 2µL PCR product added to 1µL 6X loading dye containing GelRed and 3µL ddH_2O. Bands were visualized with the UVIpro Silver gel documentation system (UVItec, Cambridge, UK). The amount of DNA in the purified PCR product was quantified using a NanoDrop 2000 (Thermo Scientific, MA, USA) in order to determine the volume required for the cloning reaction.

The pcDNA™3.1 Directional TOPO® Expression Kit (Invitrogen) was used for directional cloning of *env* genes. The system uses a topoisomerase-linked linearized mammalian expression vector. The topoisomerase binds to the 5'-CACC-3' tag sequence introduced on the 5' end of *env* amplicon to ligate it into the plasmid. The gene of interest is inserted downstream of a cytomegalovirus (CMV) promoter which ensures constitutive expression of the gene at high levels in mammalian cells. Each cloning reaction was set up in a 0.2mL tube with reagents as follows: 10ng of the desired *env* PCR product in a volume of 0.5 to 4µL, 1µL salt solution, 1µL TOPO® vector and sterile ddH_2O to a final volume of 6µL. This was mixed gently and incubated at room temperature for 20 min and then placed on ice.

Next, one Shot® Stbl3™ chemically competent *E. coli* cells (Invitrogen) were thawed on ice and transformed with the obtained *env* plasmids. Briefly, 5µL of each TOPO® cloning reaction was added to the cells, mixed gently and incubated on ice for 30 min. The transformation reactions were then heat shocked in a 42°C water bath for 30s without shaking and transferred to ice for 2min. Thereafter, 250µL Luria-Bertani medium (appendix 1) was added to each vial of cells. The vials were placed in a shaking incubator (225 rpm) for 1 hour at 37°C. After incubation, 200µL of each bacterial culture was spread onto a pre-warmed LB agar plate (Appendix 1) containing 100 mg/mL carbenicillin (Sigma-Aldrich) for positive selection of transformants. The plates were incubated at room temperature until the appearance of colonies two- to three days later.

At least eight colonies per cloning reaction were screened by colony PCR to confirm whether the desired insert was present. Colony PCR was performed in a 96-well plate format using the T7 forward (5'-TAATACGACTCACTATAGGG-3') and Rev 15 reverse (5'-ACTTTTTGACCACTTGCCACCCAT-3') primers. The final concentrations of reagents in each reaction were as follows: 1X SuperTherm Buffer, 2mM magnesium chloride ($MgCl_2$), 1mM each

dNTPs, 0.3 µM of each primer and 0.015 U/µL SuperTherm *Taq* DNA polymerase. Cycling conditions were as follows: 94°C for 3 min, then 35 cycles of 94°C for 15s, 55°C for 45s and 72°C for 2.5 min, and a final elongation step of 72°C for 7min. After 1% agarose gel electrophoresis as previously described, colonies that were identified as having the desired insert were used to inoculate 5mL LB broth containing 100 mg/mL carbenicillin which was incubated overnight (<16h) in a 32°C shaking incubator at 225 rpm. Bacteria from 4mL of the overnight cultures were pelleted at 9600 x g in a Heraeus™ Pico™ 21 microcentrifuge (Thermo Scientific) for 3 min at room temperature. After removal of all medium from the pellet, plasmid DNA was extracted using a QIAprep Spin Miniprep Kit (Qiagen). DNA was eluted in 50µL final volume of sterile ddH_2O and quantified using a NanoDrop 2000. The remaining 1mL bacterial culture was added to 1mL sterile glycerol to obtain 50% glycerol stocks which were stored at -60°C.

2.10 Generation of pseudovirus stocks

In order to identify whether clones were functional, a small-scale test for function was carried out in 96-well microtiter plates. PSVs were produced by co-transfection of HEK293T cells with an *env* clone and a plasmid containing an HIV-1 subtype B genome which has an *env* deletion, pSG3$^{\Delta env}$, as previously described (158, 172). In this way all PSVs produced had the same proteins except for Env which was participant-specific. The pSG3$^{\Delta env}$ reagent was obtained through the NIH AIDS Reagent Program, Division of AIDS, NIAID, NIH from Drs. John C. Kappes and Xiaoyun Wu (158, 172). HEK293T cells were seeded at 2 x 10^4 cells/well into a 96-well round-bottom plate in a final volume of 100µL D10F GM. For each clone, 0.15µg plasmid DNA was added to 0.3µg pSG3$^{\Delta env}$ backbone DNA and the volume adjusted to 15µL with sterile ddH_2O. PolyFect transfection reagent (2mg/mL, QIAGEN) was diluted in DMEM and 50µL added to each plasmid DNA mix such that the mass ratio of Env plasmid DNA:backbone-DNA:PolyFect was 1:2:26 (in this case 4µg per transfection). This was mixed by vortexing for 5s and then incubated at room temperature for 15 min. Each mix was subsequently added directly to the wells containing HEK293T cells up to a total well volume of 165µL. This was incubated for 48h in a 37°C humidified incubator.

Next, TZM-bl cells were seeded at a density of 1 x 10^4 cells per well in a final volume of 100 µL of GM with DEAE-dextran added at a concentration of 40 µg/mL. 50µL Pseudovirus-containing supernatant from the transfection plates was added directly to wells containing cells and DEAE-dextran in duplicate to a final volume of 150µL. After 48h incubation, the supernatant was removed, SteadyLite and luminometer readings obtained as previously described.

Functional clones were sequenced as described in section 2.8 and the clone with the fewest number of non-synonymous substitutions from the sequence selected for cloning was chosen to produce large-scale stocks for PSVs. HEK293T cells were seeded at a density of 3 x 10^6 cells per T75 flask in 10mL D10F and incubated overnight in a 37°C humidified incubator. The next day, pSG3$^{\Delta env}$ backbone and *env* clones were mixed and incubated as described previously using 8µg of backbone plasmid, 4µg of *env*-containing plasmid and 120 µg of PolyFect reagent (mass ratio of 1:2:30) per transfection in a final volume of 650µL of D10F. During incubation of the DNA with the PolyFect, the medium in each T75 flask containing cells was replaced with 15mL fresh D10F after which the DNA-PolyFect mix was added to the flasks. After 48h incubation, the supernatant was removed, aliquoted and stored at -80°C. This was replaced with 7mL fresh medium which was removed and stored as aliquots 24h later to obtain a second harvest. Determination of Gag p24 concentrations in each stock of PSVs was determined as described previously by both in-house and commercial ELISA. PSVs from the first harvest were used for all assays that followed.

2.11 Entry efficiency assays

Entry efficiency assays were performed as described for titration experiments above with the difference being that no DEAE-dextran was added to the experiments. Briefly, TZM-bl cells were seeded at a density of 1 x 10^4 cells per well in a final volume of 100µL of GM without DEAE-dextran. Three-fold dilutions of PSV stocks were made by diluting neat stocks in D10F GM. 100µL of neat supernatant and dilutions were then added to the individual wells in triplicate to a final volume of 200µL per well. After 48h incubation, the SteadyLite protocol which was described earlier was carried out. RLU measurements for each PSV were normalized on the p24 input (commercial ELISA) in each well to obtain entry efficiency measurements. Average RLU/pg p24, which was used as a measure of entry efficiency, was calculated across all replicate wells for a particular virus incorporating all dilutions within the linear range for each plate.

2.12 Inhibition assays using isolates and pseudoviruses

TZM-bl cells were seeded in a 96-well tissue culture-treated microtiter plate at a density of 1 x 10^4 cells per well in a final volume of 100µL of D10F GM with DEAE-dextran added to a final concentration of 40 µg/mL. Five-fold serial dilutions of various inhibitors were made. The inhibitors used in viral isolate inhibition assays were maraviroc (CCR5 antagonist), T20 (fusion

inhibitor), tenofovir (nucleotide reverse transcriptase inhibitor), JM-2987 (CXCR4 inhibitor), PSC-RANTES (CCR5 competitive inhibitor) and SK3 (monoclonal anti-CD4 antibody). 50µL of each dilution of inhibitor was added to wells in duplicate and plates were incubated at room temperature for 30 min. Thereafter, virus (or PSV) dilutions were added to wells such that the multiplicity of infection in each well was 200 $TCID_{50}$. Microtiter plates were incubated for 48h after which 120µL of supernatant was removed from each well and replaced with 75 µL SteadyLite. After 5 min incubation at room temperature in the dark, the contents of each well was mixed by pipette action and transferred to an opaque white 96-well microtiter plate. Luminometer readings were obtained as described in section 2.5. Antiviral activity was expressed as the percentage of viral inhibition in experiment wells compared to untreated controls wells and subsequently plotted against the compound concentration. Nonlinear regression analysis was used to calculate the EC_{50} based on at least three independent measurements. Regression analysis was performed using GraphPad Prism software, version 5.03, for Windows (GraphPad Software, CA, USA).

2.13 Statistical analysis

All *P*-values were calculated using STATA (Special Edition 11.0). Graphs were generated using GraphPad Prism. The Shapiro-Wilk test for normality was applied to each data set as well as a test for equal variances prior to calculation of the *P*-values. For all comparisons where the data was normally distributed, the *P*-values were calculated using a two-sample t-test. Where the data was not normally distributed, or had unequal variances despite being normally distributed, a non-parametric test was employed as with cases where the sample size in each group was <30. Where multiple comparisons were made, the *P*-value cut-offs were adjusted using a Bonferroni correction. Where a parametric test was employed, the 95% confidence interval (CI) was reported in the results. Where a non-parametric test was used, the interquartile range (IQR) was reported. Due to the small sample size all correlations were performed using a Spearman correlation (CI = 95%).

3. Results

3.1 Cohort and isolate description

This study characterized HIV-1 from participants who seroconverted while participating in the CAPRISA 004 1% TFV microbicide study, and who were enrolled into the CAPRISA 002 acute infection cohort. To capture features associated with the virus that founded clinical infection (transmitted/founder or T/F), only participants who were enrolled within 3 months of estimated date of infection were included. Participants assigned to TFV gel use (n= 24) were matched with PLB user controls (n=24) according to time post-infection, as well as the presence or absence of protective HLAs in both individuals of each pair. Due to the relatively small number of participants who seroconverted while enrolled in the CAPRISA 004 trial, participants could not be matched according to HLA type. Appendix 3A gives a description of the 24 matched pairs.

Of the 48 participants selected, viruses from 39 participants were successfully isolated on PBMCs (81%). Genotypic characterisation of *env* was performed to determine if these viruses were a good representation of viruses circulating *in vivo* (see section 3.2). A subset of 28 viruses (14 pairs; table 3.1) was selected for inhibition assays to evaluate whether phenotypic differences exist between viruses from the TFV and PLB arms, and whether characteristics correlate with predictors of disease progression in this study population. The subset was selected based on detectable levels of TFV in plasma samples taken at the study visit closest to the estimated date of infection. Of this subset, *env*s from 20 participants were cloned and entry efficiency was determined. For the 39 viruses isolated, VL at time of isolation did not differ between trial arms (P= 0.2567; Wilcoxon rank sum test for independent samples) with a median VL of 5.06 and 4.78 log copies/mL in the PLB and TFV arms, respectively.

Table 3.1. Participant information for the subset of matched TFV and placebo participants used for comparison of Env function

TFV arm participant	VL at isolation ǂ	VL at 3 months post-infection	Set-point VL	Weeks post-infection	TFV present ǂ	Placebo arm participant	VL at isolation ǂ	VL at 3 months post-infection	Set-point VL	Weeks post-infection	Protective HLA? ϕ
CAP320	37 500	30 550	1 607	5	Yes	CAP345**	130 000	271 500	222 000	6	No
CAP325*	127 000	66 350	10 261	3	No	CAP327*	91 600	250 500	224 579	3	No
CAP343	130 000	47 200	35 748	7	Yes	CAP317	351 000	534 000	682 000	7	No
CAP360	80 600	11 460	8 628	3	Yes	CAP301	33 500	3 670	<400	4	Yes
CAP363*	97 500	96 050	4 617	5	No	CAP292*	458 000	43 733	256 085	5	No
CAP367	3 360 000	428 500	142 970	3	No	CAP326	31 500	16 300	4 329	3	No
CAP283**	12 900	14 300	74 445	7	No	CAP306	141 000	38 900	19 530	8	Yes
CAP291	14 300	12 000	2 507	11	No	CAP349	950 000	732 000	429 247	11	No
CAP318	22 300	25 700	46 632	5	No	CAP307	174 000	107 000	147 459	5	No
CAP323	22 000	2 193	3 044	3	Yes	CAP315**	108 000	65 400	793	3	Yes
CAP334	21 200	3 150	8 077	6	Yes	CAP311	18 600	1 390	855	6	No
CAP348	305 000	112 267	21 581	8	Yes	CAP287	13 200	52 000	9 174	8	No
CAP370	28 800	8 570	12 237	5	Yes	CAP331	12 700	1 550	8 574	6	No
CAP375	192 000	110 900	20 117	5	Yes	CAP357**	14 900	7 765	22 588	7	No

VL reported as copies/mL

ǂ VL in the plasma sample from which viruses were isolated

ǂ TFV detected in plasma at the time-point used for virus isolation

ϕ Protective HLAs present or absent in both participants of the TFV-PLB pair

*Participant not selected for cloning or **cloning of *env* was not successful

VL set-point was defined as the geometric mean of HIV-1 plasma VL measurements from three consecutive study visits around 12 months post-infection in ART-naïve participants (the visit closest to 12 months post-infection as well as one visit preceding and one immediately following the 12-month visit). In participants who initiated ART before 12 months post-infection, set-point was defined as the last available VL measurement before ART initiation. ART was initiated according to National Treatment Guidelines at the time; which was a CD4+ count of <350 cells/μL. Two participants initiated ART prior to 12 months: CAP317 (PLB arm) and CAP375 (TFV arm) initiated ART at 6.3 months and 8.5 months post-infection, respectively. In the subset of 28 viruses selected for viral inhibition assays, VL at isolation, 3 months post-infection and set-point did not differ significantly between trial arms (P= 0.7304, 0.6133 and 0.4082, respectively; Wilcoxon rank sum test for independent samples).

3.2 Isolates are genotypically representative of plasma viruses

In order to demonstrate that isolates were representative of plasma viruses, the *env* gene isolate sequences were compared to sequences generated from plasma at the same time-point post-infection for 34 of the 39 isolates. A total of 105 *env* gene sequences were PCR-amplified using a single genome amplification (SGA) approach and sequenced (median= 3, range= 1; 5 sequences per participant). No more than three 'double peaks' per *env* sequence were tolerated in sequence chromatograms across the entire length of *env* for inclusion in all analyses. Full-length (n= 16 participants) and partial (n= 8 participants) *env* sequences from plasma viruses were available for the same time-point for 24 of these individuals (10 TFV and 14 PLB). These *env* sequences were generated internally (R. Thebus, C. Rademeyer, J. Marais, Z. Valley-Omar; personal communication) (median= 6, range= 1; 26 sequences per participant).

Isolate *env* sequences were compared to the plasma viruses for each of the 24 participants. To include as much sequence data as possible in the comparisons, alignments were truncated to the length of the partial plasma sequences. The two truncated alignments included one alignment from the start of *env* to the middle of gp41 (sequences between 1911- 1979 bp; HXB2 1- 1443) (n= 22 participants) and one that only included the V3V5 (sequences between 603- 642 bp; HXB2 886- 1407) regions (n= 24 participants).

For each participant, the plasma consensus (T/F) *env* sequence was derived which was assumed to represent the transmitted variant *in vivo*. The genetic distance of the isolates and plasma viruses to the plasma consensus was measured to determine if the isolate *env* variants were more

diverse than expected compared to the diversity *in vivo*. When the maximum DNA distance of the plasma consensus sequence was compared in a pairwise manner to plasma and isolate sequences for each participant (table 3.2, columns six and seven), no statistically significant difference was found (P= 0.1765; Wilcoxon signed-rank test for paired observations). However, there was significantly greater maximum intra-participant pairwise DNA distance within plasma-derived *env*s (table 3.2, columns eight and nine) compared to isolate-derived *env*s (P= 0.0016; Wilcoxon signed-rank test). Together, this implies that although viral isolation does not capture the full diversity *in vivo*, isolate sequences are a good representation of viruses *in vivo*.

Nucleotide highlighter plots (fig 3.1 and appendix 3B) allowed for closer inspection of the number of synonymous versus non-synonymous mutations in all isolate- and plasma-derived *env*s. Figure 3.1 shows examples of highlighter plots for participants whose sequences matched the plasma consensus sequence (fig 3.1a), those that have random changes compared with the plasma sequences (fig. 3.1 b and c), and those whose isolate sequences have shared mutations which were not detected in plasma variants (fig 3.1d). The maximum number of non-synonymous mutations in plasma and isolate sequences compared with the plasma consensus (table 3.2, columns four and five) revealed no statistically significant difference between the two (P= 0.2872; Wilcoxon signed-rank test). There were 12 participants for which non-synonymous mutations were present at the same position in all of the isolates *env*s sequenced which were not present in the plasma sequences. The positions of these shared non-synonymous mutations and the regions in which they occur are listed in appendix 3C.

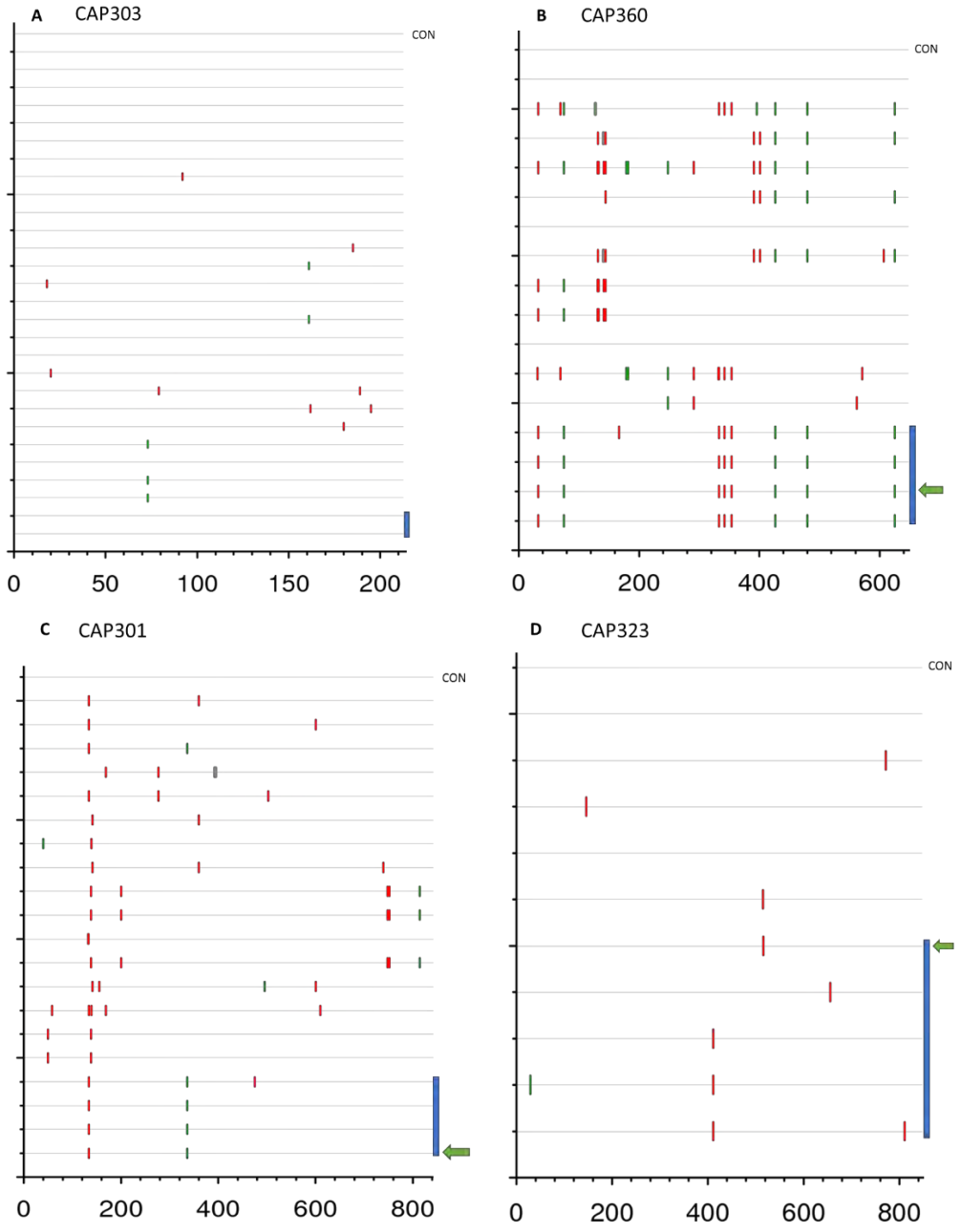

Figure 3.1. Highlighter plots comparing plasma and isolate *env* amino acid sequences for four participants. Highlighter plots show the synonymous (green vertical bars) and non-synonymous (red vertical bars) nucleotide substitutions for all sequenced *env* variants in plasma and isolate samples (grey vertical lines represent deletions). Each *env* sequence is represented by a grey horizontal line. Isolate *env*s are denoted by a blue bar on the right of the sequences. Sequences were aligned to the plasma consensus sequence representing the T/F *env* sequence (labelled 'CON' in each figure). *env*s with a green arrow to the right of them were selected for cloning. Numbers on the x-axis represent the codon number. Highlighter **plot A** is for the CAP303 alignment which was truncated to the V3V5 region and is one case where the sequenced isolate *env*s are identical to that of the plasma consensus. **Plots B and C** show CAP360 (truncated to gp41) and CAP301 (full-length *env*) alignments, respectively, which represent participants with low diversity in their isolates and where the isolate *env*s have minor changes compared to variants in the plasma. **Plot D** represents CAP323, a participant with greater diversity in the isolate *env* sequences (full length) and where the isolates represent a mixture of variants sequenced from plasma and those not seen in the plasma sequences.

Table 3.2. A comparison of plasma and isolate *env* sequence diversity for each participant.

Participant ID	Arm	Length of *env* alignment	Max. no. of non-synonymous mutations		Max. DNA distance from T/F		Max. DNA distance within group*	
			Plasma seqs	Isolate seqs	Plasma seqs	Isolate seqs	Plasma seqs	Isolate seqs
CAP303	PLB	V3V5	2	0	0.003	0.000	0.010	0.000
CAP327	PLB	Full-length	1	0	0.001	0.000	0.003	-
CAP311	PLB	Full-length	1	0	0.001	0.000	0.003	0.000
CAP331	PLB	Full-length	2	1	0.001	0.000	0.005	0.000
CAP301	PLB	Full-length	5	2	0.002	0.001	0.005	0.000
CAP323	TFV	Full-length	1	2	0.000	0.001	0.000	0.002
CAP315	PLB	Mid-gp41	4	2	0.003	0.001	0.008	-
CAP334	TFV	Full-length	3	1	0.002	0.001	0.008	0.002
CAP370	TFV	Full-length	2	1	0.001	0.001	0.003	0.000
CAP320	TFV	Full-length	3	3	0.001	0.002	0.003	-
CAP343	TFV	Mid-gp41	2	3	0.002	0.002	0.006	0.002
CAP317	PLB	Mid-gp41	3	3	0.003	0.002	0.005	0.000
CAP363	TFV	Mid-gp41	3	3	0.002	0.002	0.003	0.000
CAP292	PLB	Full-length	1	1	0.003	0.002	0.007	0.002
CAP326	PLB	Full-length		4	-	0.002	-	0.000
CAP307	PLB	Full-length	2	3	0.002	0.002	0.005	0.000
CAP314	TFV	Mid-gp41	4	3	0.003	0.003	0.008	0.000
CAP345	PLB	Full-length	3	7	0.001	0.003	0.000	-
CAP308	PLB	Full-length	4	5	0.002	0.003	0.010	0.002
CAP360	TFV	Mid-gp41	8	5	0.010	0.005	0.037	0.000
CAP287	PLB	Full-length	7	9	0.003	0.005	0.006	0.010
CAP357	PLB	Full-length	0	4	0.001	0.005	0.000	0.002
CAP375	TFV	Full-length	22	21	0.016	0.014	0.022	0.055
CAP348	TFV	Mid-gp41	21	17	0.017	0.015	0.053	0.028

*analysed using the V3V5 region only for all sequences; mid-gp41 refers to sequences that start at the start codon of *env* and end in the middle of gp41

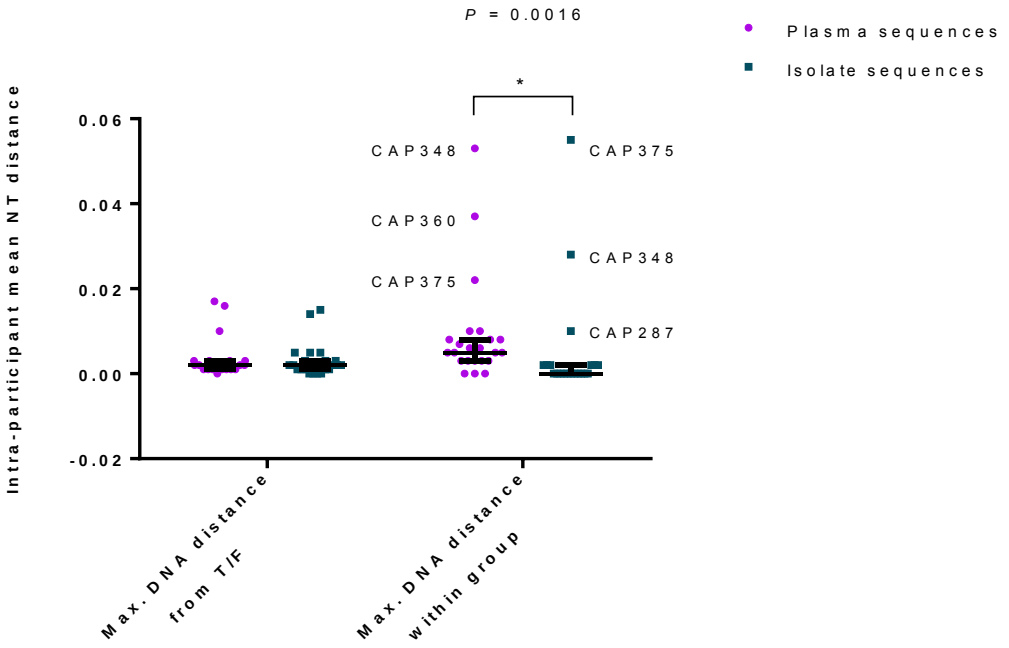

Figure 3.2. Diversity of plasma and isolate *env*s compared firstly to the transmitted/founder *env,* and secondly to other sequences within the same group. *envs* were evaluated using an alignment truncated to the V3V5 region of *env*. The intra-participant diversity was calculated in a pairwise manner for both comparisons. In the first case, each plasma- or isolate-derived *env* was compared with the plasma consensus *env* and the maximum distance was used for comparison for each. In the second case, DNA distance was calculated in a pairwise manner within the group of isolates or plasma *env*s for each participant. Each point represents the mean of DNA distances obtained for all sequences from a given participant. Black bars represent the median and IQR. The PID's of outlying points are indicated on the figure. *P*-values were calculated using a Wilcoxon signed-rank test for paired observations in STATA.

Phylogenetic analysis was performed to assess the relationship between the plasma and isolate sequences. Due to differences in the length of plasma sequences, three comparisons were made: one from a full-length *env* alignment (fig. A3D.1; appendix 3D); and two truncated alignments (HXB2 amino acids 1- 481) (fig. A3D.2; appendix 3D), and V3V5 (HXB2 amino acids 296- 469) regions (fig 3.3). All results gave quantitatively similar results with isolate sequences clustered with plasma sequences for the same participant and each participant's set of sequences forming a clade. The V3V5 analysis incorporated all 24 participants and is illustrated (fig. 3.3).

The isolate sequences for 18 of the 24 participants had low diversity and dispersed within the plasma sequences indicating that the *env* diversity of the isolates is similar to that in plasma. Of these 24 individuals, 15 had previously been classified as infected with a single variant, while two

(CAP348 and CAP360) were classified as having multivariant infections (138), and seven remained unclassified.

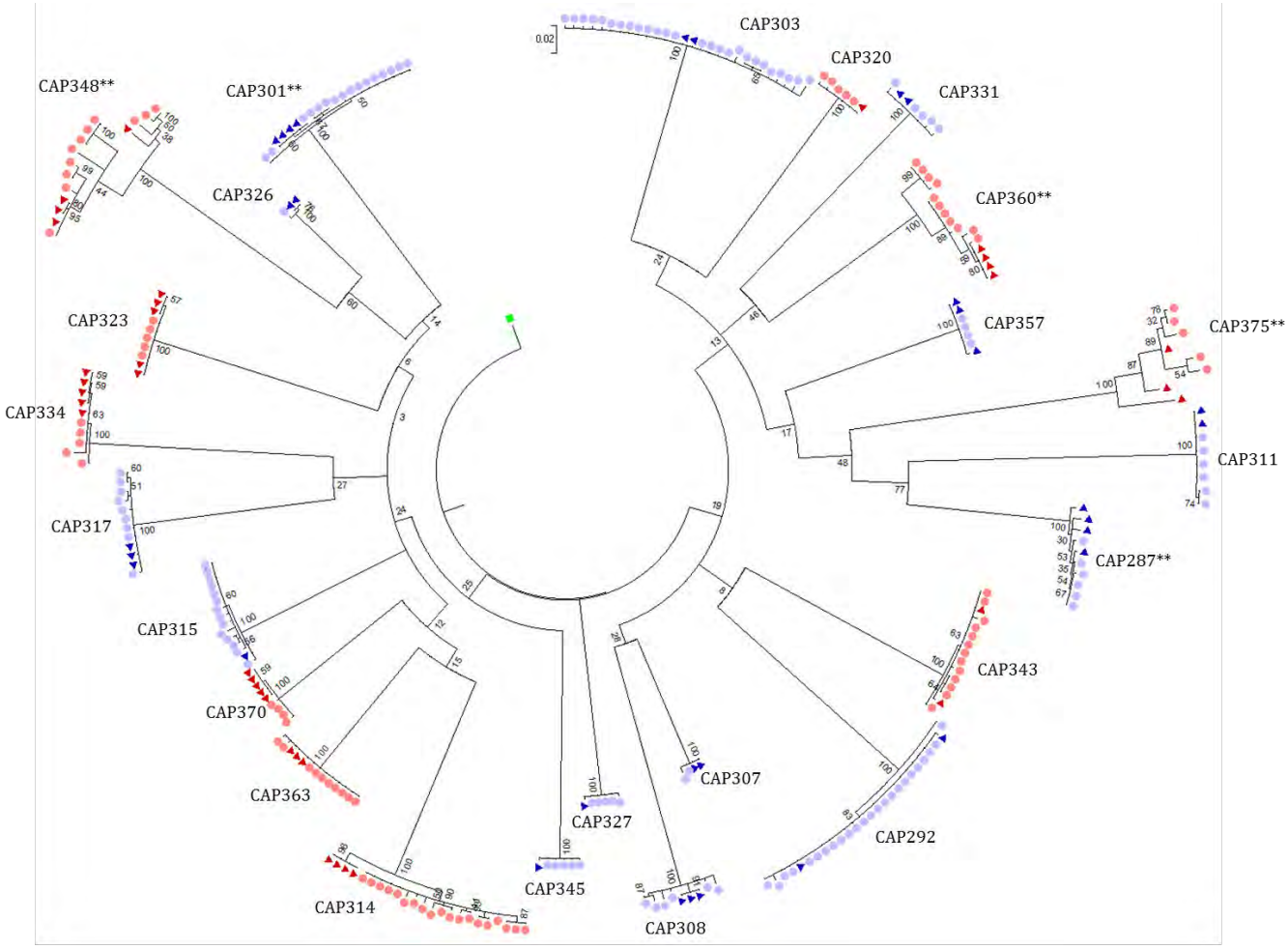

Figure 3.3. A Maximum likelihood tree of HIV-1 *env* region V3V5 plasma- and isolate-derived sequences from the same time-point post-infection in each participant. Nucleotide sequences were generated by limit dilution PCR amplification. Sequences from 24 participants from both arms of the trial (PLB depicted in blue, TFV in red) were aligned to a CAPRISA 002 cohort consensus and a maximum likelihood tree was generated. Triangles were used to represent isolate sequences while circles were used to represent plasma sequences. Sequences were truncated to the V3V5 region to include plasma-derived *env* sequences which were already available for comparison. This tree was generated using MEGA6. **denotes participants who were identified as having established infection as a result of multivariant transmission. The Subtype C acute consensus sequence was derived from available CAPRISA 002 *env* plasma sequences (n= 592 SGAs) generated from participants infected for less than 3 months.

Viruses from CAP348, CAP360 and CAP375 had a high diversity typical of multivariant transmissions (denoted by the suffix ** adjacent to participant ID's on each of the trees).

Multiplicity of infection in this cohort was previously identified by Valley-Omar *et al* (138) who identified CAP348 and CAP360 as multivariant transmissions using a heteroduplex tracking assay (HTA). However, CAP375 was identified as a high diversity, single variant transmission by the same method. It is clear from the highlighter plot for CAP375 in appendix 3B, in addition to the phylogenetic tree, that CAP375 is a multivariant transmission and thus was misclassified by HTA. The isolate sequences from multivariant transmissions show the presence of *env*s from all variants in plasma with the exception of CAP360, which appears to be a single variant transmission either because of a bottleneck created in tissue culture- where one variant grew preferentially, or it could be a result of under-sampling of isolate sequences.

There were seven participants in this study whose multiplicity of infection was not previously classified. These were classified in this study (using plasma-derived full-length *env* sequences only) by observing the pattern of non-synonymous mutations on the highlighter plots and determining whether sequence diversity followed a star phylogeny using the Poisson-Fitter tool (171) on the Los Alamos database (table 3.4). For single variant transmission, we expected a low intra-participant diversity, a star-like phylogeny and Poisson distribution of Hamming distances. We also expected the clinically estimated days post-infection to fall within the estimated timeframe of infection based on the estimated time from the most recent common ancestor (MRCA). Based on this definition, four infections (CAP326, CAP331, CAP345 and CAP357) were classified as single variant infections. Conversely, sequences were classified as multivariant transmissions if there was high genetic diversity with a multimodal distribution of pairwise Hamming distances, a non-star-like phylogeny and/or if one or more sequences were noticeably different from others in plasma. Based on these criteria, two sequences were classified into this group (CAP287 and CAP301).

Table 3.4. Genetic complexity of plasma viruses classified for participants who had not been previously identified as being infected by a single or multiple founder variants

Participant ID	Trial Arm	Mean hamming distance	Estimated days post-infection	Days post-infection (clinical)	Max. DNA distance (%)	Star phylogeny	Single/Mutivatiant infection
CAP287	PLB	6	99 (19, 179)	58	0.4	No	Multiple
CAP301	PLB	6	100 (80, 120)	25	0.5	No	Multiple
CAP311	PLB	2.7	44 (N/A)	42	0.2	No	Undetermined**
CAP326*	PLB	2.3	44 (14, 73)	23	0.3	Yes	Single
CAP331	PLB	3.4	56 (35-78)	43	0.2	Yes	Single
CAP345	PLB	2	33 (-5, 71)	43	0.2	Yes	Single
CAP357	PLB	1	17 (1,32)	25	0.1	Yes	Single
CAP375 (reclassification)	TFV	-	-	36	2.3	-	Multiple

*The plasma sequences used to classify this variant were variants present at the time of enrolment; one week prior to the plasma sample used to isolate the participant's virus
**Sequences had a low diversity amongst plasma SGAs but they did not fit the model of random evolution (a star phylogeny) therefore, multiplicity of infection could not be determined

CAP287, although the estimated date of infection was within the range calculated for date to MRCA, was classified as multivariant due to the presence of a highly diverse second variant represented by one out of six plasma sequences. CAP301 was classified as multivariant due to its maximum DNA distance between sequences being high and also the estimated date of infection according to Poisson-fitter being 75 days after the clinical estimate. The highlighter plot of CAP301 also shows the presence of a closely related, but distinct, second variant. CAP311 remains unclassified because even though it does not follow a star phylogeny, the number of sequences and the low diversity does not allow multiplicity of infection to be determined with certainty.

When these results were put together with those published (138), it was found that 17 out of 21 (81%; 95% CI, 63%- 99%) women in the PLB arm were infected with a single virus, compared to 16 out of 22 (73%; 95% CI, 53%- 93%) women in the TFV gel arm (P= 0.721; following a two-

tailed Fisher's exact test). This result supports the previous finding which showed that TFV gel did not affect the genetic bottleneck (138).

3.3 Genotypic characteristics of *env* do not differ between viruses from the TFV versus the placebo arm

Variable loop characteristics of viral envelopes are determinants of cell tropism and entry, and may undergo selection during transmission, with subtype C viruses from acute infection having shorter loop lengths and fewer glycosylation sites than *env*s from viruses in chronic infection (24, 39). Variable loop charge has been implicated in a number of functions depending on the region being investigated. For example, V1, V2 and V3 charge plays a role in fusion capacity and coreceptor tropism (173, 174). In addition, isolates from end-stage disease with enhanced fitness displayed a higher net charge of gp120 (175). We hypothesized that if TFV affected the barrier to infection, then these characteristics may differ between trial arms. Examination of altered loop length, charge or predicted sites of glycosylation between viruses of the TFV and PLB arms (fig. 3.4) showed that there was no significant difference between the trial arms for any of the characteristics investigated, including loop length, glycosylation, or charge ($P > 0.05$; two-tailed t-test or a two-tailed Wilcoxon rank-sum test for independent samples depending on the distribution of the data for each characteristic in each loop).

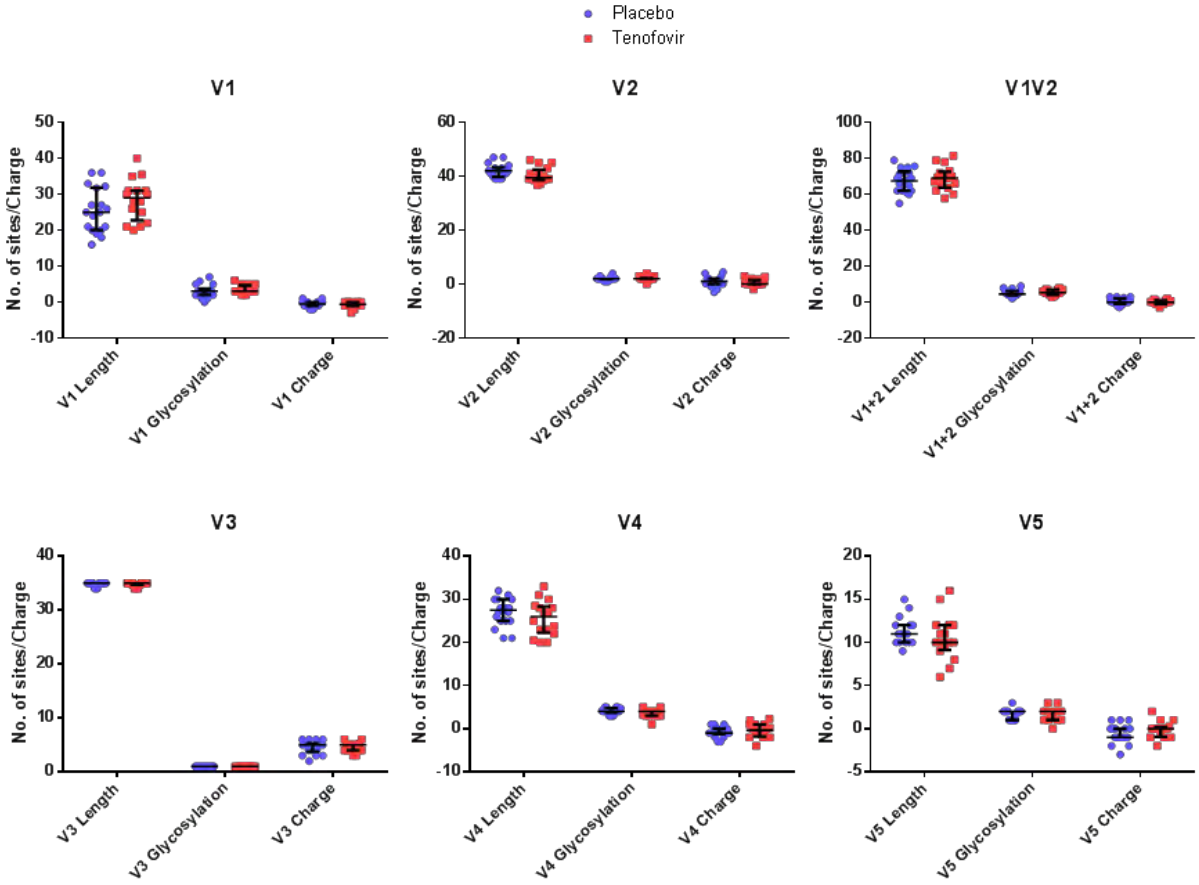

Figure 3.4. Variable loop characteristics of *envs* from PLB and TFV arm isolates do not differ. For a given characteristic within each variable loop, the average for all isolates sequenced for each participant is represented as a point in a column. The median and IQR is represented by the black bars overlapping points in each column. Statistical significance was determined by performing either a two-tailed t-test or a two-tailed Wilcoxon rank-sum test for independent samples in STATA (depending on the distribution of the data for each characteristic in each loop). All P-values were greater than the significance cut-off of 0.05.

Previously it has been shown that transmission selects for viruses which are more like consensus in amino acid identity (of Gag, Pol and Nef protein sequences) compared to chronic variants (50). Consensus-like variants are thought to have a higher *in vivo* fitness as they represent viral variants which are able to replicate to a majority in infected individuals, although they have not been shown to replicate more efficiently *in vitro* (48). Furthermore, factors that increase or decrease the transmission barrier such as female-to-male transmission, the presence of genital ulcers or inflammation, were shown to increase or decrease this selection bias for consensus-like variants (50). To identify whether breakthrough viruses from the TFV arm were more consensus-like than those of the PLB arm in Env, isolate sequences were compared to the CAPRISA 002 subtype C consensus derived from SGAs (n=592) generated from participants infected for less than 3 months (obtained from M-R. Abrahams, personal communication). Pairwise distances

between isolate sequences and the CAP 002 consensus indicate that there is no difference between trial arms in the nucleotide or amino acid distance from consensus of isolate *env* sequences (fig 3.5; two-sample t-test on data with equal variances). On the contrary, a trend can be observed for viruses from the TFV arm to be less consensus-like than those in the PLB arm.

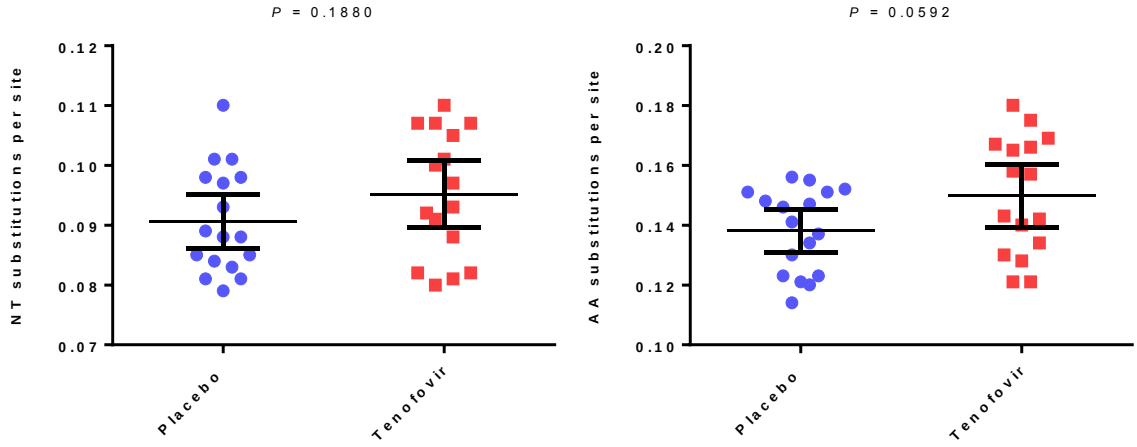

Figure 3.5. The distance to consensus does not differ between TFV and PLB arm isolates. Isolate *env* sequences were aligned to a CAPRISA 002 consensus sequence and the pairwise nucleotide (left) and amino acid (right) distances were calculated using MEGA6. The average of all distances for a given participant's sequences is plotted above with each participant represented by either a blue circle (PLB) or a red square (TFV). Black bars represent the mean with the 95% CI. *P*-values were calculated using a two-sample t-test on data with equal variances in STATA.

3.4 Phenotypic characteristics of Env do not differ between viruses from the TFV versus the placebo arm

Viral fitness is defined as the ability of a virus to survive and replicate within a given setting and fitness can be conferred by an increase in efficiency in any of the steps of the viral replication cycle, which would in turn increase its replicative capacity [reviewed in (176)]. Inhibition assays are a convenient way of measuring viral dependence on a particular step of the replication cycle by blocking that step. This method can uncover functional differences between viruses in relation to one another. Hence, we investigated the effect of various inhibitors on virus replication. Inhibition sensitivities of the isolates were determined using the effective inhibitory concentration, that is, the concentration at which viral replication, measured as RLU, was inhibited to 50% of growth in the absence of the drug (EC_{50}).

Susceptibility to TFV

The CAPRISA 004 trial found no evidence of TFV resistance based on genotypic data (95, 118). However, Lehman *et al*. (177) postulate that if TFV is present in the mucosa after participants became infected (pre-seroconversion) then viruses may have gained polymorphisms which allow it to replicate better in the face of sub-optimal levels of the drug. Here, we inhibited the replication of isolates in tissue culture using TFV, firstly, to confirm that TFV arm viruses are not phenotypically resistant to TFV, and secondly, to determine if a difference in susceptibility was associated with women who became infected while using TFV gel.

Resistance to TFV was preciously defined as a 0.4 to 2.2-fold change in inhibitor sensitivity when compared with that of HIV-1 IIIB (178). All isolates were fully inhibited by TFV (fig. A3E.1 in appendix 3E) with a median EC_{50} of 2872 nM. The two viruses that had the highest EC_{50}s for TFV were CAP292 and CAP307 with EC50s 1.6-fold higher and 1.5-fold higher than the median, respectively. In addition, there was no difference in isolate susceptibility to TFV between study arms (fig. 3.6), with all TFV arm inhibition curves falling within the range of PLB arm inhibition curves. This indicates that there was no phenotypic resistance within our TFV arm isolates.

Susceptibility to entry inhibitors

To investigate if certain phenotypic properties associated with viral entry were enriched in the TFV arm, we assayed viral attachment using CCR5 dependence (non-competitive CCR5 binding) by inhibiting with maraviroc (MVC), CD4 binding affinity with anti-CD4 antibody clone SK3 (referred to as anti-CD4 from here onwards), and CCR5 binding affinity with the use of PSC-RANTES. Fusion capacity was assayed using T20 which prevents fusion of the viral and host membranes. We used JM-2987, a CXCR4 binding inhibitor, to investigate whether any of the isolates could utilize CXCR4 as a coreceptor (see appendix 3D for all inhibition curves).

TFV, PSC RANTES and anti-CD4 all had narrow distributions of EC_{50}'s (fig. 3.6), whereas the distributions of isolate sensitivities to T20 and MVC were wider with ranges of 1.5 nM to 27 nM, and 0.68 nM to 17.37 nM, respectively. There was no difference to any of the inhibitors between isolates between isolates from the different study arms (fig 3.6; Wilcoxon rank sum test for independent observations). All isolates were sensitive to MVC and PSC-RANTES, indicating that they utilized CCR5 as a coreceptor (fig. 3E.3 and 3E.5, respectively; appendix 3E). In addition, none of the viruses displayed susceptibility to the CXCR4 inhibitor JM-2987 (fig. 3E.6; appendix 3E), confirming that all isolates are exclusively R5-tropic.

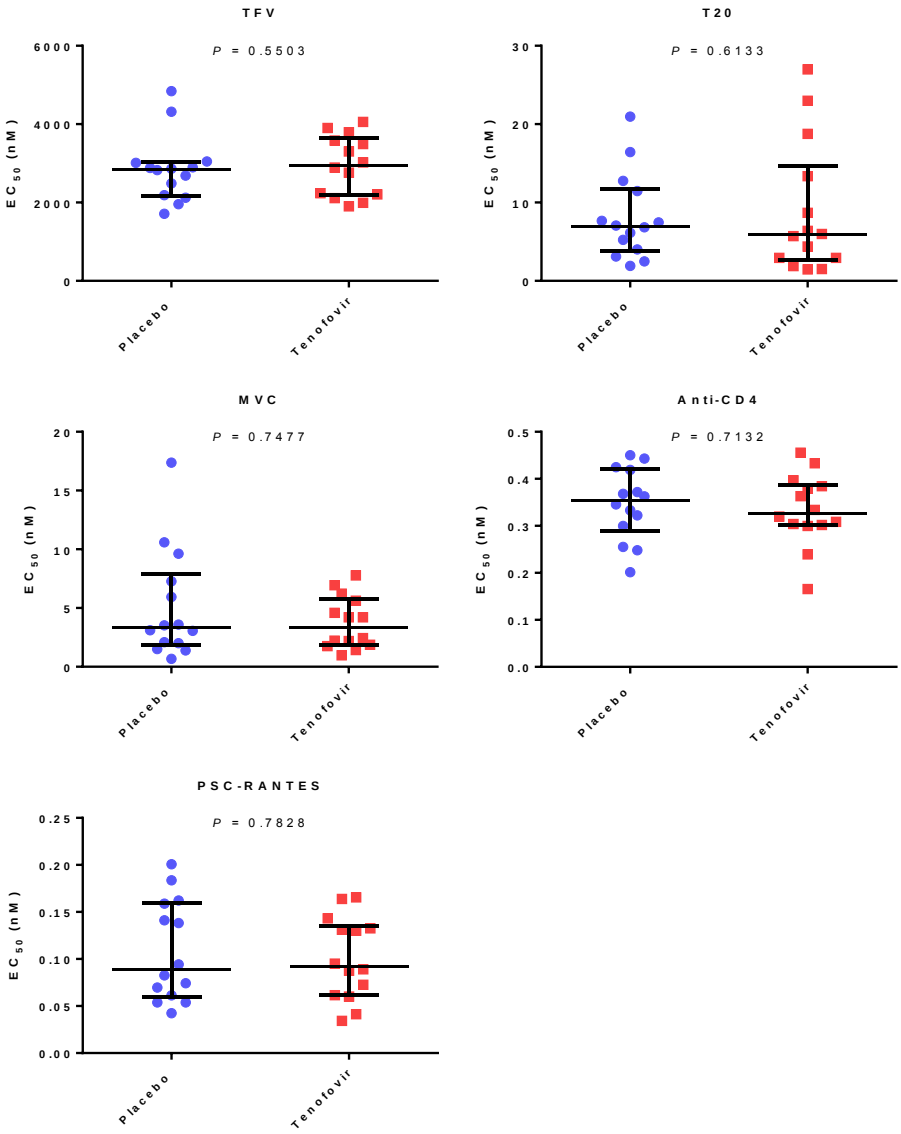

Figure 3.6. Inhibition sensitivities of isolates do not differ between trial arms. Inhibition sensitivities represented as effective inhibitory concentrations (EC_{50}) are represented on the x-axis. Each point on the graph represents an isolate from a given participant. Viruses from the PLB arm are represented as blue circles while those from the TFV arm are represented as red squares. The black bars represent the median and IQR for each group. All *P*-values on this figure were calculated using a Wilcoxon rank sum test for independent observations in STATA.

There are a few outliers on each of the plots (fig 3.6). The isolates with a lower susceptibility to T20 were CAP353 and CAP326 in the PLB arm, and CAP343, CAP320 and CAP325 in the TFV arm. There were three isolates with higher MVC EC_{50}s than all other isolates: CAP292, CAP326 and CAP345, all from the PLB arm. More importantly, two isolates, CAP291 (TFV arm) and CAP292

(PLB arm) exhibited an inhibition plateau at 18% infection and below 10% infection, respectively (fig. 3.7), suggesting that these isolates can still enter cells despite the CCR5 co-receptor being blocked by MVC.

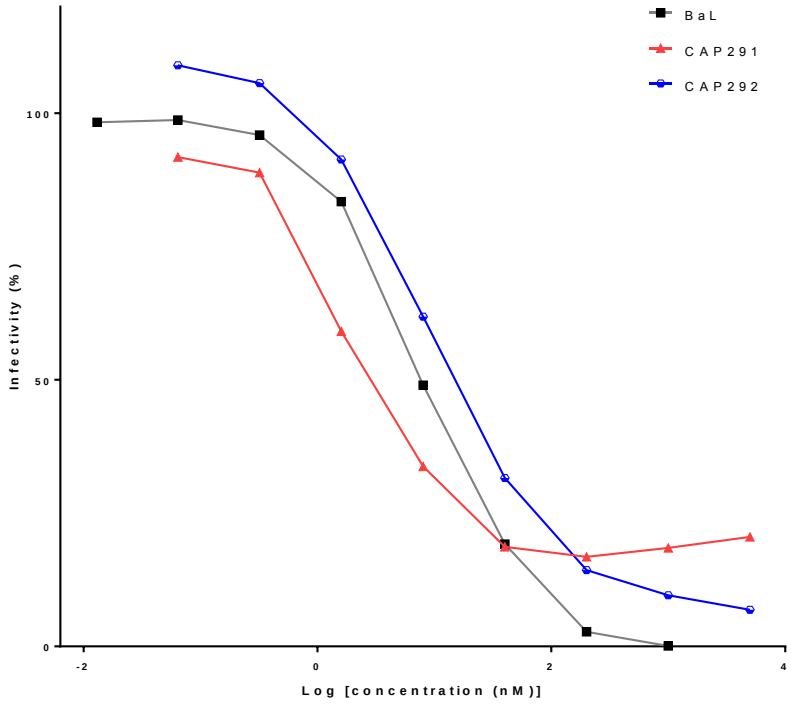

Figure 3.7. Maraviroc inhibition plateaus for CAP291 and CAP292 suggesting that these isolates can still use CCR5 despite the presence of MVC. The graph shows the decrease in the percentage infection (y-axis) by the isolates on TZM-bl cells with increasing MVC concentration (x-axis). CAP291 inhibition is represented by the red curve while CAP292 inhibition is represented by the blue curve. BAL (know R5-tropic isolate) was used as a control virus and is represented in black.

Noticeably, CAP292 and CAP326 were less susceptible to MVC and PSC-RANTES while being more susceptible to anti-CD4 than the median of the isolates from the PLB arm. This implies that these viruses had a greater CCR5 binding capacity and CCR5 affinity, while having a lower CD4 binding affinity than the majority of isolates from the PLB arm. CAP326 was also less susceptible to T20, suggesting that this virus had a greater fusion capacity. CAP325, a TFV arm isolate, was less susceptible to T20 and more susceptible to anti-CD4 inhibition than the majority of TFV arm isolates; indicating that it has a greater fusion capacity and a weaker CD4 binding affinity.

Entry efficiency

To evaluate the role of Env directly, PSVs were constructed which only differed in Env and not in any other viral proteins. The entry of Envs was examined to determine whether they differed between viruses from the two trial arms. For each participant, Env-typed PSVs were generated by cloning the *env* most representative of the majority isolate. In the highlighter plots for each of the participants (figure 3.1 and appendix 3B), the sequences which were selected for cloning are indicated by a green arrow and can be compared in relation to both plasma and isolate sequences. Of the 28 participants selected for phenotypic comparison (14 TFV and 14 PLB), PSVs were produced for 10 participants from the TFV arm and 9 participants from the PLB arm. Since CAP348 was identified as a multivariant infection, two *env* genes were cloned (one representing each transmitted virus), and the overall entry efficiency was calculated as the average entry efficiency of both clones. After multiple attempts at cloning CAP345, CAP283, CAP315, CAP343 and CAP257, no functional clones could be generated. Of the 20 functional PSV clones generated, 17 were identical to the isolate SGA amplicon while two differed in a single site. The final one, CAP287, had two synonymous and three non-synonymous changes compared with the SGA that was sequenced. These are too many changes to have been introduced during PCR and cloning. As all of the non-synonymous mutations in CAP287 were present *in vivo*, but in two different plasma variants, we concluded they were probably real changes as opposed to PCR-induced errors. Most likely when the sample was taken from the first round product for second round PCR prior to cloning, we amplified a different variant to the one sequenced, which was present as a minor variant in the first round product. Table 3.5 shows the participants for which non-synonymous mutations were introduced during the cloning process and the possible functional implications of these changes.

Table 3.5. Non-synonymous changes introduced into pseudoviruses *env*s during the cloning process

Participant ID	Number of non-synonymous changes*	Location & possible functional implications, if known
CAP360	1	V3 loop; possible effects on coreceptor binding
CAP323	1	C1; none known
CAP287	3	Any functional changes would still reflect an *in vivo*-relevant phenotype

*compared to the isolate *env* sequences selected for cloning

Finally, the *in vitro* entry efficiencies of PSVs were assessed in order to determine if they differ between the trial arms (fig 3.8). Following a two sample t-test on log-transformed data it was found that there was no difference between the entry efficiencies between the trial arms (*P*= 0. 7569).

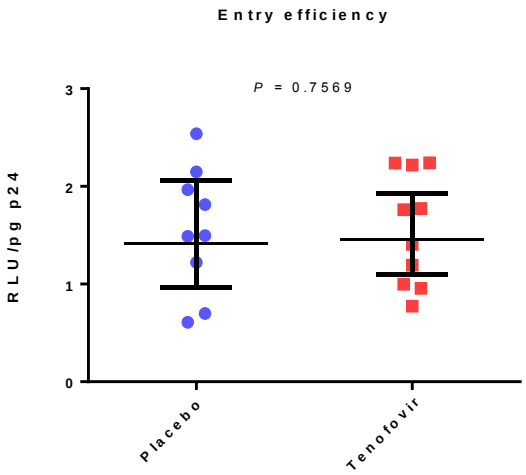

Figure 3.8. Entry efficiency does not differ between trial arms. Entry efficiency of *env*-typed PSVs was assessed using a single cycle replication assay on TZM-bl cells. The figure shows the entry efficiency expressed as RLU per pg of p24 in infection experiments with each PSV stock. Each point on the graph represents one PSV. Black bars represent the mean and 95% CI for both data sets. *P*-values were calculated by performing a two-sample t-test on log-transformed data in STATA. The figure generated using GraphPad Prism.

3.5 Env phenotype does not correlate with predictors of disease progression

In order to determine whether Env phenotype can impact disease progression in this cohort, we investigated whether inhibitor sensitivity and viral entry efficiency (i.e. PSV infectivity) correlated with VL and/or CD4 count. There was no correlation between inhibitor sensitivity and predictors of clinical progression (VL and CD4 count) (table 3.6).

Table 3.6. Spearman correlation coefficients and *P*-values showing the relationship between inhibition sensitivities to each inhibitor and various clinical markers of infection for the isolates

Inhibitor	CORRELATION WITH			
	VL at isolation	VL at 3 months post-infection	VL at set-point	$CD4^+$ count at set-point
TFV	*P*= 0.5105 r= 0.1297	*P*= 0.6377 r= 0.0930	*P*= 0.8530 r= 0.0367	*P*= 0.8574 r= 0.0356
MVC	*P*= 0.0985 r= 0.3186	*P*= 0.0979 r= 0.3191	*P*= 0.2716 r= 0.2151	*P*= 0.2393 r= -0.2299
T20	*P*= 0.8988 r= 0.0252	*P*= 0.7252 r= -0.0695	*P*= 0.7672 r= 0.0586	*P*= 0.4247 r= 0.1571
Anti-CD4	*P*= 0.7524 r= -0.0624	*P*= 0.8988 r= -0.0252	*P*= 0.4069 r= -0.1631	*P*= 0.7821 r= -0.0547
PSC-RANTES	*P*= 0.7034 r= -0.0753	*P*= 0.8077 r= -0.0482	*P*= 0.7885 r= -0.0531	*P*= 0.3163 r= -0.1965

In addition, entry efficiency measured using a PSV entry assay did not correlate with VL at isolation (*P*= 0.5520), at 3 months post-infection (*P*= 0.6165) nor with VL at set-point (*P*= 0.2272) (fig 3.9). Furthermore no correlation with CD4 count at set-point was found.

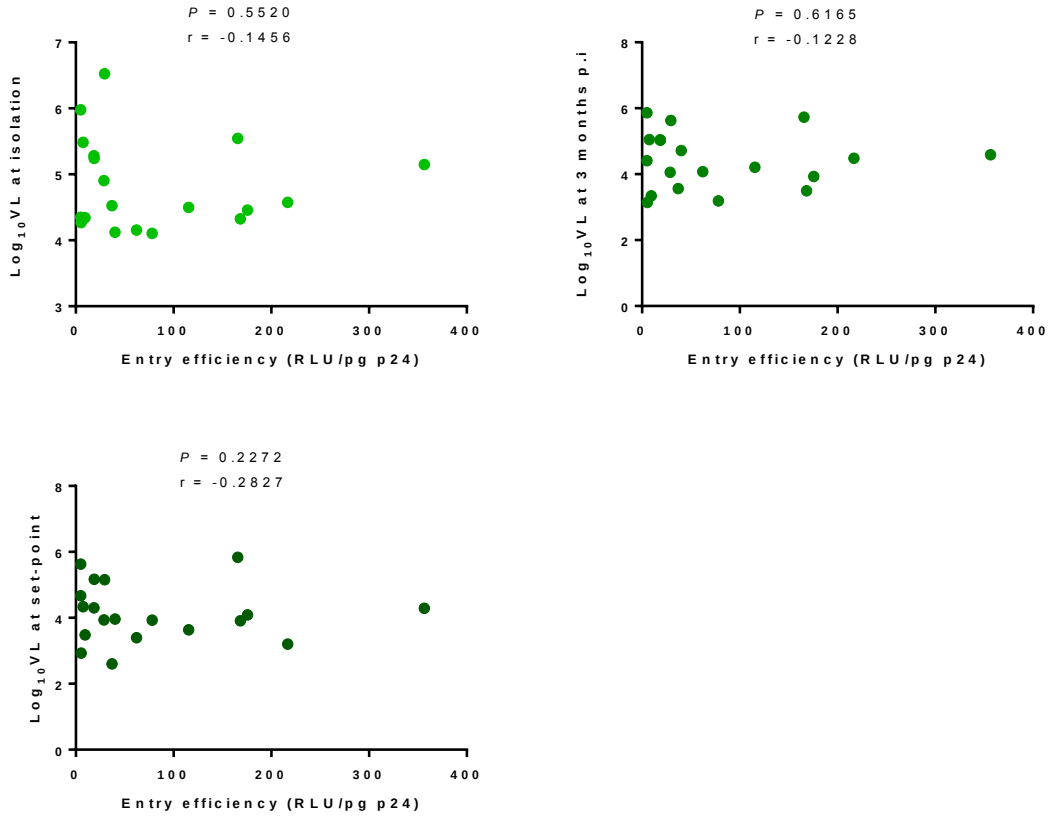

Figure 3.9. Entry efficiency does not correlate with viral load at various time-points post-infection. Entry efficiency for all PSVs is depicted on the x-axis while the VL at A) isolation, B) 3 months post-infection (p.i); and C) set-point is depicted on the y-axis. A Shapiro-Wilk test for normality was used to determine distribution of the data and then a Spearman rank correlation was applied to all data sets using STATA 11.2.

3.6 Pseudovirion Envs differ in sensitivity to entry inhibitors when compared with the corresponding isolate

It is known that native *env* trimers and PSV *env*s differ in terms of their glycosylation (179), the percentage at which they are present on the surface of virions and also the degree to which they are processed (180); all of which can affect the function of PSVs relative to their corresponding isolate. In order to evaluate the PSV system to determine whether PSVs are representative of isolates, the inhibition sensitivities of PSVs were compared to that of their corresponding isolates (fig 3.10). The PSVs which sustained PCR-induced errors compared with their corresponding SGA were excluded (that is, CAP60 and CAP 323). Data for CAP287 was included in this analysis.

Inhibition curves of the isolate and corresponding PSV can be found in appendix 3F. Median EC_{50} values for PSVs and isolates for each inhibitor are shown below (table 3.7).

Table 3.7. Median inhibition sensitivities for the comparison of pseudoviruses and isolates.

Inhibitor	**Median EC_{50}- Pseudoviruses (IQR)**	**Median EC_{50}- Isolates (IQR)**
T20 (fusion capacity)	28.47 (10.78; 57.02)	5.267 (2.986; 11.44)
MVC (CCR5 dependence)	1.904 (1.008; 6.306)	2.812 (1.826; 4.050)
SK3 (CD4 binding affinity)	0.1249 (0.1011; 0.1640)	0.3411 (0.2499; 0.3710)
PSC-RANTES (CCR5 binding affinity)	0.04661 (0.03930; 0.07912)	0.08886 (0.06440; 0.1570)

It was found that PSVs were 5-fold less susceptible to inhibition by T20 (*P*= 0.0117), and 3-fold and 19-fold more susceptible to inhibition by the anti-CD4 antibody SK3 (*P*= 0.0117) and PSC-RANTES (*P*= 0.0117) respectively, than isolates. The significance was retained even after Bonferroni correction (P-value< 0.0125 for significance). Since a Wilcoxon signed-rank test for paired data was employed to test the difference between PSV and isolate inhibition in all cases, the ranks of participant EC_{50}'s within each group can be concluded to be different. Interestingly, there was no significant difference between PSV and isolate sensitivity to MVC (1.5-fold difference, *P*= 0.2076).

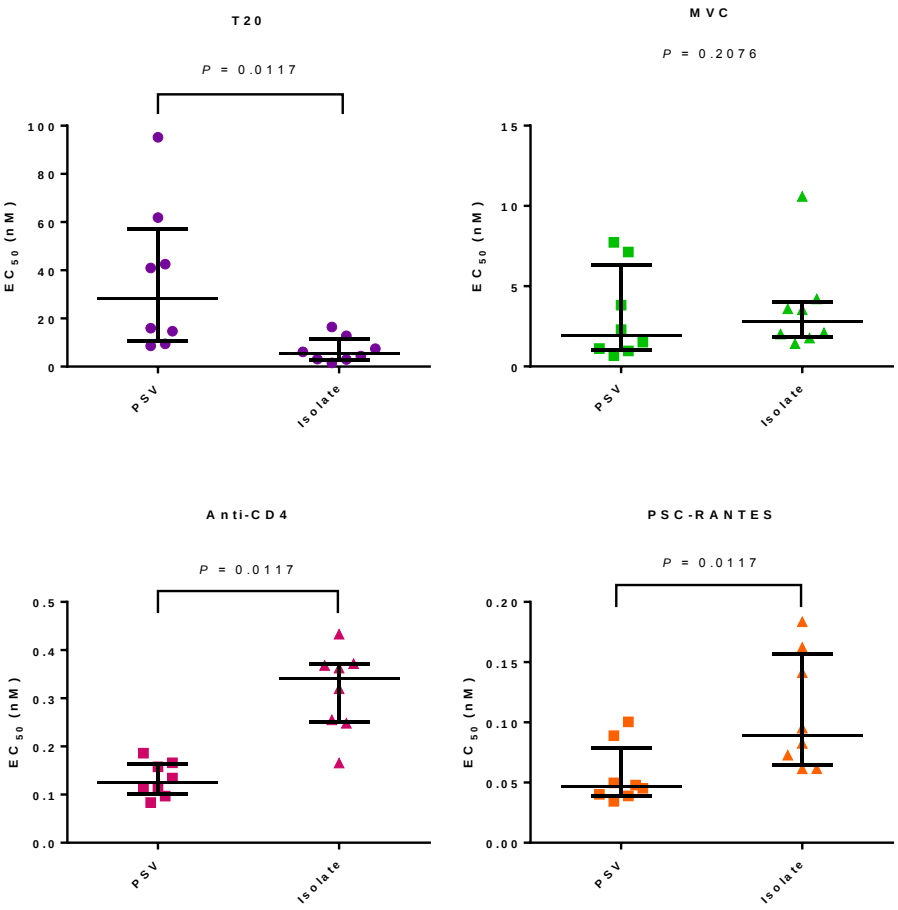

Figure 3.10. Inhibition sensitivities of pseudoviruses compared with their corresponding isolate. EC_{50} values representing the effective inhibitory concentrations for 50% inhibition are shown on the y-axis for various inhibitors (indicated above each graph). Black bars represent the median and IQR for the data. The *P*-values were calculated using a Wilcoxon signed-rank test for paired data and are significant for T20, anti-CD4 antibody clone SK3 and PSC-RANTES even after Bonferroni correction for multiple comparisons ($P < 0.0125$ for significance).

4. Discussion

Effective prevention modalities are essential if the trajectory of HIV-1 infection in Africa is to be curtailed; especially in young women who bear a disproportionate amount of the infection burden. TFV-based microbicides, if used correctly, are a safe, effective, and convenient means of protection from infection, which provides women with control over their own protection. However, when breakthrough infections occur, a potential pitfall may be that this barrier which is only partially protective might select for more virulent viruses during transmission (181). In the case of the CAPRISA 004 trial, the partial protection conferred by the microbicide could result in transmission of viruses with characteristics that may hasten disease progression or worsen clinical symptoms (119). Therefore, this study investigated the transmission of Env variants in the CAPRISA 004 1% TFV trial in order to characterise early viral variants within the CAPRISA 004 cohort, in order to identify differences in characteristics of early viruses between trial arms, and to determine their potential effect on clinical markers of disease progression.

One observation suggests the transmission of more virulent viruses in the TFV arm of the study. Garrett *et al*. found a difference in VL between study arms with participants in the TFV arm having higher VL over time (up to two years post-infection) than those in the PLB arm, despite being assigned to gel use (119). The authors state that the VL difference is explained partially by the higher number of participants in the PLB arm with protective HLA alleles. In the subset of 48 participants chosen for this study, VLs were found to be similar between trial arms at 3 months post-infection and at set-point. This could be due to the fact that trial arms were matched for the presence of protective HLAs when selecting the cohort for this study.

In fulfilment of the first objective of this study, clinical isolates were obtained for 39 women by isolating HIV-1 from cryopreserved plasma and culturing isolated virions in uninfected donor PBMCs. One of the drawbacks of using PBMCs to isolate HIV-1 is that donor cells may have differential susceptibility to infection by HIV-1 (160). To overcome this, a 3x3 stimulation protocol was employed where PBMCs were obtained from three different donors and stimulated under three different conditions (132, 161) to obtain a mix of PBMCs each time cells were added. This resulted in a high percentage (81%) of primary isolates being obtained.

The next objective was to determine whether the primary isolates used in this study were genotypically representative of viruses circulating in the plasma of these individuals. There have been a number of studies showing that PBMC-cultured viruses do not represent variants *in vivo* (182–184), however, these compared isolate sequences to proviral DNA for HIV-1 *tat* (182) and

env (183, 184). These studies found outgrowth of minor variants from infected PBMCs in the isolates. Other studies have found that isolates are similar to variants *in vivo* (160, 185), by comparing proviruses in the donor with proviruses in recipient PBMCs after co-culture. Most recently, Dalmau *et al*. have shown (using a deep sequencing approach) that viruses isolated from plasma, infected donor PBMCs, and sequences obtained from plasma RNA do not differ, and that unique variants are infrequent (186). Following these findings, we wished to confirm that our isolates were representative of circulating variants (sequences generated from plasma RNA). We compared the isolate *env* sequences to plasma-derived *env*s for 24 participants. The maximum intra-participant diversity from the plasma-derived T/F sequence (assumed to represent the virus that founded clinical infection) was not greater in the isolates than the plasma variants, indicating that there was little- to no diversification of isolate sequences during growth in tissue culture. However, the maximum intra-participant pairwise distance was greater in the plasma than in isolate *env* sequences; indicating that the isolates represent some, but not all of the diversity of the quasispecies *in vivo*. This is consistent with findings from the studies which showed preferential expansion of certain variants over others when HIV-1 was isolated on PBMCs (182–184). Our study was limited by the small number of *env* SGAs generated per participant which could, in some cases, lead to under- or overestimation of the diversity within isolates compared with plasma sequences. The case of CAP323 is a good example. Three of the five isolates sequenced had a non-synonymous mutation that was not present in any of the five plasma sequences that we had available. This could represent outgrowth of a variant that sustained a mutation during growth in tissue culture, although the fact that so few plasma sequences were available could mean that the variant that grew was a minor variant in plasma. However, as in most cases the *env* sequences sampled from the isolates were similar to sequences in the plasma, and the *env* genes of isolates were genotypically representative of plasma variants (cell-free), we concluded that it was suitable to use primary isolates for further comparisons.

The third objective was to characterise viruses genotypically and compare *env* characteristics between study arms. We attempted to classify the multiplicity of infection for seven participants not classified previously (138). Two were classified as multivariant infections, four were single variant infections and one, CAP311, remained undetermined. CAP311 posed difficult to classify due to the fact that plasma *env*s had a low diversity and a small hamming distance amongst sequences, but mutations did not follow a random distribution. Further sequencing would be needed to resolve the multiplicity of infection in this participant. An eighth participant, CAP375, which was previously classified as a single variant transmission with high diversity (138), was reclassified as a multivariant transmission. These results put together with the previous studies', and using the same statistical analysis described by the authors, confirm the finding that TFV gel

use had no impact on the transmission bottleneck. Thus, this study adds to the picture of 1% TFV gel being safe for use as a microbicide (95, 187, 188).

The genital mucosa provides an efficient barrier to HIV infection. Several lines of evidence suggest that transmission is not entirely stochastic but might involve selection of viruses with favourable characteristics that can overcome this barrier to establish a local focus of infection (24, 47, 50). T/F viruses, and more specifically their Envs, differ from viruses during chronic infection in a number of ways. For example, T/F Envs have shorter variable loop lengths and fewer glycosylation sites than chronic Envs (24, 44–46). Assessing loop length and glycosylation in early infection may give insight to the transmission fitness of the T/F. We found no difference in the median loop length, charge or number of predicted glycosylation sites in any of the variable loops between trial arms when assessing isolate Env sequences. This finding suggests that there may not be selection for viruses with Env characteristics that favour greater transmission fitness in women assigned to TFV gel use.

Another characteristic associated with heterosexual transmission of subtype C viruses is the selection of viruses which are more consensus-like in amino acid identity (48). A consensus-like identity is a proxy for transmission fitness, therefore, viruses which are more similar to consensus are more likely to be transmitted. We found no difference between trial arms in nucleotide identity of the isolates when compared to a CAPRISA 002 cohort consensus (subtype C). There was a trend towards isolates from the TFV arm being less consensus-like compared with PLB arm isolates; however, this did not reach statistical significance. If this association is real, then it would suggest that TFV use is associated with reduction in selection during transmission. An increased sample size would be needed to verify this result.

Our fourth objective was to identify the isolates' phenotypic characteristics and compare them between study arms. Therefore, we assessed the susceptibility of the isolates to TFV *in vitro* to determine if differences in susceptibility to TFV could have contributed to breakthrough infection. Tenofovir based PrEP has been a concern due to the possibility of selection of viruses with resistance mutations to TFV which could ultimately harm prevention and treatment efforts. Resistance is most commonly developed if PrEP is initiated during undiagnosed infection (189) and evidence suggests that subtype C strains have a lower barrier to resistance [reviewed in (190)]. In addition, there have been cases of breakthrough infections due to transmitted drug resistance in patients on oral PrEP [reviewed in (189)]. However, previous studies have shown no transmitted resistance in participants assigned to TFV gel use in the CAPRISA 004 cohort based on genotypic analysis (95, 118). Our study confirmed this finding as complete inhibition of the

isolates by TFV was observed with all TFV inhibition curves falling within the range of PLB inhibition curves. Furthermore, susceptibility to TFV did not differ between study arms indicating that TFV use was not a factor influencing breakthrough infection.

All isolates were confirmed phenotypically to be exclusively R5-tropic since they were all sensitive to the CCR5 binding inhibitors MVC and PSC-RANTES, but were not sensitive at all to inhibition by bicyclam JM-2987, a CXCR4 binding inhibitor. The early viruses in this study reflect previous findings that transmitted and early viruses are R5-tropic. In addition to co-receptor tropism, MVC as a non-competitive CCR5 inhibitor, was used to measure CCR5 dependence and PCS-RANTES, as a competitive CCR5 inhibitor, was used to assess co-receptor binding affinity. Neither of these traits differed between isolates from the trial arms. Ping *et al*. (39) described the presence of two conformations of CCR5 molecules on the surface of cells, a MVC resistant, and a MVC sensitive kind. Transmitted viruses almost exclusively use the MVC sensitive CCR5 to enter cells, while viruses from chronic infection are able to utilize the MVC resistant kind, reaching an inhibition plateau at 10% infection when CCR5 expression on the cell surface is high. Other groups have described similar observations of viruses that are able to utilize MVC-bound CCR5 (191). Interestingly, CAP291 (TFV arm) and CAP292 (PLB arm) both exhibit a MVC inhibition plateau, CAP291 at around 18% infection, and CAP292 below 10% infection. However, CAP291 was isolated from plasma sampled at approximately 11 weeks post-infection and CAP292 from plasma sampled at five weeks post-infection. This is too early to be considered chronic infection which perhaps suggests that these viruses represent a transmitted phenotype from donors who were in chronic stages of infection.

Neither fusion capacity, nor CCR5 dependence and binding capacity, nor CD4 binding capacity, differed between trial arms. There were, however, two isolates from the PLB arm and one from the TFV arm that showed decreased susceptibility to binding and fusion inhibitors, respectively with a concomitant decrease in CD4 binding affinity. This finding underlines the synergistic nature of the various stages of entry in determining overall entry efficiency. We evaluated the overall entry efficiency directly using PSVs expressing the majority Env of the isolates and found that entry efficiency did not differ between study arms. Thus, phenotypic characteristics of Env do not differ between viruses from the TFV and PLB arms of the CAPRISA 004 trial.

Our fifth objective was to evaluate whether sensitivity to inhibitors, or entry efficiency, correlated with VL at isolation, 3 months, and set-point, or $CD4^+$ T cell count at set-point. Neither entry efficiency, nor sensitivity to inhibitors correlated with either $CD4^+$ count at set-point or VL at any of the time-points specified. This data indicates that TFV susceptibility, CD4 binding affinity,

CCR5 binding affinity, CCR5 dependence, fusion capacity and entry efficiency does not contribute to clinical markers of disease progression in this cohort.

Finally we evaluated the PSV system in measuring characteristics of entry. The PSV assay is a widely accepted, convenient way of examining entry efficiency and evaluating host immune responses or candidate vaccines against HIV-1 (neutralising antibodies). Recently however, the functionality and neutralization sensitivity of PSVs was shown to differ from IMCs where the Env and backbone were a subtype match versus if they were mismatched (192). Similarly, we found an altered susceptibility of PSVs to certain entry inhibitors when compared with their corresponding isolate. Isolates were more susceptible to inhibition of fusion and less susceptible to inhibition of CD4 binding and CCR5 binding than PSVs. This could be due to the fact that Env incorporation has been found to be less efficient in PSVs and depends on the ratio of backbone to Env plasmid used when generating the PSVs (180). In addition, PSVs can differ greatly in the amount of fully processed Envs on the virion surface. This decrease in functional Env could lead to differences in CD4 and CCR5 binding efficiency. The lack of a difference in sensitivity between isolates and PSVs to MVC indicates that dependence on CCR5 binding does not differ between PSVs and isolates. This seems to contradict the difference in sensitivity to PSC-RANTES between isolates and PSVs. However, MVC merely decreases the amount of CCR5 available on the cell for use by the virus for entry and does not competitively inhibit CCR5 binding. Thus, generating PSVs may affect Env's ability to bind CCR5 but does not affect the amount of CCR5 needed to enter cells.

While only one *env* per isolate was cloned for all participants in this comparison, the *env* chosen was a majority variant within the isolates and therefore represents the *env* of the virus replicating most efficiently within the isolate stocks. This data highlights the importance of the context in which we study HIV-1 proteins. For example, the LLP domains in the cytoplasmic tail (CT) of gp41 (which interacts with the Gag matrix (MA) protein) have been implicated in Env fusogenicity, protein stability and cell surface expression [reviewed in (193)]. Hence, if these CT-MA interactions are changed in any way it may affect the fusogenicity and stability of Env. Similarly, the apparent affinities of CD4 and CCR5 binding might be affected as these CT-MA interaction have also been shown to be important for Env incorporation into virions (193–195). The concern that this raises is two-fold: firstly, evaluating different Envs expressed in the same backbone can have differential effects on each Env being studied, and secondly, evaluating subtype C Envs in a subtype B backbone may affect Env function across all Envs and differentially between Envs (192). While we do not have data for homologous Env-backbone PSVs, the importance of examining HIV-1 proteins in a relevant context is underscored.

Overall, our study confirms that 1% TFV gel use does not affect the genetic bottleneck, and further shows that gel use does not select for an altered Env phenotype which may lead to worsening of clinical symptoms such as higher VLs and lower CD4 counts. Although this study only evaluates Env, Chopera *et al.* have also shown no difference in Gag-Pro fitness and Nef function between study arms (146). This means that, in addition to a slightly higher number of protective HLA-bearing participants in the PLB arm (119), other factors are responsible for the VL difference between study arms. Further investigation into the causes of this VL discrepancy is needed.

5. Conclusion

In summary, the analysis of early viruses from participants who became infected while enrolled in the CAPRISA 004 1% TFV gel microbicide trial showed that the genetic bottleneck was not affected by the use of 1% TFV gel and that viruses from the both study arms were similar in genotypic and phenotypic characteristics of their Envs. Furthermore, characteristics of Env did not correlate with disease progression or VL at isolation, 3 months or at set-point, regardless of trial arm. Overall this suggest that the partial protection of 1% TFV gel does not result in the selection of viruses that worsen disease outcome and further supports the use of TFV as a safe and effective microbicide.

Appendices

Appendix 1. Reagents and buffers

The materials described hereafter and the methods in which they can be used are described in *Molecular Cloning: A Laboratory Manual* (196).

For Carbenicillin: (100 mg/mL) - stored at -20^{0}C

1. Weigh 1000 mg carbenicilin disodium salt (98-100% anhydrous)
2. Dissolve in 10 mL distilled, de-ionized H_2O in a 15 mL tube
3. Vortex to ensure that all the salt is dissolved
4. Using a syringe, pass the solution through a 0.22 μm filter into a fresh, sterile tube

For Luria-Bertani Broth : -stored at room temperature

1. Add the following to 800 mL H_2O:
   10 g Bacto-tryptone
   5 g yeast extract
   10 g NaCl
2. Adjust pH to 7.5 with NaOH or HCl
3. Adjust the volume to 1 L with dH_2O
4. Sterilize by autoclaving at 121^{0}C for 15 minutes

For Luria-Bertani Agar: -stored at 4^{0}C

1. Add the following to 800 mL H_2O:
   10 g Bacto-tryptone
   5 g yeast extract
   10 g NaCl
2. Adjust pH to 7.5 with NaOH or HCl
3. Add 15 g agar and dissolve by heating in the microwave
4. Adjust the volume to 1 L with dH_2O
5. Sterilize by autoclaving at 121^{0}C for 15 minutes

Pouring agar plates:

1. Prepare LB Agar as above and allow to cool
2. Add 1 µL carbenicilin (100 mg/mL as above) per mL of agar using sterile technique
3. Add to sterile petri dishes until the height of the liquid ~1 cm thick
4. Allow to set before storing the plate with the lid facing down

For Tris- buffered saline (TBS) buffer: -stored at 4^0C for up to 3 months

1. Dissolve 6.05g Tris and 8.76g NaCl in 800mL H_20
2. Adjust to pH 7.6 with 1M HCl
3. Adjust volume to 1L with ddH_20

Appendix 2. Table A2. HIV-1 subtype C *envelope*, full-length primers.

Primer Name	Sequencing Direction	Primer Sequence	Length (mer)	HXB2 position of first 5' nucleotide
EF00	Forward	5' GGG AAA GAG CAG AAG ACA GTG GCA ATG A 3'	28	6204
EF15	Reverse	5' CTT GCT CTC CAC CTT CTT CTT C 3'	22	8442
EF55	Reverse	5' GCC CCA GAC CGT GAG TTG CAA CAT ATG 3'	27	7937
EF115	Reverse	5' AGA AAA ATT CTC CTC TAC AAT TAA 3'	24	7371
EF170	Forward	5' AGC AGG AAG CAC TAT GGG 3'	18	7802
EF175	Reverse	5' TTT AGC ATC TGA TGC ACA GAA TAG 3'	24	6398
EF200	Forward	5' GGG ATA ACA TGA CCT GGA TGC AGT GGG 3'	27	8095
EF260	Forward	5' TTC AGC TAC CAC CGA TTG AGA GAC T 3'	25	8523
For14	Forward	5' TAT GGG ACC AAA GCC TAA AGC CAT GTG 3'	27	6559
For16	Forward	5' TTT AAT TGT GGA GGA GAA TTT TTC TA 3'	26	7353
Rev 15	Reverse	5' CTG CCA TTT AAC AGC AGT TGA GTT GA 3'	26	7012
Rev19	Reverse	5' ACT TTT TGA CCA CTT GCC ACC CAT 3'	24	8817

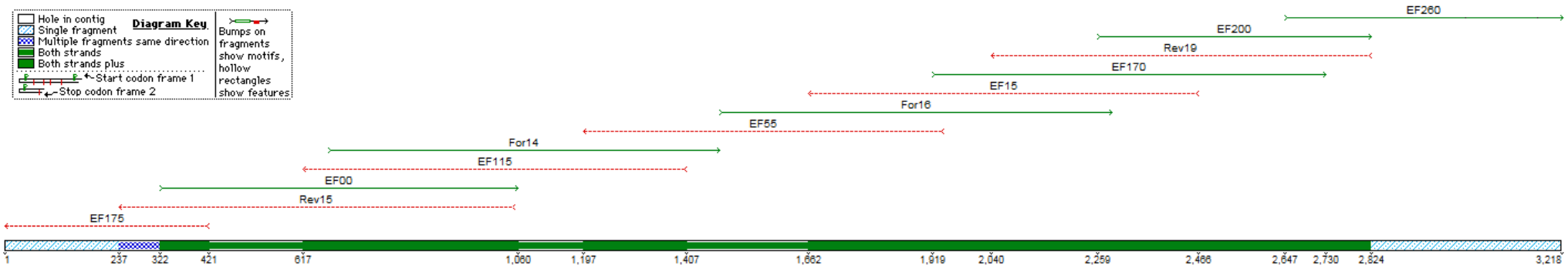

Figure A2. The order and direction of the sequencing primers along the *envelope* amplicon, from 5' to 3' end, as depicted in Sequencher v5.2.4

Appendix 3A. Table A3A. A description of the CAPRISA 004 participants selected for this study.

TFV arm participant	Viral load ł	Time Post-infection		TFV Present ǂ	Placebo arm participant	Viral load ł	Time Post-infection		Protective HLA? ϕ
		Weeks	Days				Weeks	Days	
CAP304 [x]	94 900	5	34		**CAP321**	338 000	5	35	No
CAP305 [x]	45 600	11	77	No	**CAP337**	114 000	10	71	Yes
CAP310 [x]	305 000	4	29	No	**CAP303**	344 000	4	29	No
CAP314	166 000	12	87	Yes	**CAP340** [x]	72 500	13	89	No
CAP320	37 500	5	34	Yes	**CAP345**	130 000	6	43	No
CAP325	127 000	3	20	No	**CAP327**	91 600	3	20	No
CAP343	130 000	7	51	Yes	**CAP317**	351 000	7	51	No
CAP355	19 700	5	32	No	**CAP353**	487 000	5	32	No
CAP360	80 600	3	24	Yes	**CAP301**	33 500	4	25	Yes
CAP362 [x]	44 200	4	29	Yes	**CAP335** [x]	214 000	4	28	No
CAP363	97 500	5	36	No	**CAP292**	458 000	5	38	No
CAP367	3 360 000	3	22	No	**CAP326**	31 500	3	23	No
CAP283	12 900	7	52	No	**CAP306**	141 000	8	54	Yes
CAP291	14 300	11	79	No	**CAP349**	950 000	11	77	No
CAP318	22 300	5	37	No	**CAP307**	174 000	5	37	No
CAP323	22 000	3	22	Yes	**CAP315**	108 000	3	22	Yes
CAP334	21 200	6	42	Yes	**CAP311**	18 600	6	42	No
CAP348	305 000	8	57	Yes	**CAP287**	13 200	8	58	No
CAP352	113 000	7	50	No	**CAP365**	14 500	9	63	Yes
CAP358 [x]	717	9	66	No	**CAP308**	37 100	9	66	No
CAP368	1 180	4	31	Yes	**CAP351** [x]	151 000	4	28	No
CAP370	28 800	5	33	Yes	**CAP331**	12 700	6	43	No
CAP372	107 000	3	21	Yes	**CAP330** [x]	21 200	2	15	No
CAP375	192 000	5	36	Yes	**CAP357**	14 900	7	47	No

[x] Indicates participants whose viruses could not be isolated in tissue culture; ł viral load of sample used for isolation;
ǂ Measurements of TFV taken from plasma samples; ϕ Presence of protective HLAs in both participants.

Appendix 3B. Highlighter plots

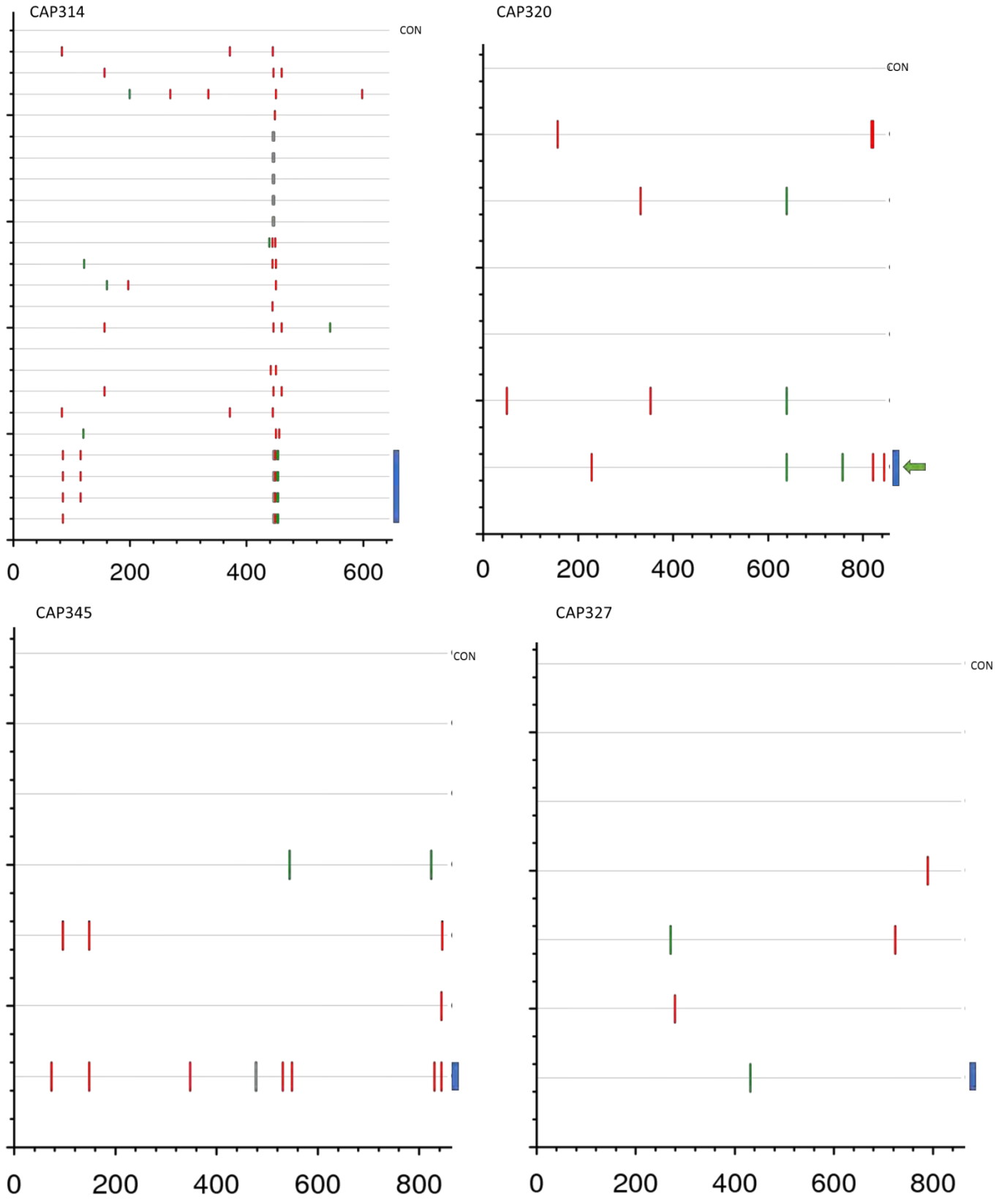

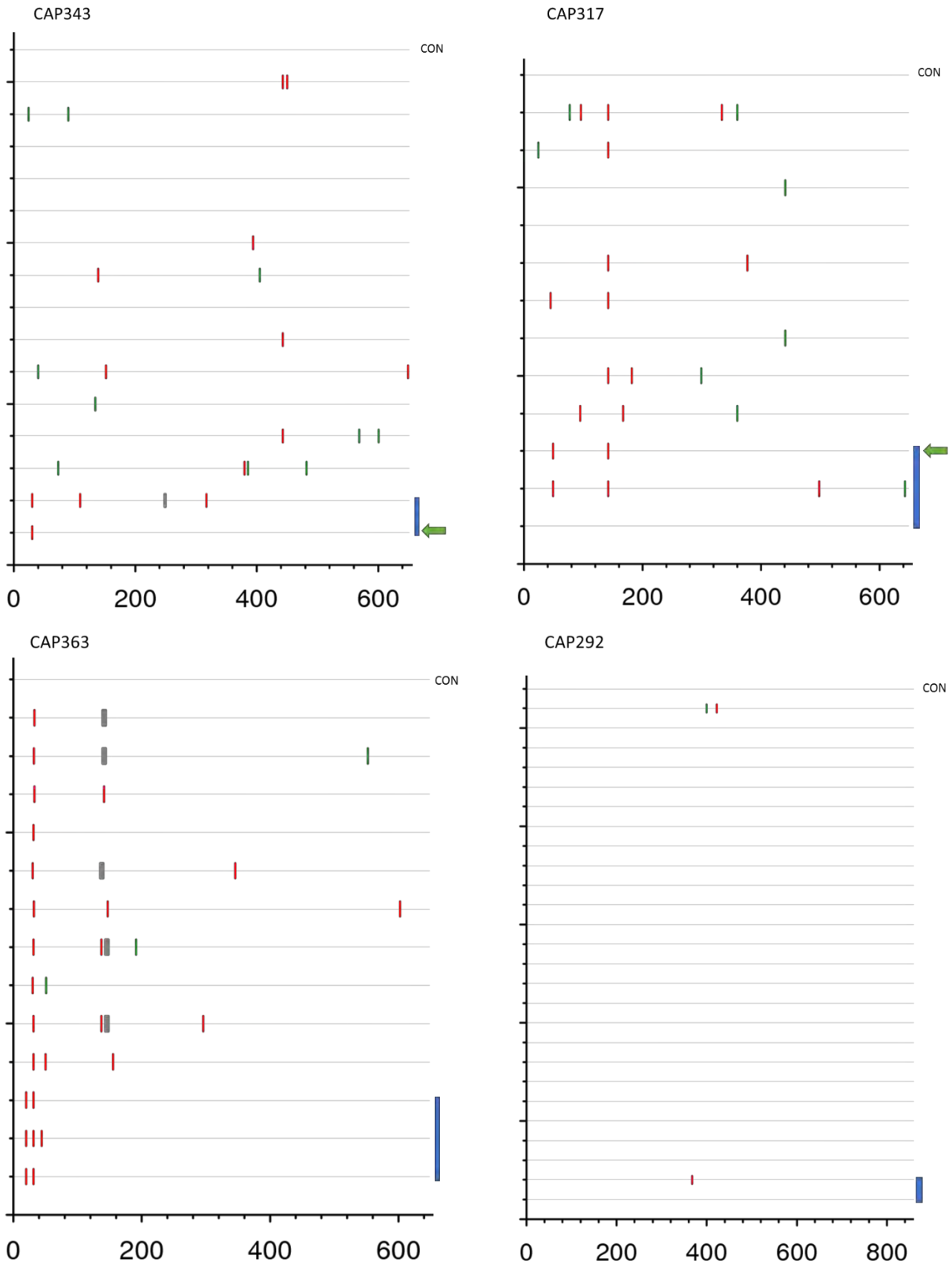
CAP343
CON
0
200
400
600
CAP317
CON
0
200
400
600
CAP363
CON
0
200
400
600
CAP292
CON
0
200
400
600
800

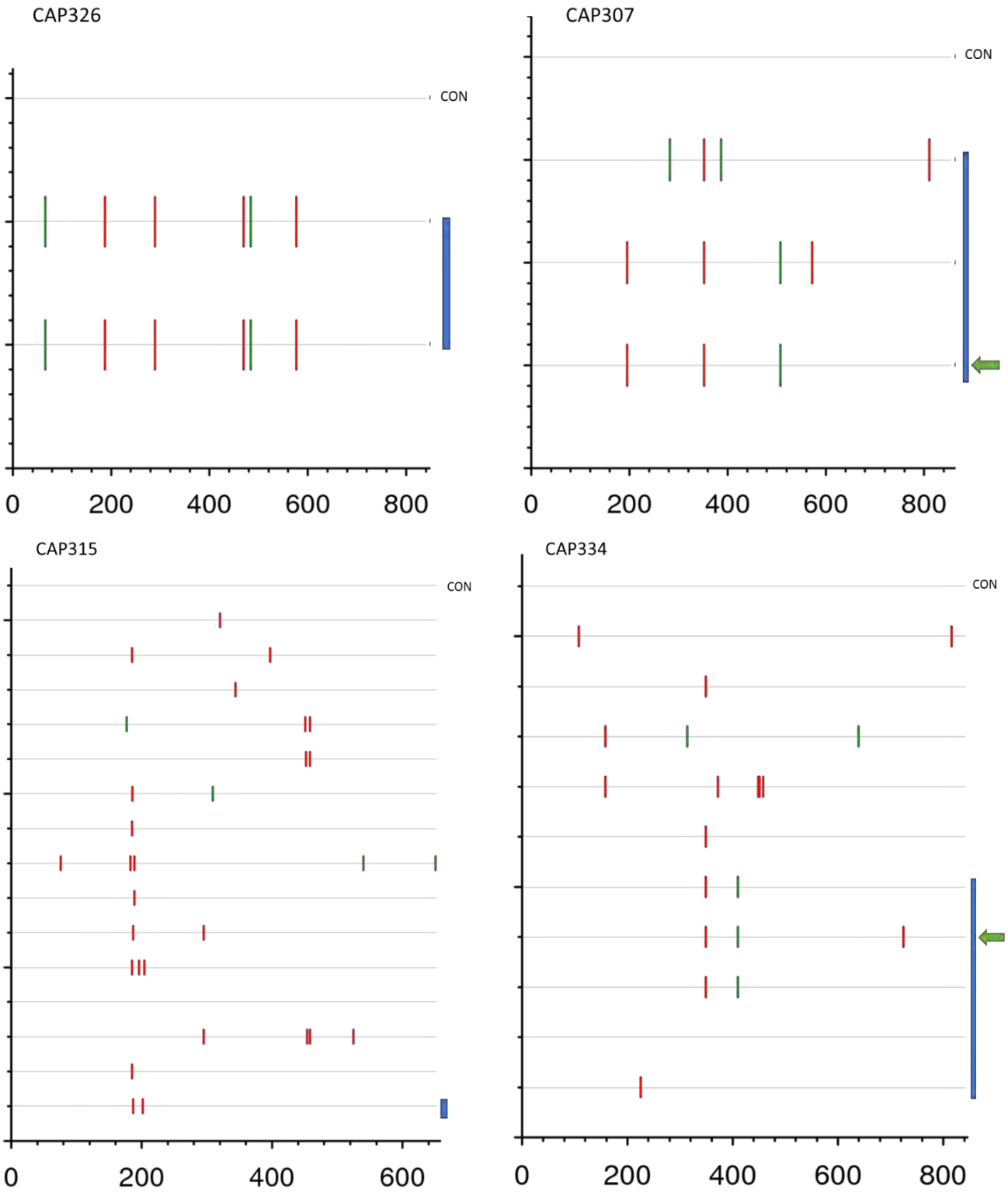
CAP326
CON
0
200
400
600
800
CAP307
CON
0
200
400
600
800
CAP315
CON
0
200
400
600
CAP334
CON
0
200
400
600
800

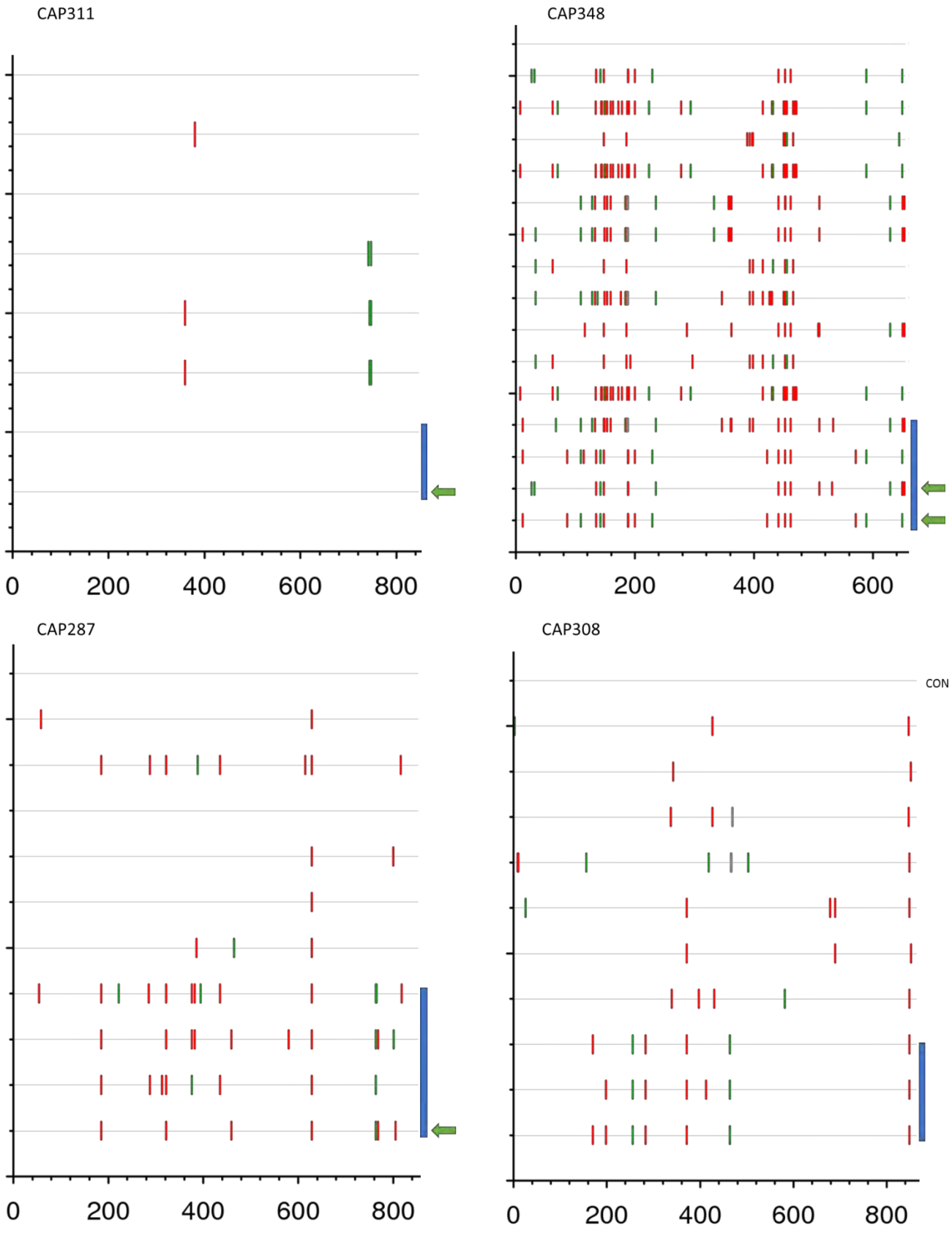
CAP311
0
200
400
600
800
CAP348
0
200
400
600
CAP287
0
200
400
600
800
CAP308
CON
0
200
400
600
800

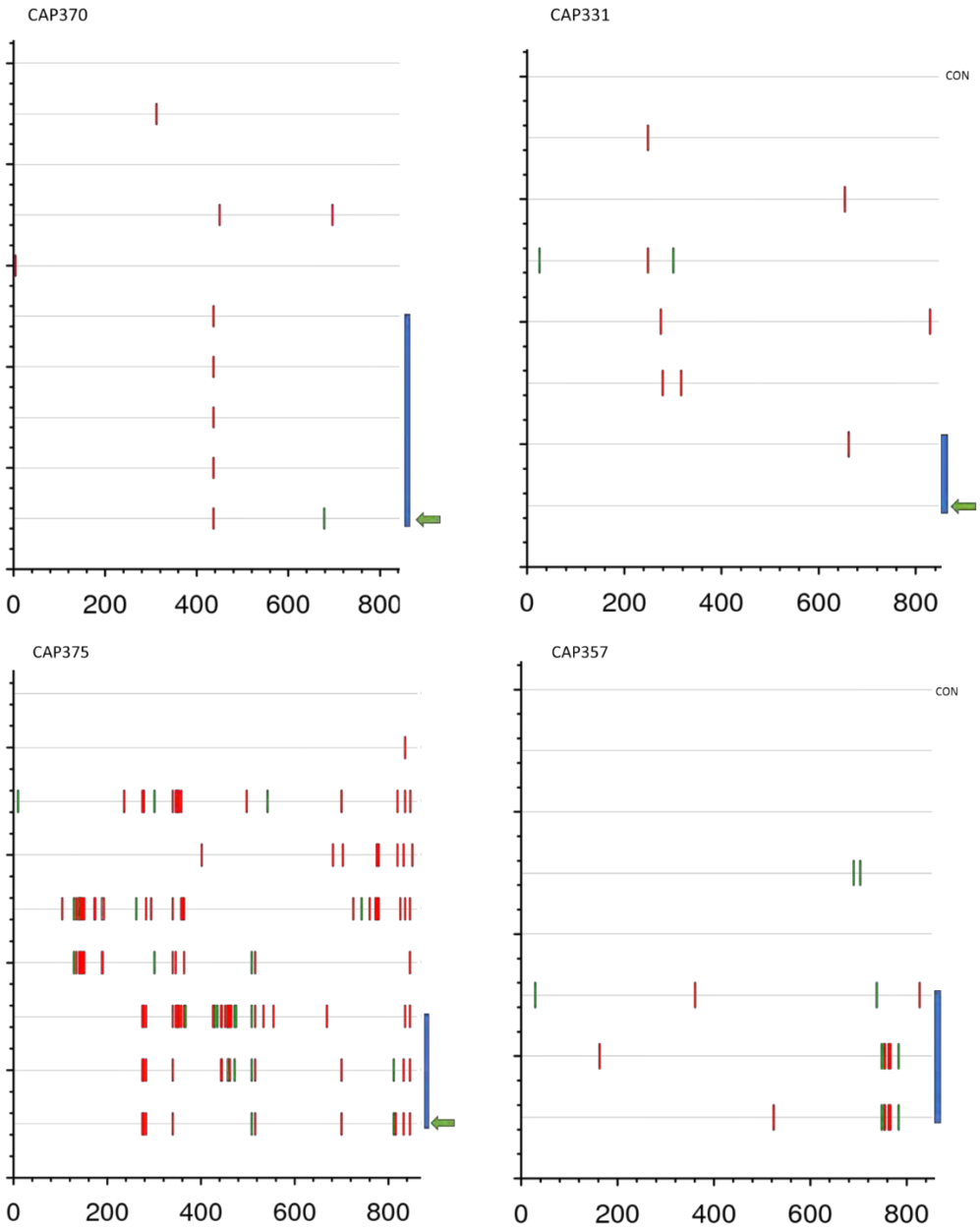

Figure A3B. Highlighter plots comparing plasma and isolate *env* sequences for 20 participants. Highlighter plots show the synonymous (green) and non-synonymous (red) nucleotide substitutions for all sequenced *env* variants in plasma and isolate samples (grey vertical bars represent deletions). Each *env* sequence is represented by a grey horizontal line. Isolate *env*s are denoted by a blue bar on the right of the sequences. Sequences were aligned to the plasma consensus sequence representing the T/F *env* sequence (labelled 'CON' in each figure). *env*s with a green arrow to the right of them were selected for cloning. Numbers on the x-axis represent the codon number. Highlighter plot A is for the CAP303 alignment which was truncated to the V3V5 region and is one case where the sequenced isolate *env*s are identical to that of the plasma consensus. Plots B and C show CAP360 (truncated to gp41) and CAP301 (full-length *env*) alignments, respectively, which represent participants with low diversity in their isolates and where the isolate *env*s have minor changes compared to variants in the plasma. Plot C represents CAP323, a participant with greater diversity in the isolate *env* sequences (full length) and where the isolates represent a mixture of variants sequenced from plasma and those not seen in the plasma sequences.

Appendix 3C. Table A3C. Non-synonymous mutations shared in isolates *env*s that were not represented in plasma *env* sequences

Participant ID	HXB2 Env gp160 position (change from T/F)	Known function(s) of residue or region	Reference(s) *
CAP314	V86 (L->M)	Adjacent to V85, a gp120 point of contact with gp41	(197)
	L116 (L->I)	Adjacent to K117, a coreceptor binding site outside of V3	(197) (198)
	After N460 (deletion of three amino acids, SRI)	V5 hypervariable loop close to CD4 contact residue S461 (side-chain only); removes one N-linked glycosylation site compared to the majority of the isolates and two compared to the T/F	
CAP345	V75 (V->I); R350 (K->E)	No known function	-
	Y484- Y486 (deletion in C5)	No known function	-
	V539 (V->A)	Residue immediately precedes the Leucine/Isoleucine zipper-like sequence of gp41	(199)
	R557 (R->K)	Within the Leucine/Isoleucine zipper-like sequence of gp41	(199)
CAP343	T31 (M->V)	First amino acid residue of GP120; adjacent to the Env signal peptide cleavage site	(200)
CAP363	L21 (G->S)	Amino acid 20 of signal peptide	-
	E32 (E->G)	Amino acid 2 of gp120; Env signal peptide cleavage site	(200)
CAP326	V2 loop, residues not present in HXB2 (P->L)	No known function	-
	I284 (M->I)	Residue adjacent to Loop D, a CD4 contact site	(198)
CAP307	T194 (K->I)	In the V1 loop adjacent to a coreceptor-specific site	(197)
CAP323	K429 (G->R)	CD4 contact residue for both main- and side-chain contact	(198)
CAP287	S190 (E->D)	V2 hypervariable loop	-
	R327 (N->K)	Coreceptor binding site inside the V3 loop	(197)
CAP308	G167 (D->N)	V1 loop, adjacent to a coreceptor-specific site	(197)
	S190 (E->K)	V2 hypervariable loop	-
	V275 (E->K)	First residue of Loop D; adjacent to a neutralising antibody binding site	(198)
CAP370	Q442 (N->S)	Coreceptor binding site outside of the V3 loop and an N-linked glycosylation site	(197)

Participant ID	HXB2 Env gp160 position (change from T/F)	Known function(s) of residue or region	Reference(s) *
CAP375	L518 (V->M)	Fusion peptide of gp41	(201)
	R828 (R->G)	First residue of LLP-1	(199)
	R841 (C->Y)	Residue in the LLP-1	(199)
CAP357	S767 (C->S)	Residue preceding the LLP-2 domain of gp41; no known function	-
	L774- V778 (**FI**L**IA**->**LA**L**VI**)	Series of 4 mutations in the LLP-2; overlaps with the Rev Leucine-rich domain	(199)

*Obtained from the HXB2 Genome Annotation document available on the Los Alamos website at http://www.hiv.lanl.gov/content/sequence/HIV/MAP/annotation.html and the N Glycosite tool at http://www.hiv.lanl.gov/content/sequence/GLYCOSITE/glycosite.html (170).

Appendix 3D. Maximum likelihood trees of isolate and plasma *env* sequences

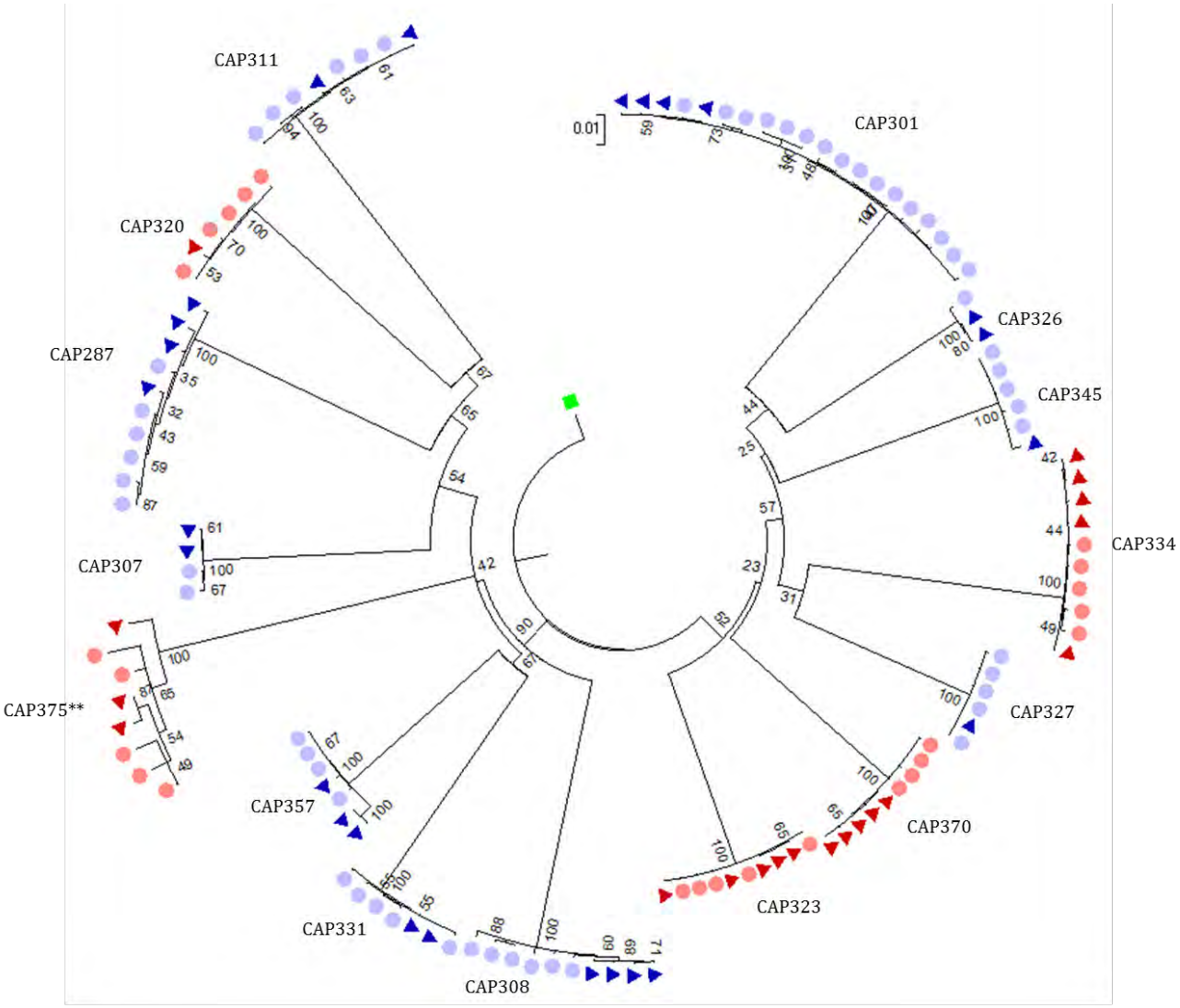

Figure A3D.1. Phylogenetic analysis of full-length plasma- and isolate-derived *env* sequences of HIV-1 from the same time-point post-infection in each participant. Nucleotide sequences were generated by limit dilution PCR amplification. Sequences from 24 participants from both arms of the trial (PLB depicted in blue, TFV in red) were aligned to a CAPRISA 002 cohort consensus and a maximum likelihood tree was generated. Triangles were used to represent isolate sequences while circles were used to represent plasma sequences. Only participants with full-length plasma-derived *env* sequences full-length sequences were used to generate this tree. **denotes participants who were identified as having established infection as a result of multivariant transmission.

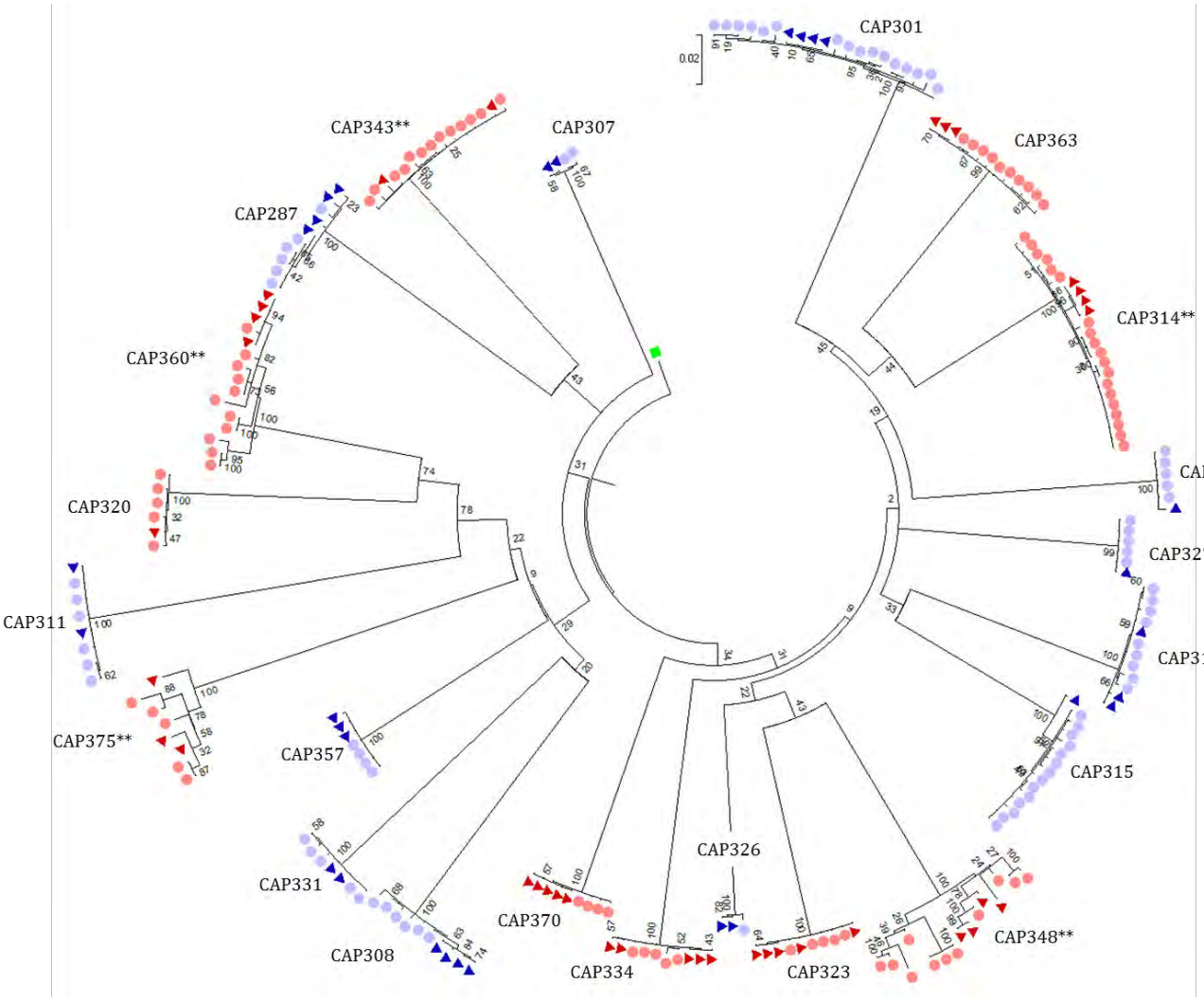

Figure A3D.2. Phylogenetic analysis of truncated plasma- and isolate-derived *env* sequences of HIV-1 from the same time-point post-infection in each participant. Nucleotide sequences were generated by limit dilution PCR amplification. Sequences from 22 participants from both arms of the trial (PLB depicted in blue, TFV in red) were aligned to a CAPRISA 002 cohort consensus and a maximum likelihood tree was generated. Triangles were used to represent isolate sequences while circles were used to represent plasma sequences. Sequences were truncated to the middle of gp41 within the *env* sequence due to a number of plasma-derived *env* sequences being only partially sequenced. **denotes participants who were identified as having established infection as a result of multivariant transmission.

Appendix 3E. Isolate inhibition curves

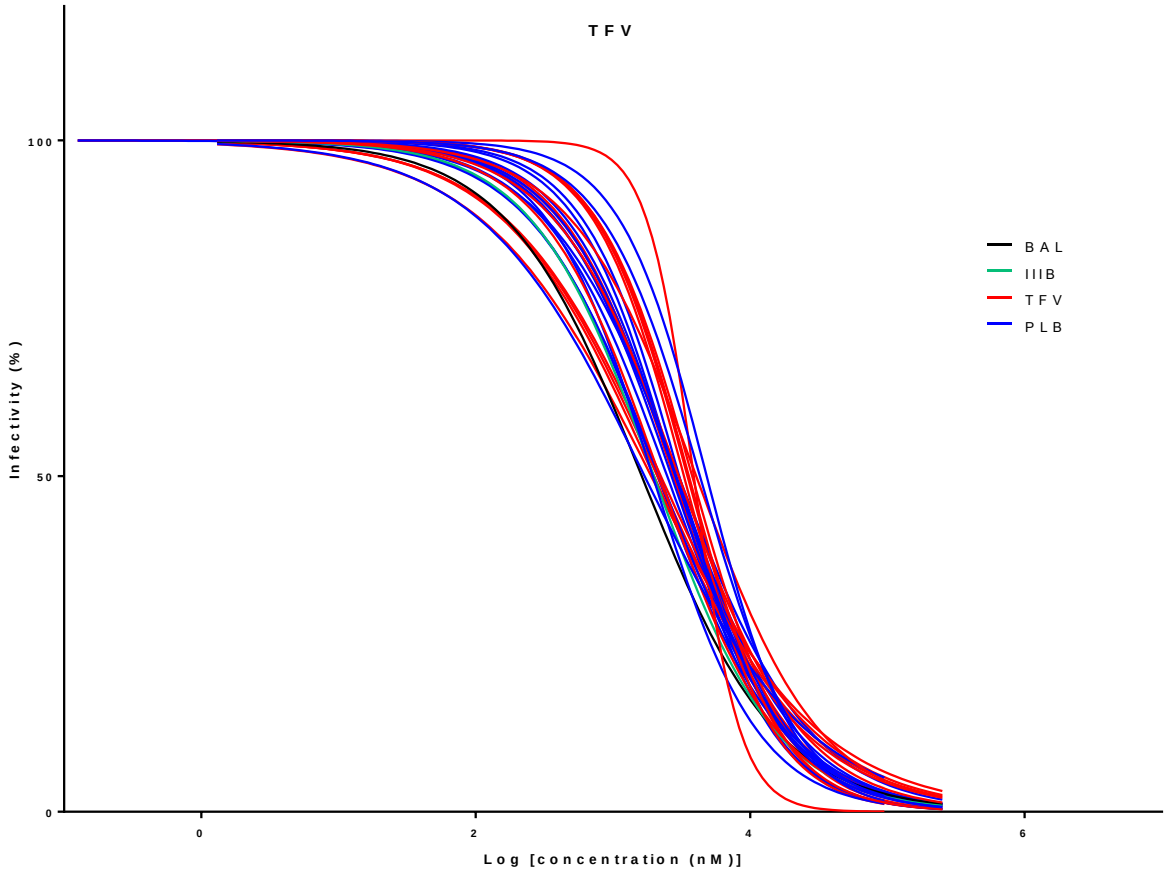

Figure 3E.1. Isolate inhibition with TFV, a reverse transcriptase inhibitor. The graph shows the decrease in the percentage infectivity of isolates (y-axis) on TZM-bl cells with increasing TFV concentration (x-axis). TFV arm isolate inhibition is represented as red curves while PLB arm isolate inhibition is depicted in blue. BAL (black) and IIB (turquoise) isolates were used as control within each experiment. As both controls are sensitive to TFV, they are inhibited as expected. The figure was generated using GraphPad Prism.

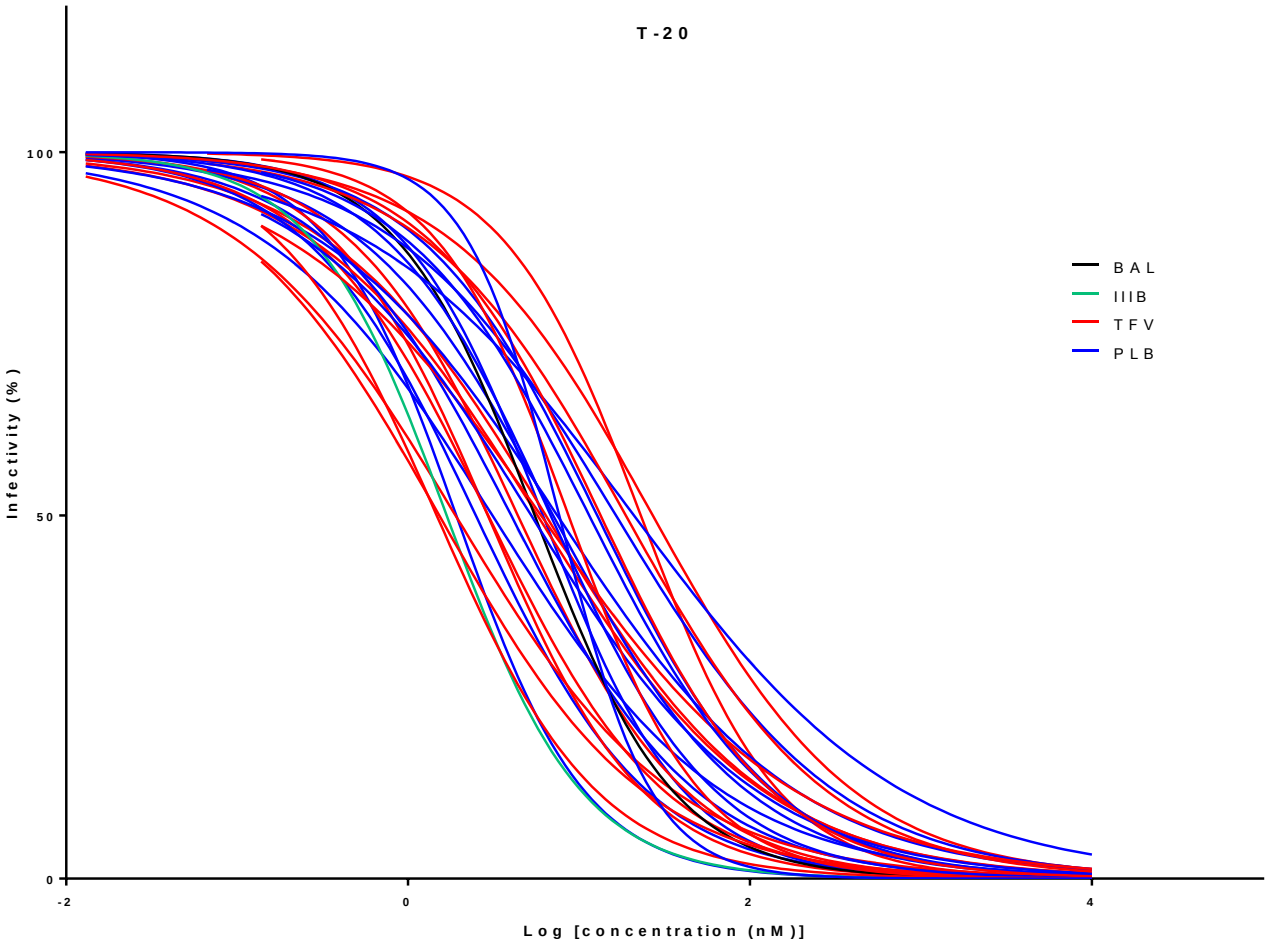

Figure 3E.2. Isolate inhibition with T20, a fusion inhibitor. The graph shows the decrease in the percentage infectivity of isolates (y-axis) on TZM-bl cells with increasing T20 concentration (x-axis). TFV arm isolate inhibition is represented as red curves while PLB arm isolate inhibition is depicted in blue. BAL (black) and IIB (turquoise) isolates were used as control within each experiment. As both controls are sensitive to T20 they behave as expected. The figure was generated using GraphPad Prism.

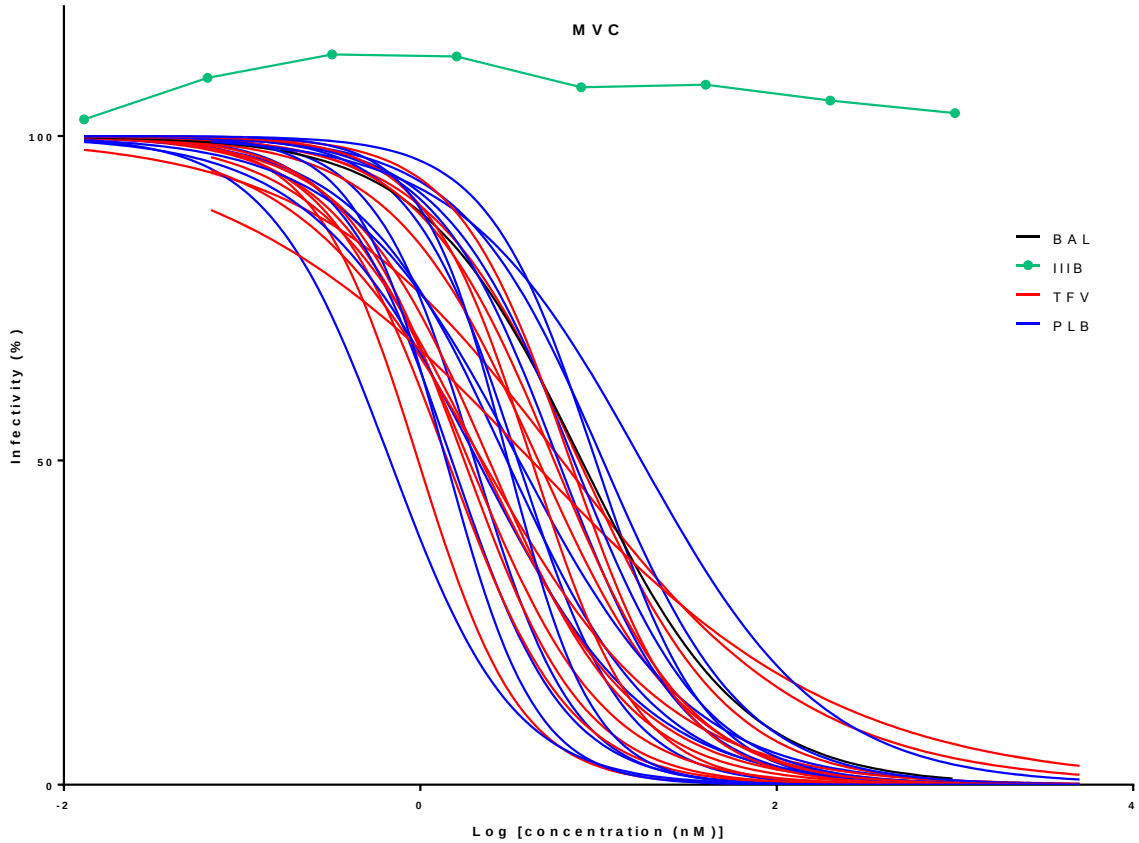

Figure 3E.3. Isolate inhibition with maraviroc, a non-competitive CCR5 binding inhibitor. The graph shows the decrease in the percentage infectivity of isolates (y-axis) on TZM-bl cells with increasing MVC concentration (x-axis). TFV arm isolate inhibition is represented as red curves while PLB arm isolate inhibition is depicted in blue. BAL (black) and IIB (turquoise) isolates were used as control within each experiment. As BAL is a known R5-tropic virus it is inhibited as expected. IIIB is an X4-tropic virus and is not sensitive to inhibition by MVC, as expected. The figure was generated using GraphPad Prism.

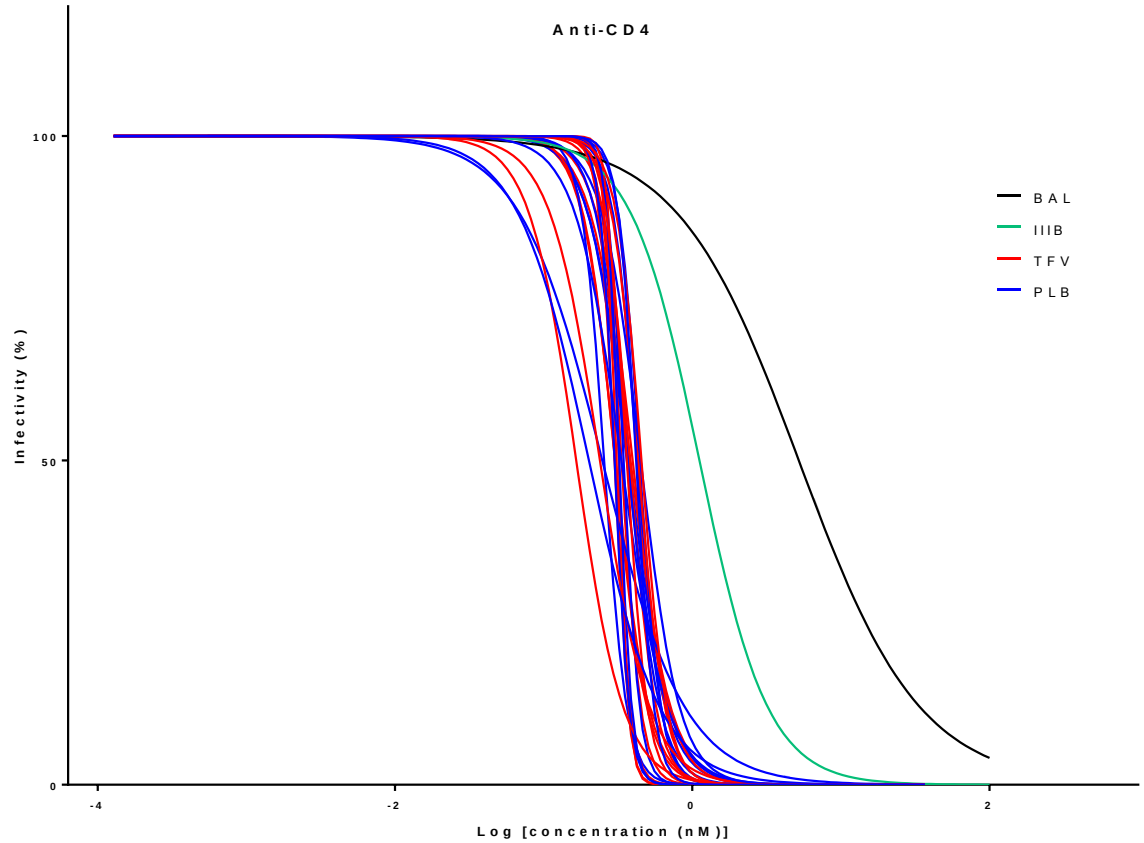

Figure 3E.4. Isolate inhibition with SK3, a competitive CD4 binding inhibitor. The graph shows the decrease in the percentage infectivity of isolates (y-axis) on TZM-bl cells with increasing SK3 concentration (x-axis). TFV arm isolate inhibition is represented as red curves while PLB arm isolate inhibition is depicted in blue. BAL (black) and IIB (turquoise) isolates were used as control within each experiment. Both controls are susceptible to inhibition by anti-CD4 antibodies and re inhibited as expected. The figure was generated using GraphPad Prism.

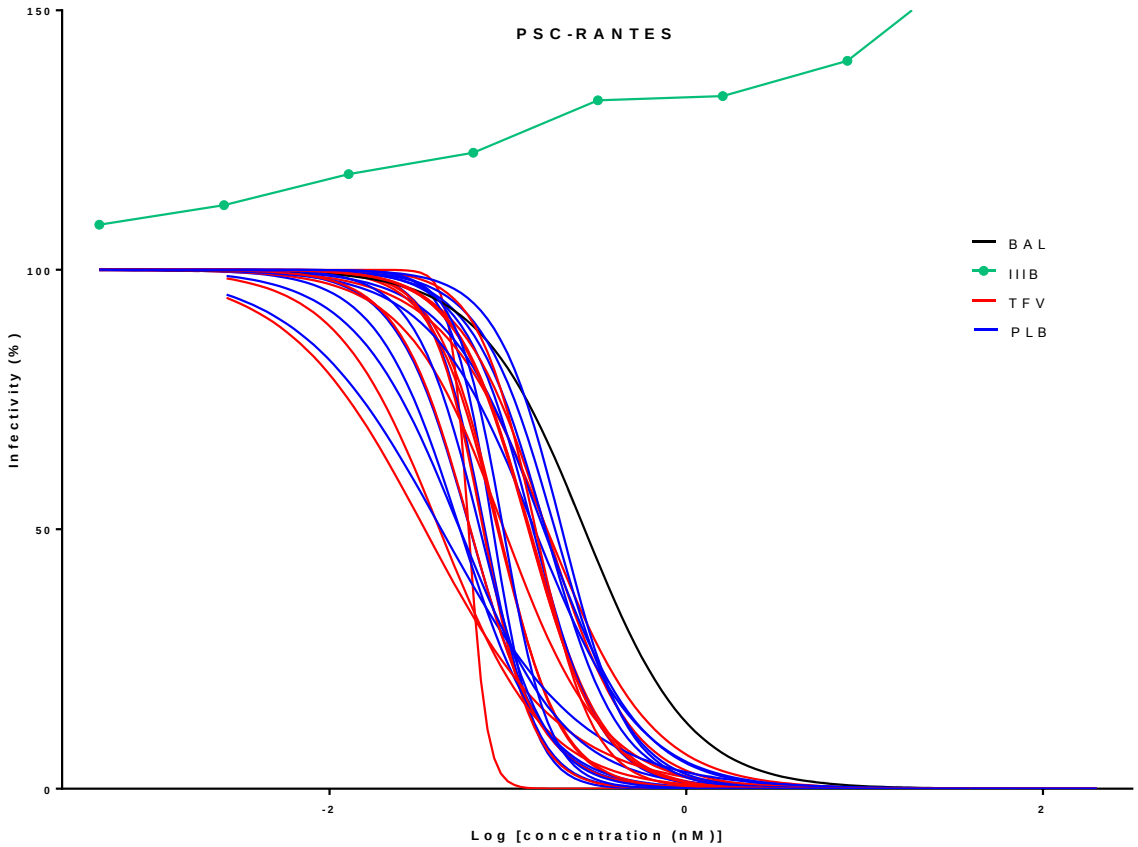

Figure 3E.5. Isolate inhibition with PSC-RANTES, a competitive CCR5 binding inhibitor. The graph shows the decrease in the percentage infectivity of isolates (y-axis) on TZM-bl cells with increasing PSC-RANTES concentration (x-axis). TFV arm isolate inhibition is represented as red curves while PLB arm isolate inhibition is depicted in blue. BAL (black) and IIB (turquoise) isolates were used as control within each experiment. As BAL is a known R5-tropic virus it is inhibited as expected. IIIB is an X4-tropic virus and is not sensitive to inhibition by PSC-RANTES, as expected. The figure was generated using GraphPad Prism.

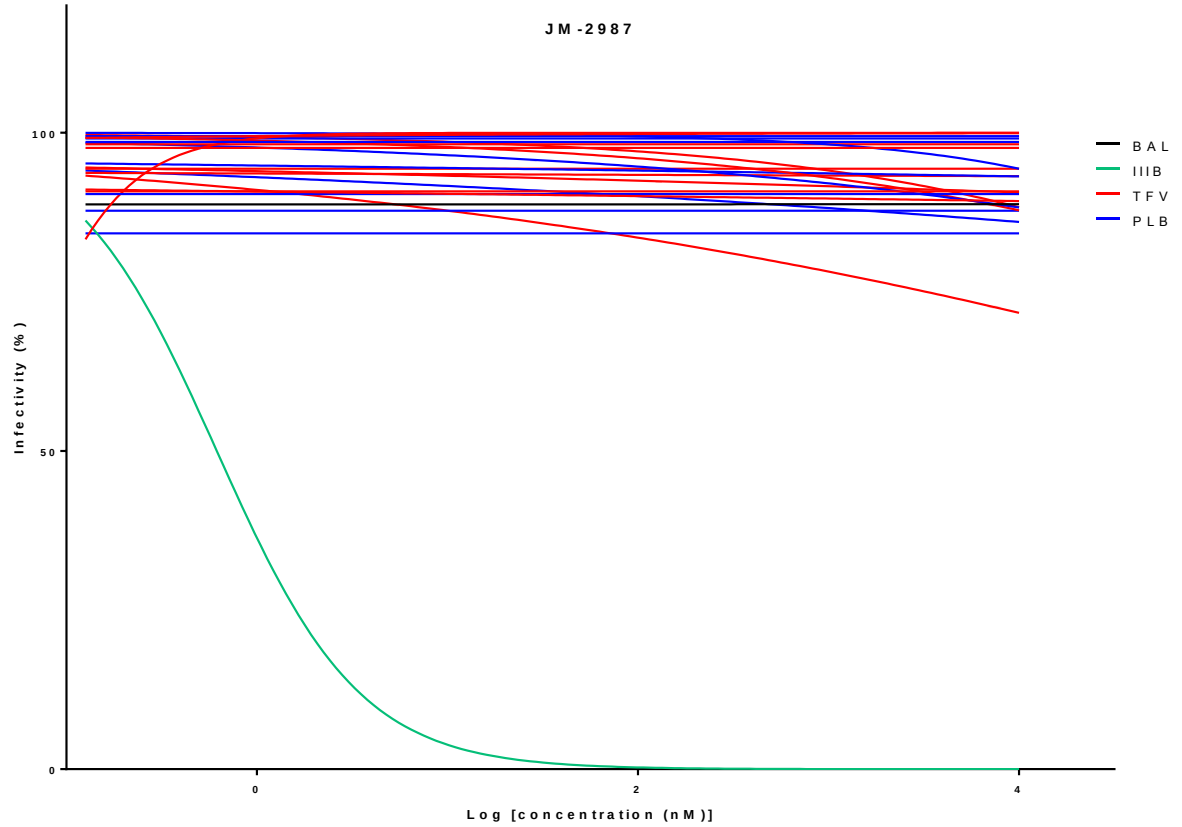

Figure 3E.6. Isolate inhibition with bicyclam JM-2987, a non-competitive CXCR4 binding inhibitor. The graph shows the decrease in the percentage infectivity of isolates (y-axis) on TZM-bl cells with increasing JM-2987 concentration (x-axis). TFV arm isolate inhibition is represented as red curves while PLB arm isolate inhibition is depicted in blue. BAL (black) and IIB (turquoise) isolates were used as control within each experiment. As BAL is a known R5-tropic virus it is not inhibited, as expected. IIIB is an X4-tropic virus and is sensitive to inhibition by JM-2987, as expected. The figure was generated using GraphPad Prism.

Appendix 3F. Inhibition of pseudoviruses with their corresponding isolate.

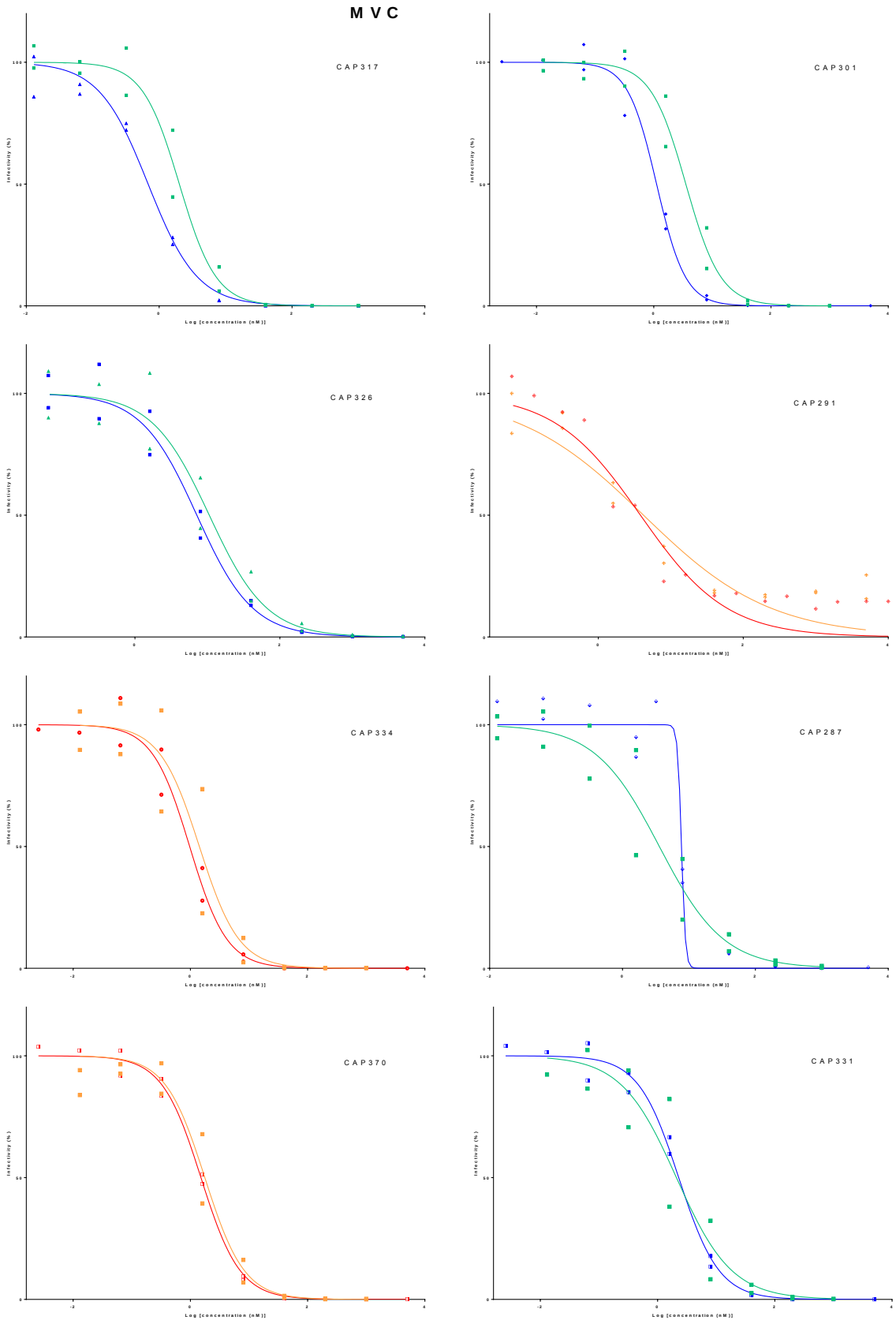

T 2 0

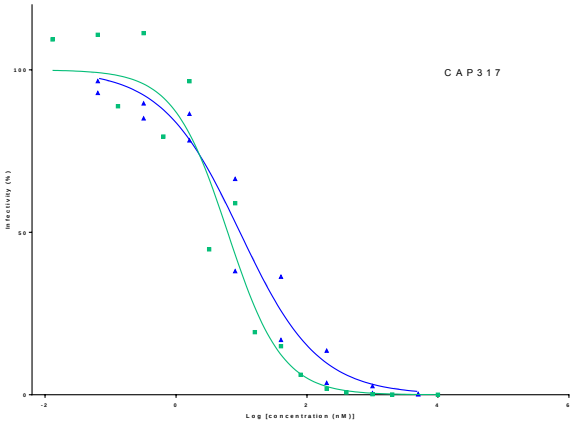
CAP317
Infectivity (%)
Log [concentration (nM)]

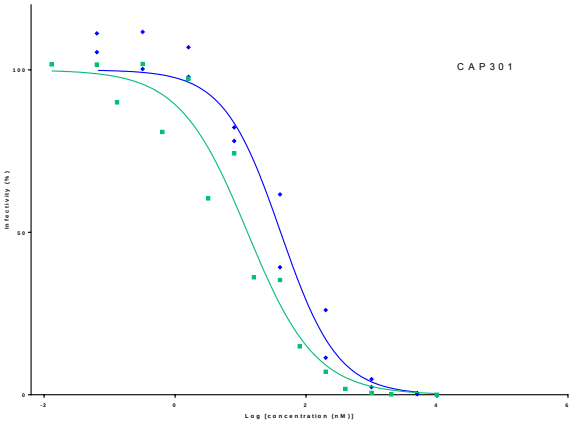
CAP301
Infectivity (%)
Log [concentration (nM)]

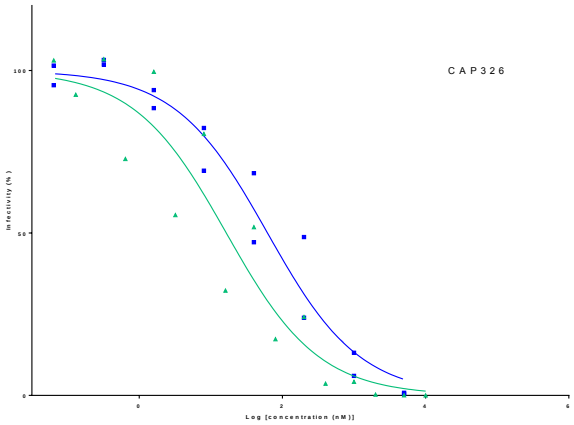
CAP326
Infectivity (%)
Log [concentration (nM)]

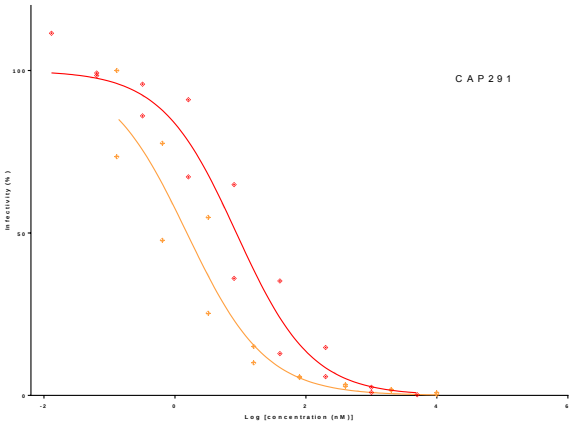
CAP291
Infectivity (%)
Log [concentration (nM)]

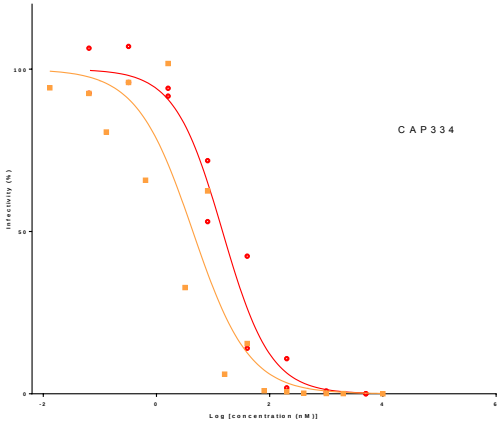
CAP334
Infectivity (%)
Log [concentration (nM)]

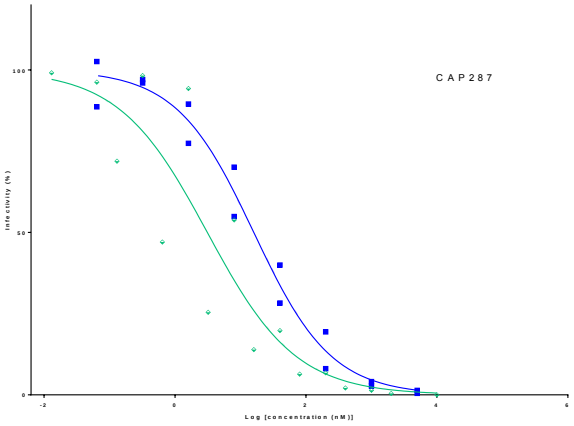
CAP287
Infectivity (%)
Log [concentration (nM)]

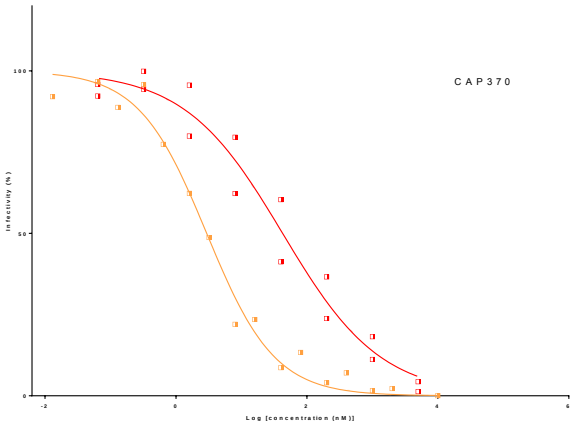
CAP370
Infectivity (%)
Log [concentration (nM)]

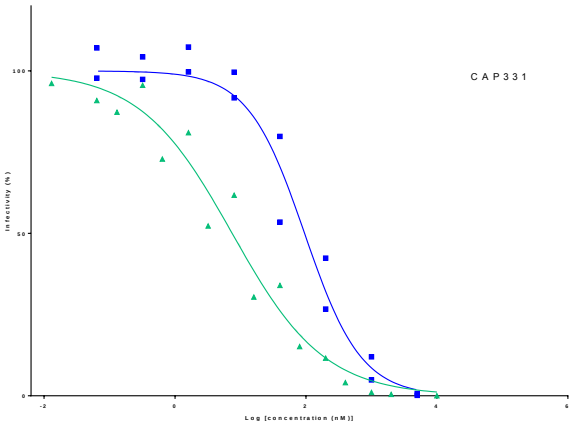
CAP331
Infectivity (%)
Log [concentration (nM)]

Anti-CD4

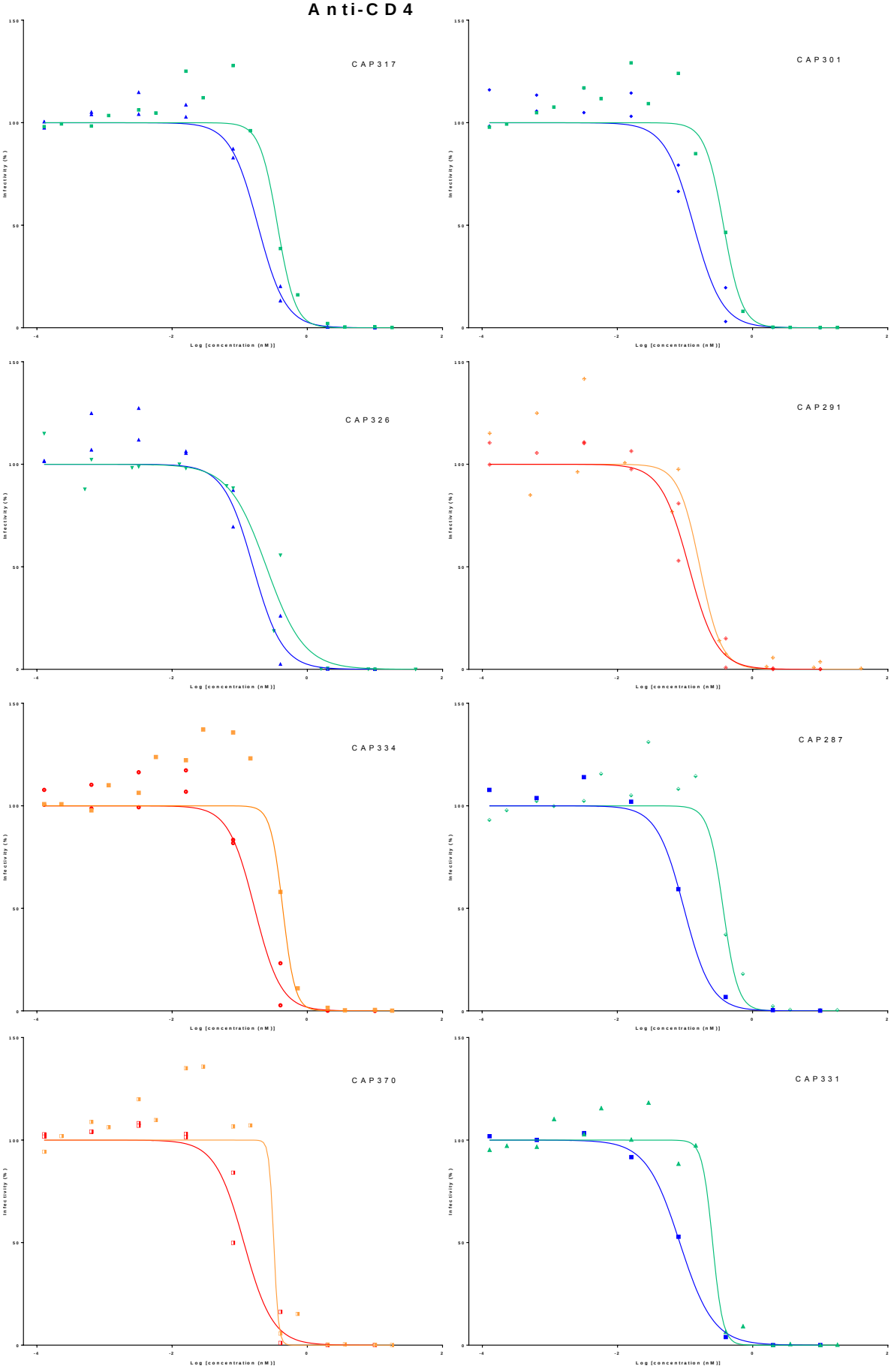
CAP317
CAP301
CAP326
CAP291
CAP334
CAP287
CAP370
CAP331
Infectivity (%)
Log [concentration (nM)]

PSC-RANTES

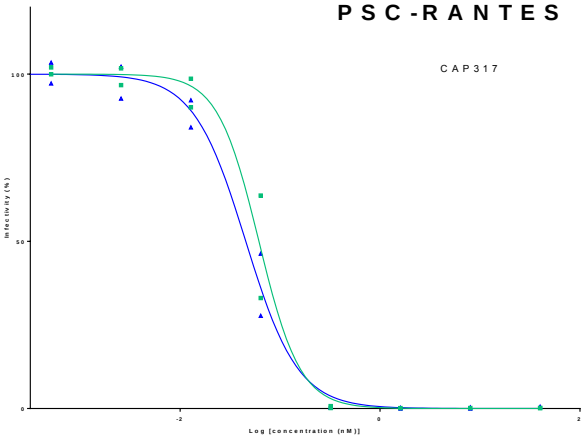
CAP317
Infectivity (%)
Log [concentration (nM)]

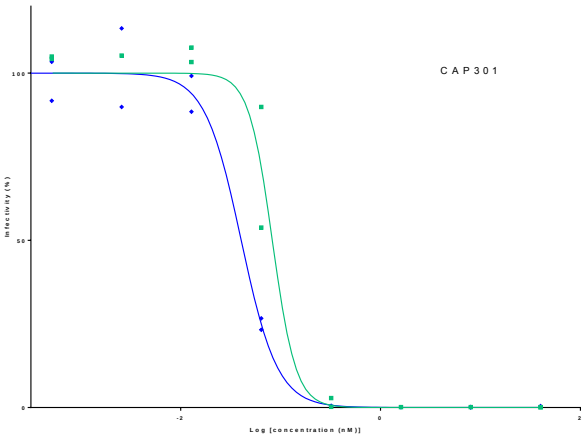
CAP301
Infectivity (%)
Log [concentration (nM)]

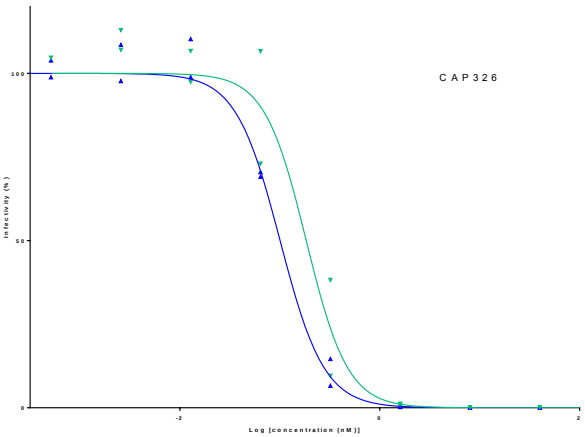
CAP326
Infectivity (%)
Log [concentration (nM)]

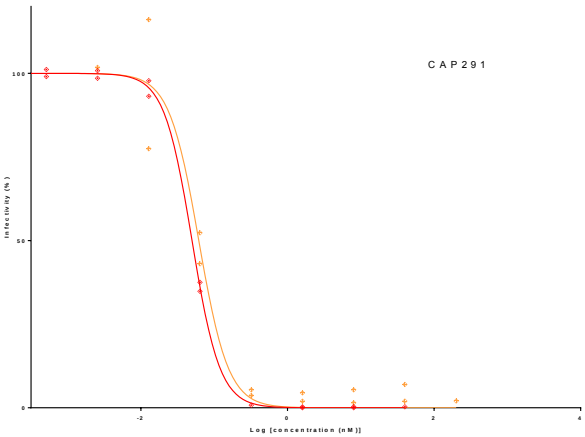
CAP291
Infectivity (%)
Log [concentration (nM)]

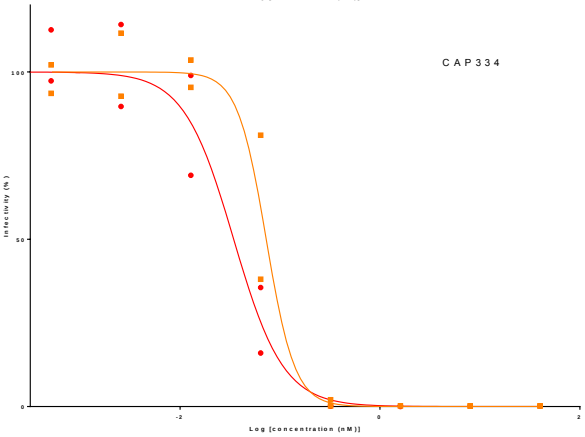
CAP334
Infectivity (%)
Log [concentration (nM)]

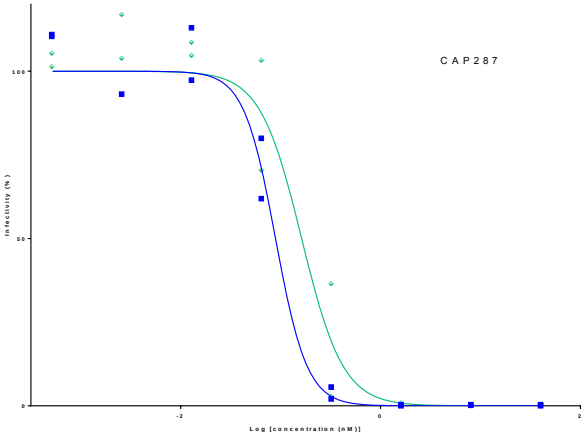
CAP287
Infectivity (%)
Log [concentration (nM)]

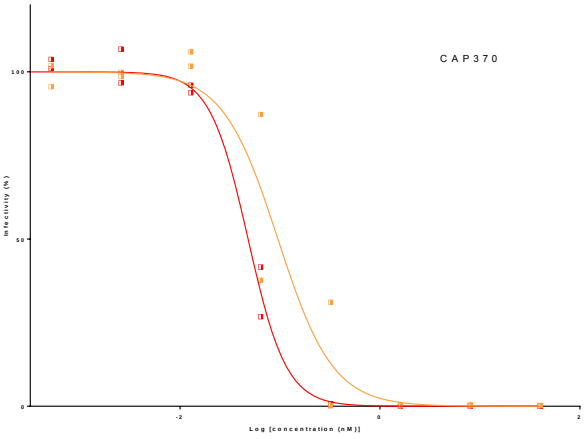
CAP370
Infectivity (%)
Log [concentration (nM)]

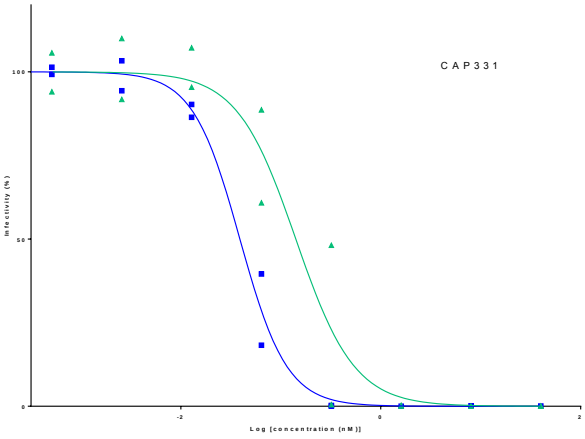
CAP331
Infectivity (%)
Log [concentration (nM)]

Figure 3F. Inhibition curves of pseudoviruses and their corresponding isolate. Inhibition curves show the log of the drug concentration on the x-axis and the percentage inhibition on the y-axis. Experiments were performed on TZM-bl cells with an incubation period of 48h after addition of the virus to the cells. Cool colours represent participants from the placebo arm while warm colours represent those from the TFV arm. On each figure, the darkly coloured curve (blue or red) represents inhibition of PSV growth while the lighter colour (turquoise or orange) shows inhibition of isolate replication. This experiment was performed using eight PSVs for each of four inhibitors (labelled at the top of each set of inhibition curves). Participant ID's are indicated in each figure to the right of the inhibition curve.

References

1. **UNAIDS**. 2013. Global Report: UNAIDS Report on the Global AIDS Epidemic 2013.
2. **Leclerc-Madlala S**, **Simbayi L**, **Cloete A**. 2009. The Sociocultural Aspects of HIV/AIDS in South Africa 25 Years On. Psychosocial Perspectives. Springer Science + Business Media, LLC.
3. **E. Ordóñez C**, **C. Marconi V**. 2012. Understanding HIV Risk Behavior from a Sociocultural Perspective. J AIDS Clin Res **3**:online.
4. **Mbonye M**, **Nalukenge W**, **Nakamanya S**, **Nalusiba B**, **King R**, **Vandepitte J**, **Seeley J**. 2012. Gender inequity in the lives of women involved in sex work in Kampala, Uganda. J Int AIDS Soc **15 Suppl 1**:1–9.
5. **Leclerc-Madlala S**. 2008. Age-disparate and intergenerational sex in southern Africa: the dynamics of hypervulnerability. AIDS **22 Suppl 4**:S17-25.
6. **Leclerc-Madlala S**. 2009. Cultural scripts for multiple and concurrent partnerships in southern Africa: why HIV prevention needs anthropology. Sex Health **6**:103.
7. **Dunkle KL**, **Jewkes RK**, **Brown HC**, **Gray GE**, **McIntryre JA**, **Harlow SD**. 2004. Gender-based violence, relationship power, and risk of HIV infection in women attending antenatal clinics in South Africa. Lancet **363**:1415–1421.
8. **MacPherson EE**, **Sadalaki J**, **Njoloma M**, **Nyongopa V**, **Nkhwazi L**, **Mwapasa V**, **Lalloo DG**, **Desmond N**, **Seeley J**, **Theobald S**. 2012. Transactional sex and HIV: understanding the gendered structural drivers of HIV in fishing communities in Southern Malawi. J Int AIDS Soc **15 Suppl 1**:1–9.
9. **Patel P**, **Borkowf CB**, **Brooks JT**, **Lasry A**, **Lansky A**, **Mermin J**. 2014. Estimating per-act HIV transmission risk: a systematic review. AIDS **28**:1509–19.
10. **Boily M-C**, **Baggaley RF**, **Wang L**, **Masse B**, **White RG**, **Hayes RJ**, **Alary M**. 2009. Heterosexual risk of HIV-1 infection per sexual act: systematic review and meta-analysis of observational studies. Lancet Infect Dis **9**:118–129.
11. **Hughes JP**, **Baeten JM**, **Lingappa JR**, **Magaret AS**, **Wald A**, **de Bruyn G**, **Kiarie J**, **Inambao M**, **Kilembe W**, **Farquhar C**, **Celum C**, **Partners in Prevention HSV/HIV Transmission Study Team**. 2012. Determinants of per-coital-act HIV-1 infectivity among African HIV-1-serodiscordant couples. J Infect Dis **205**:358–65.
12. **Long EM**, **Martin HL**, **Kreiss JK**, **Rainwater SM**, **Lavreys L**, **Jackson DJ**, **Rakwar J**, **Mandaliya K**, **Overbaugh J**. 2000. Gender differences in HIV-1 diversity at time of infection. Nat Med **6**:71–5.
13. **Barreto-de-Souza V**, **Arakelyan A**, **Margolis L**, **Vanpouille C**. 2014. HIV-1 Vaginal Transmission: Cell-Free or Cell-Associated Virus? Am J Reprod Immunol **71**:589–599.

14. **Haase AT**. 2010. Targeting early infection to prevent HIV-1 mucosal transmission. Nature **464**:217–23.
15. **Plummer FA**, **Simonsen JN**, **Cameron DW**, **Ndinya-Achola JO**, **Kreiss JK**, **Gakinya MN**, **Waiyaki P**, **Cheang M**, **Piot P**, **Ronald AR**. 1991. Cofactors in male-female sexual transmission of human immunodeficiency virus type 1. J Infect Dis **163**:233–9.
16. **Shey MS**, **Garrett NJ**, **McKinnon LR**, **Passmore J-AS**. 2015. The role of dendritic cells in driving genital tract inflammation and HIV transmission risk: are there opportunities to intervene? Innate Immun **21**:99–112.
17. **Heffron R**, **Donnell D**, **Rees H**, **Celum C**, **Mugo N**, **Were E**, **de Bruyn G**, **Nakku-Joloba E**, **Ngure K**, **Kiarie J**, **Coombs RW**, **Baeten JM**, **Partners in Prevention HSV/HIV Transmission Study Team**. 2012. Use of hormonal contraceptives and risk of HIV-1 transmission: a prospective cohort study. Lancet Infect Dis **12**:19–26.
18. **Royce RA**, **Seña A**, **Cates W**, **Cohen MS**. 1997. Sexual transmission of HIV. N Engl J Med **336**:1072–1078.
19. **Laga M**, **Manoka A**, **Kivuvu M**, **Malele B**, **Tuliza M**, **Nzila N**, **Goeman J**, **Behets F**, **Batter V**, **Alary M**. 1993. Non-ulcerative sexually transmitted diseases as risk factors for HIV-1 transmission in women: results from a cohort study. AIDS **7**:95–102.
20. **Pellett Madan R**, **Masson L**, **Tugetman J**, **Werner L**, **Grobler A**, **Mlisana K**, **Lo Y**, **Che D**, **Arnold KB**, **Abdool Karim SS**, **Passmore J-AS**, **Herold BC**. 2015. Innate Antibacterial Activity in Female Genital Tract Secretions Is Associated with Increased Risk of HIV Acquisition. AIDS Res Hum Retroviruses **31**:1153–1159.
21. **Masson L**, **Passmore J-AS**, **Liebenberg LJ**, **Werner L**, **Baxter C**, **Arnold KB**, **Williamson C**, **Little F**, **Mansoor LE**, **Naranbhai V**, **Lauffenburger D a.**, **Ronacher K**, **Walzl G**, **Garrett NJ**, **Williams BL**, **Couto-Rodriguez M**, **Hornig M**, **Lipkin WI**, **Grobler A**, **Abdool Karim QA**, **Abdool Karim SS**. 2015. Genital Inflammation and the Risk of HIV Acquisition in Women. Clin Infect Dis **61**:260–269.
22. **Maartens G**, **Celum C**, **Lewin SR**. 2014. HIV infection: epidemiology, pathogenesis, treatment, and prevention. Lancet **384**:258–271.
23. **Keele BF**, **Giorgi EE**, **Salazar-Gonzalez JF**, **Decker JM**, **Pham KT**, **Salazar MG**, **Sun C**, **Grayson T**, **Wang S**, **Li H**, **Wei X**, **Jiang C**, **Kirchherr JL**, **Gao F**, **Anderson JA**, **Ping L-H**, **Swanstrom R**, **Tomaras GD**, **Blattner WA**, **Goepfert PA**, **Kilby JM**, **Saag MS**, **Delwart EL**, **Busch MP**, **Cohen MS**, **Montefiori DC**, **Haynes BF**, **Gaschen B**, **Athreya GS**, **Lee HY**, **Wood N**, **Seoighe C**, **Perelson AS**, **Bhattacharya T**, **Korber BT**, **Hahn BH**, **Shaw GM**. 2008. Identification and characterization of transmitted and early founder virus envelopes in primary HIV-1 infection. Proc Natl Acad Sci U S A **105**:7552–7.
24. **Derdeyn CA**. 2004. Envelope-Constrained Neutralization-Sensitive HIV-1 After

Heterosexual Transmission. Science **303**:2019–2022.

25. **Haaland RE**, **Hawkins PA**, **Salazar-Gonzalez J**, **Johnson A**, **Tichacek A**, **Karita E**, **Manigart O**, **Mulenga J**, **Keele BF**, **Shaw GM**, **Hahn BH**, **Allen SA**, **Derdeyn CA**, **Hunter E**. 2009. Inflammatory genital infections mitigate a severe genetic bottleneck in heterosexual transmission of subtype A and C HIV-1. PLoS Pathog **5**:e1000274.
26. **Salazar-Gonzalez JF**, **Salazar MG**, **Keele BF**, **Learn GH**, **Giorgi EE**, **Li H**, **Decker JM**, **Wang S**, **Baalwa J**, **Kraus MH**, **Parrish NF**, **Shaw KS**, **Guffey MB**, **Bar KJ**, **Davis KL**, **Ochsenbauer-Jambor C**, **Kappes JC**, **Saag MS**, **Cohen MS**, **Mulenga J**, **Derdeyn CA**, **Allen S**, **Hunter E**, **Markowitz M**, **Hraber P**, **Perelson AS**, **Bhattacharya T**, **Haynes BF**, **Korber BT**, **Hahn BH**, **Shaw GM**. 2009. Genetic identity, biological phenotype, and evolutionary pathways of transmitted/founder viruses in acute and early HIV-1 infection. J Exp Med **206**:1273–89.
27. **Abrahams M-R**, **Anderson JA**, **Giorgi EE**, **Seoighe C**, **Mlisana K**, **Ping L-H**, **Athreya GS**, **Treurnicht FK**, **Keele BF**, **Wood N**, **Salazar-Gonzalez JF**, **Bhattacharya T**, **Chu H**, **Hoffman I**, **Galvin S**, **Mapanje C**, **Kazembe P**, **Thebus R**, **Fiscus S**, **Hide W**, **Cohen MS**, **Karim SA**, **Haynes BF**, **Shaw GM**, **Hahn BH**, **Korber BT**, **Swanstrom R**, **Williamson C**. 2009. Quantitating the Multiplicity of Infection with Human Immunodeficiency Virus Type 1 Subtype C Reveals a Non-Poisson Distribution of Transmitted Variants. J Virol **83**:3556–3567.
28. **Bar KJ**, **Li H**, **Chamberland A**, **Tremblay C**, **Routy JP**, **Grayson T**, **Sun C**, **Wang S**, **Learn GH**, **Morgan CJ**, **Schumacher JE**, **Haynes BF**, **Keele BF**, **Hahn BH**, **Shaw GM**. 2010. Wide Variation in the Multiplicity of HIV-1 Infection among Injection Drug Users. J Virol **84**:6241–6247.
29. **Li H**, **Bar KJ**, **Wang S**, **Decker JM**, **Chen Y**, **Sun C**, **Salazar-Gonzalez JF**, **Salazar MG**, **Learn GH**, **Morgan CJ**, **Schumacher JE**, **Hraber P**, **Giorgi EE**, **Bhattacharya T**, **Korber BT**, **Perelson AS**, **Eron JJ**, **Cohen MS**, **Hicks CB**, **Haynes BF**, **Markowitz M**, **Keele BF**, **Hahn BH**, **Shaw GM**. 2010. High Multiplicity Infection by HIV-1 in Men Who Have Sex with Men. PLoS Pathog **6**:e1000890.
30. **Sagar M**, **Lavreys L**, **Baeten JM**, **Richardson BA**, **Mandaliya K**, **Chohan BH**, **Kreiss JK**, **Overbaugh J**. 2003. Infection with multiple human immunodeficiency virus type 1 variants is associated with faster disease progression. J Virol **77**:12921–6.
31. **Shaw GM**, **Hunter E**. 2012. HIV Transmission. Cold Spring Harb Perspect Med **2**:a006965–a006965.
32. **Masharsky AE**, **Dukhovlinova EN**, **Verevochkin SV.**, **Toussova OV.**, **Skochilov RV.**, **Anderson JA**, **Hoffman I**, **Cohen MS**, **Swanstrom R**, **Kozlov AP**. 2010. A substantial transmission bottleneck among newly and recently HIV-1-infected injection drug users in

St Petersburg, Russia. J Infect Dis **201**:1697–702.

33. **Weiss RA**. 1993. How does HIV cause AIDS? Science **260**:1273–9.
34. **Levy JA**. 1993. Pathogenesis of human immunodeficiency virus infection. Microbiol Rev **57**:183–289.
35. **Mellors JW**, **Rinaldo CR**, **Gupta P**, **White RM**, **Todd JA**, **Kingsley LA**. 1996. Prognosis in HIV-1 infection predicted by the quantity of virus in plasma. Science **272**:1167–70.
36. **Mellors JW**, **Muñoz A**, **Giorgi JV**, **Margolick JB**, **Tassoni CJ**, **Gupta P**, **Kingsley LA**, **Todd JA**, **Saah AJ**, **Detels R**, **Phair JP**, **Rinaldo CR**. 1997. Plasma viral load and CD4+ lymphocytes as prognostic markers of HIV-1 infection. Ann Intern Med **126**:946–54.
37. **Lavreys L**, **Baeten JM**, **Chohan V**, **McClelland RS**, **Hassan WM**, **Richardson BA**, **Mandaliya K**, **Achola JON**, **Overbaugh J**. 2006. Higher Set Point Plasma Viral Load and More-Severe Acute HIV Type 1 (HIV-1) Illness Predict Mortality among High-Risk HIV-1-Infected African Women. Clin Infect Dis **42**:1333–1339.
38. **van't Wout AB**, **Kootstra NA**, **Mulder-Kampinga GA**, **Albrecht-van Lent N**, **Scherpbier HJ**, **Veenstra J**, **Boer K**, **Coutinho RA**, **Miedema F**, **Schuitemaker H**. 1994. Macrophage-tropic variants initiate human immunodeficiency virus type 1 infection after sexual, parenteral, and vertical transmission. J Clin Invest **94**:2060–7.
39. **Ping L-H**, **Joseph SB**, **Anderson JA**, **Abrahams M-R**, **Salazar-Gonzalez JF**, **Kincer LP**, **Treurnicht FK**, **Arney L**, **Ojeda S**, **Zhang M**, **Keys J**, **Potter EL**, **Chu H**, **Moore P**, **Salazar MG**, **Iyer SS**, **Jabara C**, **Kirchherr J**, **Mapanje C**, **Ngandu N**, **Seoighe C**, **Hoffman I**, **Gao F**, **Tang Y**, **Labranche C**, **Lee B**, **Saville A**, **Vermeulen M**, **Fiscus S**, **Morris L**, **Abdool Karim SS**, **Haynes BF**, **Shaw GM**, **Korber BT**, **Hahn BH**, **Cohen MS**, **Montefiori D**, **Williamson C**, **Swanstrom R**, **CAPRISA Acute Infection Study and the Center for HIV-AIDS Vaccine Immunology Consortium**. 2013. Comparison of viral Env proteins from acute and chronic infections with subtype C human immunodeficiency virus type 1 identifies differences in glycosylation and CCR5 utilization and suggests a new strategy for immunogen design. J Virol **87**:7218–33.
40. **Zhang Z**. 1999. Sexual Transmission and Propagation of SIV and HIV in Resting and Activated CD4+ T Cells. Science **286**:1353–1357.
41. **Connor RI**, **Sheridan KE**, **Ceradini D**, **Choe S**, **Landau NR**. 1997. Change in Coreceptor Use Correlates with Disease Progression in HIV-1–Infected Individuals. J Exp Med **185**:621–628.
42. **Scarlatti G**, **Tresoldi E**, **Björndal Å**, **Fredriksson R**, **Colognesi C**, **Deng HK**, **Malnati MS**, **Plebani A**, **Siccardi AG**, **Littman DR**, **Fenyö EM**, **Lusso P**. 1997. In vivo evolution of HIV-1 co-receptor usage and sensitivity to chemokine-mediated suppression. Nat Med **3**:1259–65.

43. **Long EM**, **Rainwater SMJ**, **Lavreys L**, **Mandaliya K**, **Overbaugh J**. 2002. HIV type 1 variants transmitted to women in Kenya require the CCR5 coreceptor for entry, regardless of the genetic complexity of the infecting virus. AIDS Res Hum Retroviruses **18**:567–76.

44. **Chohan B**, **Lang D**, **Sagar M**, **Korber B**, **Lavreys L**, **Richardson B**, **Overbaugh J**. 2005. Selection for Human Immunodeficiency Virus Type 1 Envelope Glycosylation Variants with Shorter V1-V2 Loop Sequences Occurs during Transmission of Certain Genetic Subtypes and May Impact Viral RNA Levels. J Virol **79**:6528–6531.

45. **Sagar M**, **Laeyendecker O**, **Lee S**, **Gamiel J**, **Wawer MJ**, **Gray RH**, **Serwadda D**, **Sewankambo NK**, **Shepherd JC**, **Toma J**, **Huang W**, **Quinn TC**. 2009. Selection of HIV variants with signature genotypic characteristics during heterosexual transmission. J Infect Dis **199**:580–9.

46. **Gnanakaran S**, **Bhattacharya T**, **Daniels M**. 2011. Recurrent signature patterns in HIV-1 B clade envelope glycoproteins associated with either early or chronic infections. PLoS ….

47. **Parrish NF**, **Gao F**, **Li H**, **Giorgi EE**, **Barbian HJ**, **Parrish EH**, **Zajic L**, **Iyer SS**, **Decker JM**, **Kumar A**, **Hora B**, **Berg A**, **Cai F**, **Hopper J**, **Denny TN**, **Ding H**, **Ochsenbauer C**, **Kappes JC**, **Galimidi RP**, **West AP**, **Bjorkman PJ**, **Wilen CB**, **Doms RW**, **O'Brien M**, **Bhardwaj N**, **Borrow P**, **Haynes BF**, **Muldoon M**, **Theiler JP**, **Korber B**, **Shaw GM**, **Hahn BH**. 2013. Phenotypic properties of transmitted founder HIV-1. Proc Natl Acad Sci **110**:6626–6633.

48. **Deymier MJ**, **Ende Z**, **Fenton-May AE**, **Dilernia DA**, **Kilembe W**, **Allen SA**, **Borrow P**, **Hunter E**. 2015. Heterosexual Transmission of Subtype C HIV-1 Selects Consensus-Like Variants without Increased Replicative Capacity or Interferon-α Resistance. PLoS Pathog **11**:e1005154.

49. **Wilen CB**, **Parrish NF**, **Pfaff JM**, **Decker JM**, **Henning EA**, **Haim H**, **Petersen JE**, **Wojcechowskyj JA**, **Sodroski J**, **Haynes BF**, **Montefiori DC**, **Tilton JC**, **Shaw GM**, **Hahn BH**, **Doms RW**. 2011. Phenotypic and immunologic comparison of clade B transmitted/founder and chronic HIV-1 envelope glycoproteins. J Virol **85**:8514–27.

50. **Carlson JM**, **Schaefer M**, **Monaco DC**, **Batorsky R**, **Claiborne DT**, **Prince J**, **Deymier MJ**, **Ende ZS**, **Klatt NR**, **DeZiel CE**, **Lin T-H**, **Peng J**, **Seese AM**, **Shapiro R**, **Frater J**, **Ndung'u T**, **Tang J**, **Goepfert P**, **Gilmour J**, **Price MA.**, **Kilembe W**, **Heckerman D**, **Goulder PJR**, **Allen TM**, **Allen S**, **Hunter E**. 2014. Selection bias at the heterosexual HIV-1 transmission bottleneck. Science **345**:1254031–1254031.

51. **Boeras DI**, **Hraber PT**, **Hurlston M**, **Evans-Strickfaden T**, **Bhattacharya T**, **Giorgi EE**, **Mulenga J**, **Karita E**, **Korber BT**, **Allen S**, **Hart CE**, **Derdeyn CA**, **Hunter E**. 2011. Role of donor genital tract HIV-1 diversity in the transmission bottleneck. Proc Natl Acad Sci **108**:E1156–E1163.

52. **Fanales-Belasio E**, **Raimondo M**, **Suligoi B**, **Buttò S**. 2010. HIV virology and pathogenetic mechanisms of infection: a brief overview. Ann Ist Super Sanita **46**:5–14.
53. **Hallenberger S**, **Bosch V**, **Angliker H**, **Shaw E**, **Klenk HD**, **Garten W**. 1992. Inhibition of furin-mediated cleavage activation of HIV-1 glycoprotein gp160. Nature **360**:358–61.
54. **Gu M**, **Rappaport J**, **Leppla SH**. 1995. Furin is important but not essential for the proteolytic maturation of gp160 of HIV-1. FEBS Lett **365**:95–7.
55. **Moulard M**, **Hallenberger S**, **Garten W**, **Klenk HD**. 1999. Processing and routage of HIV glycoproteins by furin to the cell surface. Virus Res **60**:55–65.
56. **Earl PL**, **Doms RW**, **Moss B**. 1990. Oligomeric structure of the human immunodeficiency virus type 1 envelope glycoprotein. Proc Natl Acad Sci **87**:648–652.
57. **Weiss CD**, **Levy JA**, **White JM**. 1990. Oligomeric organization of gp120 on infectious human immunodeficiency virus type 1 particles. J Virol **64**:5674–7.
58. **Carr JM**, **Hocking H**, **Li P**, **Burrell CJ**. 1999. Rapid and Efficient Cell-to-Cell Transmission of Human Immunodeficiency Virus Infection from Monocyte-Derived Macrophages to Peripheral Blood Lymphocytes. Virology **265**:319–329.
59. **Sattentau Q**. 2008. Avoiding the void: cell-to-cell spread of human viruses. Nat Rev Microbiol **6**:815–26.
60. **Zhong P**, **Agosto LM**, **Ilinskaya A**, **Dorjbal B**, **Truong R**, **Derse D**, **Uchil PD**, **Heidecker G**, **Mothes W**. 2013. Cell-to-Cell Transmission Can Overcome Multiple Donor and Target Cell Barriers Imposed on Cell-Free HIV. PLoS One **8**:e53138.
61. **McDonald D**. 2003. Recruitment of HIV and Its Receptors to Dendritic Cell-T Cell Junctions. Science **300**:1295–1297.
62. **Hübner W**, **McNerney GP**, **Chen P**, **Dale BM**, **Gordon RE**, **Chuang FYS**, **Li X-D**, **Asmuth DM**, **Huser T**, **Chen BK**. 2009. Quantitative 3D video microscopy of HIV transfer across T cell virological synapses. Science **323**:1743–7.
63. **Martin N**, **Welsch S**, **Jolly C**, **Briggs JAG**, **Vaux D**, **Sattentau QJ**. 2010. Virological synapse-mediated spread of human immunodeficiency virus type 1 between T cells is sensitive to entry inhibition. J Virol **84**:3516–27.
64. **Felts RL**, **Narayan K**, **Estes JD**, **Shi D**, **Trubey CM**, **Fu J**, **Hartnell LM**, **Ruthel GT**, **Schneider DK**, **Nagashima K**, **Bess JW**, **Bavari S**, **Lowekamp BC**, **Bliss D**, **Lifson JD**, **Subramaniam S**. 2010. 3D visualization of HIV transfer at the virological synapse between dendritic cells and T cells. Proc Natl Acad Sci **107**:13336–13341.
65. **Jolly C**. 2004. HIV-1 Cell to Cell Transfer across an Env-induced, Actin-dependent Synapse. J Exp Med **199**:283–293.
66. **Groot F**, **Welsch S**, **Sattentau QJ**. 2008. Efficient HIV-1 transmission from macrophages to T cells across transient virological synapses. Blood **111**:4660–4663.

67. **Jolly C**, **Mitar I**, **Sattentau QJ**. 2007. Adhesion molecule interactions facilitate human immunodeficiency virus type 1-induced virological synapse formation between T cells. J Virol **81**:13916–21.
68. **Duncan CJA**, **Williams JP**, **Schiffner T**, **Gartner K**, **Ochsenbauer C**, **Kappes J**, **Russell RA**, **Frater J**, **Sattentau QJ**. 2014. High-Multiplicity HIV-1 Infection and Neutralizing Antibody Evasion Mediated by the Macrophage-T Cell Virological Synapse. J Virol **88**:2025–2034.
69. **Agosto LM**, **Uchil PD**, **Mothes W**. 2015. HIV cell-to-cell transmission: effects on pathogenesis and antiretroviral therapy. Trends Microbiol **23**:289–295.
70. **Russell RA**, **Martin N**, **Mitar I**, **Jones E**, **Sattentau QJ**. 2013. Multiple proviral integration events after virological synapse-mediated HIV-1 spread. Virology **443**:143–149.
71. **Sigal A**, **Kim JT**, **Balazs AB**, **Dekel E**, **Mayo A**, **Milo R**, **Baltimore D**. 2011. Cell-to-cell spread of HIV permits ongoing replication despite antiretroviral therapy. Nature **477**:95–8.
72. **Duncan CJA**, **Russell RA**, **Sattentau QJ**. 2013. High multiplicity HIV-1 cell-to-cell transmission from macrophages to CD4+ T cells limits antiretroviral efficacy. AIDS **27**:2201–2206.
73. **Abela IA**, **Berlinger L**, **Schanz M**, **Reynell L**, **Günthard HF**, **Rusert P**, **Trkola A**. 2012. Cell-Cell Transmission Enables HIV-1 to Evade Inhibition by Potent CD4bs Directed Antibodies. PLoS Pathog **8**:e1002634.
74. **Schiffner T**, **Sattentau QJ**, **Duncan CJA**. 2013. Cell-to-cell spread of HIV-1 and evasion of neutralizing antibodies. Vaccine **31**:5789–5797.
75. **Wilen CB**, **Tilton JC**, **Doms RW**. 2012. HIV: cell binding and entry. Cold Spring Harb Perspect Med **2**:1–14.
76. **Rangel HR**, **Weber J**, **Chakraborty B**, **Gutierrez A**, **Marotta ML**, **Mirza M**, **Kiser P**, **Martinez MA**, **Este JA**, **Quin ME**. 2003. Role of the Human Immunodeficiency Virus Type 1 Envelope Gene in Viral Fitness **77**:9069–9073.
77. **Marozsan AJ**, **Moore DM**, **Lobritz MA**, **Fraundorf E**, **Abraha A**, **Reeves JD**, **Arts EJ**. 2005. Differences in the Fitness of Two Diverse Wild-Type Human Immunodeficiency Virus Type 1 Isolates Are Related to the Efficiency of Cell Binding and Entry. J Virol **79**:7121–7134.
78. FDA-Approved HIV Medicines | HIV/AIDS Fact Sheets | Education Materials | AIDSinfo.
79. **Attia S**, **Egger M**, **Müller M**, **Zwahlen M**, **Low N**. 2009. Sexual transmission of HIV according to viral load and antiretroviral therapy: systematic review and meta-analysis. AIDS **23**:1397–1404.
80. **Donnell D**, **Baeten JM**, **Kiarie J**, **Thomas KK**, **Stevens W**, **Cohen CR**, **McIntyre J**,

Lingappa JR, **Celum C**. 2010. Heterosexual HIV-1 transmission after initiation of antiretroviral therapy: a prospective cohort analysis. Lancet **375**:2092–2098.

81. **Reynolds SJ**, **Makumbi F**, **Nakigozi G**, **Kagaayi J**, **Gray RH**, **Wawer M**, **Quinn TC**, **Serwadda D**. 2011. HIV-1 transmission among HIV-1 discordant couples before and after the introduction of antiretroviral therapy. AIDS **25**:473–7.
82. **Del Romero J**, **Castilla J**, **Hernando V**, **Rodriguez C**, **Garcia S**. 2010. Combined antiretroviral treatment and heterosexual transmission of HIV-1: cross sectional and prospective cohort study. BMJ **340**:c2205–c2205.
83. **Bunnell R**, **Ekwaru JP**, **Solberg P**, **Wamai N**, **Bikaako-Kajura W**, **Were W**, **Coutinho A**, **Liechty C**, **Madraa E**, **Rutherford G**, **Mermin J**. 2006. Changes in sexual behavior and risk of HIV transmission after antiretroviral therapy and prevention interventions in rural Uganda. AIDS **20**:85–92.
84. **Anglemyer A**, **Horvath T**, **Rutherford G**. 2013. Antiretroviral Therapy for Prevention of HIV Transmission in HIV-Discordant Couples. JAMA **310**:1619.
85. **Cohen MS**, **Chen YQ**, **McCauley M**, **Gamble T**, **Hosseinipour MC**, **Kumarasamy N**, **Hakim JG**, **Kumwenda J**, **Grinsztejn B**, **Pilotto JHS**, **Godbole S V**, **Mehendale S**, **Chariyalertsak S**, **Santos BR**, **Mayer KH**, **Hoffman IF**, **Eshleman SH**, **Piwowar-Manning E**, **Wang L**, **Makhema J**, **Mills LA**, **de Bruyn G**, **Sanne I**, **Eron J**, **Gallant J**, **Havlir D**, **Swindells S**, **Ribaudo H**, **Elharrar V**, **Burns D**, **Taha TE**, **Nielsen-Saines K**, **Celentano D**, **Essex M**, **Fleming TR**. 2011. Prevention of HIV-1 Infection with Early Antiretroviral Therapy. N Engl J Med **365**:493–505.
86. **Lallemant M**, **Jourdain G**, **Le Coeur S**, **Mary JY**, **Ngo-Giang-Huong N**, **Koetsawang S**, **Kanshana S**, **McIntosh K**, **Thaineua V**, **Perinatal HIV Prevention Trial (Thailand) Investigators**. 2004. Single-dose perinatal nevirapine plus standard zidovudine to prevent mother-to-child transmission of HIV-1 in Thailand. N Engl J Med **351**:217–28.
87. **Jackson JB**, **Musoke P**, **Fleming T**, **Guay LA**, **Bagenda D**, **Allen M**, **Nakabiito C**, **Sherman J**, **Bakaki P**, **Owor M**, **Ducar C**, **Deseyve M**, **Mwatha A**, **Emel L**, **Duefield C**, **Mirochnick M**, **Fowler MG**, **Mofenson L**, **Miotti P**, **Gigliotti M**, **Bray D**, **Mmiro F**. 2003. Intrapartum and neonatal single-dose nevirapine compared with zidovudine for prevention of mother-to-child transmission of HIV-1 in Kampala, Uganda: 18-month follow-up of the HIVNET 012 randomised trial. Lancet (London, England) **362**:859–68.
88. **Townsend CL**, **Cortina-Borja M**, **Peckham CS**, **de Ruiter A**, **Lyall H**, **Tookey PA**. 2008. Low rates of mother-to-child transmission of HIV following effective pregnancy interventions in the United Kingdom and Ireland, 2000-2006. AIDS **22**:973–81.
89. **Grant RM**, **Lama JR**, **Anderson PL**, **McMahan V**, **Liu AY**, **Vargas L**, **Goicochea P**, **Casapía M**, **Guanira-Carranza JV**, **Ramirez-Cardich ME**, **Montoya-Herrera O**,

Fernández T, **Veloso VG**, **Buchbinder SP**, **Chariyalertsak S**, **Schechter M**, **Bekker L-G**, **Mayer KH**, **Kallás EG**, **Amico KR**, **Mulligan K**, **Bushman LR**, **Hance RJ**, **Ganoza C**, **Defechereux P**, **Postle B**, **Wang F**, **McConnell JJ**, **Zheng J-H**, **Lee J**, **Rooney JF**, **Jaffe HS**, **Martinez AI**, **Burns DN**, **Glidden DV.** 2010. Preexposure Chemoprophylaxis for HIV Prevention in Men Who Have Sex with Men. N Engl J Med **363**:2587–2599.

90. **Baeten JM**, **Donnell D**, **Ndase P**, **Mugo NR**, **Campbell JD**, **Wangisi J**, **Tappero JW**, **Bukusi EA**, **Cohen CR**, **Katabira E**, **Ronald A**, **Tumwesigye E**, **Were E**, **Fife KH**, **Kiarie J**, **Farquhar C**, **John-Stewart G**, **Kakia A**, **Odoyo J**, **Mucunguzi A**, **Nakku-Joloba E**, **Twesigye R**, **Ngure K**, **Apaka C**, **Tamooh H**, **Gabona F**, **Mujugira A**, **Panteleeff D**, **Thomas KK**, **Kidoguchi L**, **Krows M**, **Revall J**, **Morrison S**, **Haugen H**, **Emmanuel-Ogier M**, **Ondrejcek L**, **Coombs RW**, **Frenkel L**, **Hendrix C**, **Bumpus NN**, **Bangsberg D**, **Haberer JE**, **Stevens WS**, **Lingappa JR**, **Celum C**. 2012. Antiretroviral Prophylaxis for HIV Prevention in Heterosexual Men and Women. N Engl J Med **367**:399–410.

91. **Thigpen MC**, **Kebaabetswe PM**, **Paxton LA**, **Smith DK**, **Rose CE**, **Segolodi TM**, **Henderson FL**, **Pathak SR**, **Soud FA**, **Chillag KL**, **Mutanhaurwa R**, **Chirwa LI**, **Kasonde M**, **Abebe D**, **Buliva E**, **Gvetadze RJ**, **Johnson S**, **Sukalac T**, **Thomas VT**, **Hart C**, **Johnson JA**, **Malotte CK**, **Hendrix CW**, **Brooks JT**, **TDF2 Study Group**. 2012. Antiretroviral preexposure prophylaxis for heterosexual HIV transmission in Botswana. N Engl J Med **367**:423–34.

92. **Van Damme L**, **Corneli A**, **Ahmed K**, **Agot K**, **Lombaard J**, **Kapiga S**, **Malahleha M**, **Owino F**, **Manongi R**, **Onyango J**, **Temu L**, **Monedi MC**, **Mak'Oketch P**, **Makanda M**, **Reblin I**, **Makatu SE**, **Saylor L**, **Kiernan H**, **Kirkendale S**, **Wong C**, **Grant R**, **Kashuba A**, **Nanda K**, **Mandala J**, **Fransen K**, **Deese J**, **Crucitti T**, **Mastro TD**, **Taylor D**. 2012. Preexposure Prophylaxis for HIV Infection among African Women. N Engl J Med **367**:411–422.

93. **Marrazzo JM**, **Ramjee G**, **Richardson BA**, **Gomez K**, **Mgodi N**, **Nair G**, **Palanee T**, **Nakabiito C**, **van der Straten A**, **Noguchi L**, **Hendrix CW**, **Dai JY**, **Ganesh S**, **Mkhize B**, **Taljaard M**, **Parikh UM**, **Piper J**, **Mâsse B**, **Grossman C**, **Rooney J**, **Schwartz JL**, **Watts H**, **Marzinke MA**, **Hillier SL**, **McGowan IM**, **Chirenje ZM**. 2015. Tenofovir-Based Preexposure Prophylaxis for HIV Infection among African Women. N Engl J Med **372**:509–518.

94. **Andrews CD**, **Heneine W**. 2015. Cabotegravir long-acting for HIV-1 prevention. Curr Opin HIV AIDS **10**:258–263.

95. **Abdool Karim Q**, **Abdool Karim SS**, **Frohlich JA**, **Grobler AC**, **Baxter C**, **Mansoor LE**, **Kharsany ABM**, **Sibeko S**, **Mlisana KP**, **Omar Z**, **Gengiah TN**, **Maarschalk S**, **Arulappan N**, **Mlotshwa M**, **Morris L**, **Taylor D**. 2010. Effectiveness and Safety of Tenofovir Gel, an

Antiretroviral Microbicide, for the Prevention of HIV Infection in Women. Science **329**:1168–1174.

96. **Baeten JM**, **Palanee-Phillips T**, **Brown ER**, **Schwartz K**, **Soto-Torres LE**, **Govender V**, **Mgodi NM**, **Matovu Kiweewa F**, **Nair G**, **Mhlanga F**, **Siva S**, **Bekker L-G**, **Jeenarain N**, **Gaffoor Z**, **Martinson F**, **Makanani B**, **Pather A**, **Naidoo L**, **Husnik M**, **Richardson BA**, **Parikh UM**, **Mellors JW**, **Marzinke MA**, **Hendrix CW**, **van der Straten A**, **Ramjee G**, **Chirenje ZM**, **Nakabiito C**, **Taha TE**, **Jones J**, **Mayo A**, **Scheckter R**, **Berthiaume J**, **Livant E**, **Jacobson C**, **Ndase P**, **White R**, **Patterson K**, **Germuga D**, **Galaska B**, **Bunge K**, **Singh D**, **Szydlo DW**, **Montgomery ET**, **Mensch BS**, **Torjesen K**, **Grossman CI**, **Chakhtoura N**, **Nel A**, **Rosenberg Z**, **McGowan I**, **Hillier S**. 2016. Use of a Vaginal Ring Containing Dapivirine for HIV-1 Prevention in Women. N Engl J Med NEJMoa1506110.

97. **Karim QA**, **Baxter C**, **Karim SA**. 2013. Topical Microbicides—What's New? JAIDS J Acquir Immune Defic Syndr **63**:S144–S149.

98. **Williams BG**, **Abdool Karim SS**, **Abdool Karim QA**, **Gouws E**. 2011. Epidemiological impact of tenofovir gel on the HIV epidemic in South Africa. J Acquir Immune Defic Syndr **58**:207–10.

99. **McCormack S**, **Ramjee G**, **Kamali A**, **Rees H**, **Crook AM**, **Gafos M**, **Jentsch U**, **Pool R**, **Chisembele M**, **Kapiga S**, **Mutemwa R**, **Vallely A**, **Palanee T**, **Sookrajh Y**, **Lacey CJ**, **Darbyshire J**, **Grosskurth H**, **Profy A**, **Nunn A**, **Hayes R**, **Weber J**. 2010. PRO2000 vaginal gel for prevention of HIV-1 infection (Microbicides Development Programme 301): a phase 3, randomised, double-blind, parallel-group trial. Lancet (London, England) **376**:1329–37.

100. **Roddy RE**, **Zekeng L**, **Ryan KA**, **Tamoufé U**, **Weir SS**, **Wong EL**. 1998. A controlled trial of nonoxynol 9 film to reduce male-to-female transmission of sexually transmitted diseases. N Engl J Med **339**:504–10.

101. **Niruthisard S**, **Roddy RE**, **Chutivongse S**. 1991. The effects of frequent nonoxynol-9 use on the vaginal and cervical mucosa. Sex Transm Dis **18**:176–9.

102. **Fichorova RN**, **Tucker LD**, **Anderson DJ**. 2001. The molecular basis of nonoxynol-9-induced vaginal inflammation and its possible relevance to human immunodeficiency virus type 1 transmission. J Infect Dis **184**:418–28.

103. **De Clercq E**. 2007. Acyclic nucleoside phosphonates: Past, present and future. Biochem Pharmacol **73**:911–922.

104. **Barditch-Crovo P**, **Deeks SG**, **Collier A**, **Safrin S**, **Coakley DF**, **Miller M**, **Kearney BP**, **Coleman RL**, **Lamy PD**, **Kahn JO**, **McGowan I**, **Lietman PS**. 2001. Phase I/II Trial of the Pharmacokinetics, Safety, and Antiretroviral Activity of Tenofovir Disoproxil Fumarate in Human Immunodeficiency Virus-Infected Adults. Antimicrob Agents Chemother

45:2733–2739.

105. **Abdool Karim SS**, **Abdool Karim Q**, **Kharsany ABM**, **Baxter C**, **Grobler AC**, **Werner L**, **Kashuba A**, **Mansoor LE**, **Samsunder N**, **Mindel A**, **Gengiah TN**. 2015. Tenofovir Gel for the Prevention of Herpes Simplex Virus Type 2 Infection. N Engl J Med **373**:530–539.
106. **Mansoor LE**, **Abdool Karim QA**, **Werner L**, **Madlala B**, **Ngcobo N**, **Cornman DH**, **Amico KR**, **Fisher J**, **Fisher WA**, **Macqueen KM**, **Abdool Karim SS**. 2014. Impact of an adherence intervention on the effectiveness of tenofovir gel in the CAPRISA 004 trial. AIDS Behav **18**:841–8.
107. **Mansoor LE**, **Abdool Karim QA**, **Yende-Zuma N**, **MacQueen KM**, **Baxter C**, **Madlala BT**, **Grobler A**, **Abdool Karim SS**. 2014. Adherence in the CAPRISA 004 tenofovir gel microbicide trial. AIDS Behav **18**:811–9.
108. **Delany-Moretlwe SA**, **Lombard C**, **Baron D**, **Panchia R**, **Myer L**, **Schwartz JL**, **Doncel GF**, **Gray GE**, **Rees H**. 2015. FACTS 001 Phase III Trial of Pericoital Tenofovir 1% Gel for HIV Prevention in Women, p. 90–91. *In* CROI, Seattle, Washington.
109. **Sethi AK**, **Celentano DD**, **Gange SJ**, **Moore RD**, **Gallant JE**. 2003. Association between adherence to antiretroviral therapy and human immunodeficiency virus drug resistance. Clin Infect Dis **37**:1112–8.
110. **Brenner BG**, **Oliveira M**, **Doualla-Bell F**, **Moisi DD**, **Ntemgwa M**, **Frankel F**, **Essex M**, **Wainberg MA**. 2006. HIV-1 subtype C viruses rapidly develop K65R resistance to tenofovir in cell culture. AIDS **20**:F9–F13.
111. **White KL**, **Margot NA**, **Wrin T**, **Petropoulos CJ**, **Miller MD**, **Naeger LK**. 2002. Molecular Mechanisms of Resistance to Human Immunodeficiency Virus Type 1 with Reverse Transcriptase Mutations K65R and K65R+M184V and Their Effects on Enzyme Function and Viral Replication Capacity. Antimicrob Agents Chemother **46**:3437–3446.
112. **Hoffmann CJ**, **Ledwaba J**, **Li J-F**, **Johnston V**, **Hunt G**, **Fielding KL**, **Chaisson RE**, **Churchyard GJ**, **Grant AD**, **Johnson JA**, **Charalambous S**, **Morris L**. 2013. Resistance to tenofovir-based regimens during treatment failure of subtype C HIV-1 in South Africa. Antivir Ther **18**:915–20.
113. **Van Zyl GU**, **Liu TF**, **Claassen M**, **Engelbrecht S**, **de Oliveira T**, **Preiser W**, **Wood NT**, **Travers S**, **Shafer RW**. 2013. Trends in Genotypic HIV-1 Antiretroviral Resistance between 2006 and 2012 in South African Patients Receiving First- and Second-Line Antiretroviral Treatment Regimens. PLoS One **8**:e67188.
114. **Sunpath H**, **Wu B**, **Gordon M**, **Hampton J**, **Johnson B**, **Moosa M-YS**, **Ordonez C**, **Kuritzkes DR**, **Marconi VC**. 2012. High rate of K65R for antiretroviral therapy-naive patients with subtype C HIV infection failing a tenofovir-containing first-line regimen. AIDS **26**:1679–84.

115. **Skhosana L**, **Steegen K**, **Bronze M**, **Lukhwareni A**, **Letsoalo E**, **Papathanasopoulos MA**, **Carmona SC**, **Stevens WS**. 2015. High prevalence of the K65R mutation in HIV-1 subtype C infected patients failing tenofovir-based first-line regimens in South Africa. PLoS One **10**:e0118145.

116. **von Wyl V**, **Yerly S**, **Böni J**, **Bürgisser P**, **Klimkait T**, **Battegay M**, **Bernasconi E**, **Cavassini M**, **Furrer H**, **Hirschel B**, **Vernazza PL**, **Rickenbach M**, **Ledergerber B**, **Günthard HF**, **Swiss HIV Cohort Study**. 2008. Factors associated with the emergence of K65R in patients with HIV-1 infection treated with combination antiretroviral therapy containing tenofovir. Clin Infect Dis **46**:1299–309.

117. **Yang W-L**, **Kouyos RD**, **Böni J**, **Yerly S**, **Klimkait T**, **Aubert V**, **Scherrer AU**, **Shilaih M**, **Hinkley T**, **Petropoulos C**, **Bonhoeffer S**, **Günthard HF**. 2015. Persistence of Transmitted HIV-1 Drug Resistance Mutations Associated with Fitness Costs and Viral Genetic Backgrounds. PLoS Pathog **11**:e1004722.

118. **Wei X**, **Hunt G**, **Abdool Karim SS**, **Naranbhai V**, **Sibeko S**, **Abdool Karim QA**, **Li J-F**, **Kashuba ADM**, **Werner L**, **Passmore J-AS**, **Morris L**, **Heneine W**, **Johnson JA**. 2014. Sensitive tenofovir resistance screening of HIV-1 from the genital and blood compartments of women with breakthrough infections in the CAPRISA 004 tenofovir gel trial. J Infect Dis **209**:1916–20.

119. **Garrett NJ**, **Werner L**, **Naicker N**, **Naranbhai V**, **Sibeko S**, **Samsunder N**, **Gray C**, **Williamson C**, **Morris L**, **Abdool Karim QA**, **Abdool Karim SS**. 2015. HIV disease progression in seroconvertors from the CAPRISA 004 tenofovir gel pre-exposure prophylaxis trial. J Acquir Immune Defic Syndr **68**:55–61.

120. **Naranbhai V**, **Abdool Karim SS**, **Altfeld M**, **Samsunder N**, **Durgiah R**, **Sibeko S**, **Abdool Karim QA**, **Carr WH**, **CAPRISA004 TRAPS team**. 2012. Innate immune activation enhances hiv acquisition in women, diminishing the effectiveness of tenofovir microbicide gel. J Infect Dis **206**:993–1001.

121. **Baeten JM**, **Chohan B**, **Lavreys L**, **Chohan V**, **McClelland RS**, **Certain L**, **Mandaliya K**, **Jaoko W**, **Overbaugh J**. 2007. HIV-1 Subtype D Infection Is Associated with Faster Disease Progression than Subtype A in Spite of Similar Plasma HIV-1 Loads. J Infect Dis **195**:1177–1180.

122. **Kaleebu P**, **French N**, **Mahe C**, **Yirrell D**, **Watera C**, **Lyagoba F**, **Nakiyingi J**, **Rutebemberwa A**, **Morgan D**, **Weber J**, **Gilks C**, **Whitworth J**. 2002. Effect of Human Immunodeficiency Virus (HIV) Type 1 Envelope Subtypes A and D on Disease Progression in a Large Cohort of HIV-1–Positive Persons in Uganda. J Infect Dis **185**:1244–1250.

123. **Mlisana K**, **Werner L**, **Garrett NJ**, **McKinnon LR**, **Loggerenberg F Van**, **Passmore JAS**,

Gray CM, **Morris L**, **Williamson C**, **AbdoolKarim SS**. 2014. Rapid disease progression in HIV-1 subtype C-infected South African women. Clin Infect Dis **59**:1322–1331.

124. **Schuitemaker H**, **Koot M**, **Kootstra NA**, **Dercksen MW**, **de Goede RE**, **van Steenwijk RP**, **Lange JM**, **Schattenkerk JK**, **Miedema F**, **Tersmette M**. 1992. Biological phenotype of human immunodeficiency virus type 1 clones at different stages of infection: progression of disease is associated with a shift from monocytotropic to T-cell-tropic virus population. J Virol **66**:1354–60.
125. **Karlsson A**, **Parsmyr K**, **Sandstrom E**, **Fenyo EM**, **Albert J**. 1994. MT-2 cell tropism as prognostic marker for disease progression in human immunodeficiency virus type 1 infection [see comments]. J Clin Microbiol **32**:364–370.
126. **Miura T**, **Brockman MA**, **Schneidewind A**, **Lobritz M**, **Pereyra F**, **Rathod A**, **Block BL**, **Brumme ZL**, **Brumme CJ**, **Baker B**, **Rothchild AC**, **Li B**, **Trocha A**, **Cutrell E**, **Frahm N**, **Brander C**, **Toth I**, **Arts EJ**, **Allen TM**, **Walker BD**. 2009. HLA-B57/B*5801 human immunodeficiency virus type 1 elite controllers select for rare gag variants associated with reduced viral replication capacity and strong cytotoxic T-lymphocyte [corrected] recognition. J Virol **83**:2743–55.
127. **Miura T**, **Brumme ZL**, **Brockman MA**, **Rosato P**, **Sela J**, **Brumme CJ**, **Pereyra F**, **Kaufmann DE**, **Trocha A**, **Block BL**, **Daar ES**, **Connick E**, **Jessen H**, **Kelleher AD**, **Rosenberg E**, **Markowitz M**, **Schafer K**, **Vaida F**, **Iwamoto A**, **Little S**, **Walker BD**. 2010. Impaired replication capacity of acute/early viruses in persons who become HIV controllers. J Virol **84**:7581–91.
128. **Brumme ZL**, **Li C**, **Miura T**, **Sela J**, **Rosato PC**, **Brumme CJ**, **Markle TJ**, **Martin E**, **Block BL**, **Trocha A**, **Kadie CM**, **Allen TM**, **Pereyra F**, **Heckerman D**, **Walker BD**, **Brockman MA**. 2011. Reduced Replication Capacity of NL4-3 Recombinant Viruses Encoding Reverse Transcriptase–Integrase Sequences From HIV-1 Elite Controllers. JAIDS J Acquir Immune Defic Syndr **56**:100–108.
129. **Mwimanzi P**, **Markle TJ**, **Martin E**, **Ogata Y**, **Kuang XT**, **Tokunaga M**, **Mahiti M**, **Pereyra F**, **Miura T**, **Walker BD**, **Brumme ZL**, **Brockman MA**, **Ueno T**. 2013. Attenuation of multiple Nef functions in HIV-1 elite controllers. Retrovirology **10**:1.
130. **Chopera DR**, **Woodman Z**, **Mlisana K**, **Mlotshwa M**, **Martin DP**, **Seoighe C**, **Treurnicht F**, **de Rosa DA**, **Hide W**, **Karim SA**, **Gray CM**, **Williamson C**. 2008. Transmission of HIV-1 CTL Escape Variants Provides HLA-Mismatched Recipients with a Survival Advantage. PLoS Pathog **4**:e1000033.
131. **Ntale R**, **Chopera D**, **Ngandu N**, **Abrahams M-R**, **Debra A**, **Mlotswa M**, **Werner L**, **Woodman Z**, **Mlisana K**, **Abdool Karim SS**, **Gray C**, **Williamson C**. 2012. Beneficial HLA-mediated viral polymorphisms on the transmitted virus additively influence disease

progression in HIV-1, subtype C infection. Retrovirology **9**:O60.

132. **Trkola A**, **Kuster H**, **Leemann C**, **Ruprecht C**, **Joos B**, **Telenti A**, **Hirschel B**, **Weber R**, **Bonhoeffer S**, **Gunthard HF**. 2003. Human Immunodeficiency Virus Type 1 Fitness Is a Determining Factor in Viral Rebound and Set Point in Chronic Infection. J Virol **77**:13146–13155.
133. **Claiborne DT**, **Prince JL**, **Scully E**, **Macharia G**, **Micci L**, **Lawson B**, **Kopycinski J**, **Deymier MJ**, **Vanderford TH**, **Nganou-Makamdop K**, **Ende Z**, **Brooks K**, **Tang J**, **Yu T**, **Lakhi S**, **Kilembe W**, **Silvestri G**, **Douek D**, **Goepfert PA.**, **Price MA.**, **Allen SA**, **Paiardini M**, **Altfeld M**, **Gilmour J**, **Hunter E**. 2015. Replicative fitness of transmitted HIV-1 drives acute immune activation, proviral load in memory CD4 + T cells, and disease progression. Proc Natl Acad Sci 201421607.
134. **Hollingsworth TD**, **Laeyendecker O**, **Shirreff G**, **Donnelly CA**, **Serwadda D**, **Wawer MJ**, **Kiwanuka N**, **Nalugoda F**, **Collinson-Streng A**, **Ssempijja V**, **Hanage WP**, **Quinn TC**, **Gray RH**, **Fraser C**. 2010. HIV-1 Transmitting Couples Have Similar Viral Load Set-Points in Rakai, Uganda. PLoS Pathog **6**:e1000876.
135. **Hecht FM**, **Hartogensis W**, **Bragg L**, **Bacchetti P**, **Atchison R**, **Grant R**, **Barbour J**, **Deeks SG**. 2010. HIV RNA level in early infection is predicted by viral load in the transmission source. AIDS **24**:941–945.
136. **Gottlieb GS**, **Nickle DC**, **Jensen MA**, **Wong KG**, **Grobler J**, **Li F**, **Liu S-L**, **Rademeyer C**, **Learn GH**, **abdool Karim SS**, **Williamson C**, **Corey L**, **Margolick JB**, **Mullins JI**. 2004. Dual HIV-1 infection associated with rapid disease progression. Lancet (London, England) **363**:619–22.
137. **Grobler J**, **Gray CM**, **Rademeyer C**, **Seoighe C**, **Ramjee G**, **Abdool Karim SS**, **Morris L**, **Williamson C**. 2004. Incidence of HIV-1 dual infection and its association with increased viral load set point in a cohort of HIV-1 subtype C-infected female sex workers. J Infect Dis **190**:1355–9.
138. **Valley-Omar Z**, **Sibeko S**, **Anderson JA**, **Goodier S**, **Werner L**, **Arney L**, **Naranbhai V**, **Treurnicht F**, **Abrahams M-R**, **Bandawe G**, **Swanstrom R**, **Abdool Karim QA**, **Abdool Karim SS**, **Williamson C**. 2012. CAPRISA 004 tenofovir microbicide trial: no impact of tenofovir gel on the HIV transmission bottleneck. J Infect Dis **206**:35–40.
139. **Laeyendecker O**, **Redd AD**, **Nason M**, **Longosz AF**, **Abdool Karim QA**, **Naranbhai V**, **Garrett N**, **Eshleman SH**, **Abdool Karim SS**, **Quinn TC**. 2015. Antibody Maturation in Women Who Acquire HIV Infection While Using Antiretroviral Preexposure Prophylaxis. J Infect Dis **212**:754–759.
140. Avidity-Wikipedia Definition.
141. **Curtis KA**, **Kennedy MS**, **Luckay A**, **Cong M-E**, **Youngpairoj AS**, **Zheng Q**, **Smith J**,

Hanson D, **Heneine W**, **Owen SM**, **García-Lerma JG**. 2011. Delayed Maturation of Antibody Avidity but Not Seroconversion in Rhesus Macaques Infected With Simian HIV During Oral Pre-Exposure Prophylaxis. JAIDS J Acquir Immune Defic Syndr **57**:355–362.

142. **Kersh EN**, **Luo W**, **Zheng Q**, **Adams DR**, **Hanson D**, **Youngpairoj AS**, **Cong M**, **Butler K**, **Hendry RM**, **McNicholl JM**, **Heneine W**, **Garcia-Lerma JG**. 2012. Reduced inflammation and CD4 loss in acute SHIV infection during oral pre-exposure prophylaxis. J Infect Dis **206**:770–9.
143. **Campbell TB**, **Schneider K**, **Wrin T**, **Petropoulos CJ**, **Connick E**. 2003. Relationship between In Vitro Human Immunodeficiency Virus Type 1 Replication Rate and Virus Load in Plasma. J Virol **77**:12105–12112.
144. **Prince JL**, **Claiborne DT**, **Carlson JM**, **Schaefer M**, **Yu T**, **Lahki S**, **Prentice HA**, **Yue L**, **Vishwanathan SA**, **Kilembe W**, **Goepfert P**, **Price MA**, **Gilmour J**, **Mulenga J**, **Farmer P**, **Derdeyn CA**, **Tang J**, **Heckerman D**, **Kaslow RA**, **Allen SA**, **Hunter E**. 2012. Role of transmitted Gag CTL polymorphisms in defining replicative capacity and early HIV-1 pathogenesis. PLoS Pathog **8**:e1003041.
145. **Troyer RM**, **Collins KR**, **Abraha A**, **Fraundorf E**, **Moore DM**, **Krizan RW**, **Toossi Z**, **Colebunders RL**, **Jensen MA**, **Mullins JI**, **Vanham G**, **Arts EJ**. 2005. Changes in human immunodeficiency virus type 1 fitness and genetic diversity during disease progression. J Virol **79**:9006–18.
146. **Chopera DR**, **Mann JK**, **Mwimanzi P**, **Omarjee S**, **Kuang XT**, **Ndabambi N**, **Goodier S**, **Martin E**, **Naranbhai V**, **Karim SA**, **Karim QA**, **Brumme ZL**, **Ndung'u T**, **Williamson C**, **Brockman MA**. 2013. No Evidence for Selection of HIV-1 with Enhanced Gag-Protease or Nef Function among Breakthrough Infections in the CAPRISA 004 Tenofovir Microbicide Trial. PLoS One **8**:e71758.
147. **Garcia J V**, **Miller AD**. 1991. Serine phosphorylation-independent downregulation of cell-surface CD4 by nef. Nature **350**:508–11.
148. **Piguet V**, **Wan L**, **Borel C**, **Mangasarian A**, **Demaurex N**, **Thomas G**, **Trono D**. 2000. HIV-1 Nef protein binds to the cellular protein PACS-1 to downregulate class I major histocompatibility complexes. Nat Cell Biol **2**:163–7.
149. **Gorry PR**, **McPhee DA**, **Verity E**, **Dyer WB**, **Wesselingh SL**, **Learmont J**, **Sullivan JS**, **Roche M**, **Zaunders JJ**, **Gabuzda D**, **Crowe SM**, **Mills J**, **Lewin SR**, **Brew BJ**, **Cunningham AL**, **Churchill MJ**. 2007. Pathogenicity and immunogenicity of attenuated, nef-deleted HIV-1 strains in vivo. Retrovirology **4**:66.
150. **Verity EE**, **Zotos D**, **Wilson K**, **Chatfield C**, **Lawson VA**, **Dwyer DE**, **Cunningham A**, **Learmont J**, **Dyer W**, **Sullivan J**, **Churchill M**, **Wesselingh SL**, **Gabuzda D**, **Gorry PR**, **McPhee DA**. 2007. Viral Phenotypes and Antibody Responses in Long-Term Survivors

Infected with Attenuated Human Immunodeficiency Virus Type 1 Containing Deletions in the nef and Long Terminal Repeat Regions. J Virol **81**:9268–9278.

151. **Salazar-Gonzalez JF**, **Bailes E**, **Pham KT**, **Salazar MG**, **Guffey MB**, **Keele BF**, **Derdeyn CA**, **Farmer P**, **Hunter E**, **Allen S**, **Manigart O**, **Mulenga J**, **Anderson JA**, **Swanstrom R**, **Haynes BF**, **Athreya GS**, **Korber BTM**, **Sharp PM**, **Shaw GM**, **Hahn BH**. 2008. Deciphering human immunodeficiency virus type 1 transmission and early envelope diversification by single-genome amplification and sequencing. J Virol **82**:3952–70.
152. **Bagasra O**, **Pomerantz RJ**. 1993. The role of CD8-positive lymphocytes in the control of HIV-1 infection of peripheral blood mononuclear cells. Immunol Lett **35**:83–92.
153. **DuBridge RB**, **Tang P**, **Hsia HC**, **Leong PM**, **Miller JH**, **Calos MP**. 1987. Analysis of mutation in human cells by using an Epstein-Barr virus shuttle system. Mol Cell Biol **7**:379–387.
154. **Pear WS**, **Nolan GP**, **Scott ML**, **Baltimore D**. 1993. Production of high-titer helper-free retroviruses by transient transfection. Proc Natl Acad Sci U S A **90**:8392–6.
155. **Platt EJ**, **Wehrly K**, **Kuhmann SE**, **Chesebro B**, **Kabat D**. 1998. Effects of CCR5 and CD4 cell surface concentrations on infections by macrophagetropic isolates of human immunodeficiency virus type 1. J Virol **72**:2855–64.
156. **Platt EJ**, **Bilska M**, **Kozak SL**, **Kabat D**, **Montefiori DC**. 2009. Evidence that ecotropic murine leukemia virus contamination in TZM-bl cells does not affect the outcome of neutralizing antibody assays with human immunodeficiency virus type 1. J Virol **83**:8289–92.
157. **Derdeyn CA**, **Decker JM**, **Sfakianos JN**, **Wu X**, **O'Brien WA**, **Ratner L**, **Kappes JC**, **Shaw GM**, **Hunter E**. 2000. Sensitivity of Human Immunodeficiency Virus Type 1 to the Fusion Inhibitor T-20 Is Modulated by Coreceptor Specificity Defined by the V3 Loop of gp120. J Virol **74**:8358–8367.
158. **Wei X**, **Decker JM**, **Liu H**, **Zhang Z**, **Arani RB**, **Kilby JM**, **Saag MS**, **Wu X**, **Shaw GM**, **Kappes JC**. 2002. Emergence of resistant human immunodeficiency virus type 1 in patients receiving fusion inhibitor (T-20) monotherapy. Antimicrob Agents Chemother **46**:1896–905.
159. **Takeuchi Y**, **McClure MO**, **Pizzato M**. 2008. Identification of gammaretroviruses constitutively released from cell lines used for human immunodeficiency virus research. J Virol **82**:12585–8.
160. **Spira AI**, **Ho DD**. 1995. Effect of different donor cells on human immunodeficiency virus type 1 replication and selection in vitro. J Virol **69**:422–429.
161. **Trkola A**, **Matthews J**, **Gordon C**, **Ketas T**, **Moore JP**. 1999. A cell line-based neutralization assay for primary human immunodeficiency virus type 1 isolates that use

either the CCR5 or the CXCR4 coreceptor. J Virol **73**:8966–74.

162. **Rohr O**, **Marban C**, **Aunis D**, **Schaeffer E**. 2003. Regulation of HIV-1 gene transcription: from lymphocytes to microglial cells. J Leukoc Biol **74**:736–49.
163. **Terry VH**, **Johnston ICD**, **Spina CA**. 2009. CD44 MicroBeads accelerate HIV-1 infection in T cells. Virology **388**:294–304.
164. **Vogt PK**. 1967. DEAE-dextran: Enhancement of cellular transformation induced by avian sarcoma viruses. Virology **33**:175–177.
165. **Reed LJ**, **Muench H**. 1938. A Simple Method of Estimating Fifty Percent Endpoints. Am J Epidemiol **27**:493–497.
166. Limit dilution endpoint PCR for single molecules of DNA (Single Genome Amplification, SGA).
167. **Larsson A**. 2014. AliView: a fast and lightweight alignment viewer and editor for large datasets. Bioinformatics **30**:3276–8.
168. **Ranwez V**, **Harispe S**, **Delsuc F**, **Douzery EJP**. 2011. MACSE: Multiple alignment of coding SEquences accounting for frameshifts and stop codons. PLoS One **6**.
169. **Tamura K**, **Stecher G**, **Peterson D**, **Filipski A**, **Kumar S**. 2013. MEGA6: Molecular Evolutionary Genetics Analysis version 6.0. Mol Biol Evol **30**:2725–9.
170. **Zhang M**. 2004. Tracking global patterns of N-linked glycosylation site variation in highly variable viral glycoproteins: HIV, SIV, and HCV envelopes and influenza hemagglutinin. Glycobiology **14**:1229–1246.
171. **Giorgi EE**, **Funkhouser B**, **Athreya GS**, **Perelson AS**, **Korber BTM**. 2010. Estimating time since infection in early homogeneous HIV-1 samples using a poisson model. BMC Bioinformatics **11**:28.
172. **Wei X**, **Decker JM**, **Wang S**, **Hui H**, **Kappes JC**, **Wu X**, **Salazar-Gonzalez JF**, **Salazar MG**, **Kilby JM**, **Saag MS**, **Komarova NL**, **Nowak M a**, **Hahn BH**, **Kwong PD**, **Shaw GM**. 2003. Antibody neutralization and escape by HIV-1. Nature **422**:307–12.
173. **Fouchier RA**, **Groenink M**, **Kootstra NA**, **Tersmette M**, **Huisman HG**, **Miedema F**, **Schuitemaker H**. 1992. Phenotype-associated sequence variation in the third variable domain of the human immunodeficiency virus type 1 gp120 molecule. J Virol **66**:3183–7.
174. **Hoffman, TL**, **Doms RW**. 1999. HIV-1 envelope determinants for cell tropism and chemokine receptor use. Mol Membr Biol **16**:57–65.
175. **Repits J**, **Sterjovski J**, **Badia-Martinez D**, **Mild M**, **Gray L**, **Churchill MJ**, **Purcell DFJ**, **Karlsson A**, **Albert J**, **Fenyö EM**, **Achour A**, **Gorry PR**, **Jansson M**. 2008. Primary HIV-1 R5 isolates from end-stage disease display enhanced viral fitness in parallel with increased gp120 net charge. Virology **379**:125–134.
176. **Clementi M**, **Lazzarin A**. 2010. Human immunodeficiency virus type 1 fitness and

tropism: concept, quantification, and clinical relevance. Clin Microbiol Infect **16**:1532–1538.

177. **Lehman DA**, **Baeten JM**, **McCoy CO**, **Weis JF**, **Peterson D**, **Mbara G**, **Donnell D**, **Thomas KK**, **Hendrix CW**, **Marzinke MA**, **Frenkel L**, **Ndase P**, **Mugo NR**, **Celum C**, **Overbaugh J**, **Matsen FA**, **Partners PrEP Study Team**. 2015. Risk of drug resistance among persons acquiring HIV within a randomized clinical trial of single- or dual-agent preexposure prophylaxis. J Infect Dis **211**:1211–8.
178. **Palmer S**, **Margot N**, **Gilbert H**, **Shaw N**, **Buckheit R**, **Miller M**. 2001. Tenofovir, adefovir, and zidovudine susceptibilities of primary human immunodeficiency virus type 1 isolates with non-B subtypes or nucleoside resistance. AIDS Res Hum Retroviruses **17**:1167–1173.
179. **Pritchard LK**, **Harvey DJ**, **Bonomelli C**, **Crispin M**, **Doores KJ**. 2015. Cell- and Protein-Directed Glycosylation of Native Cleaved HIV-1 Envelope. J Virol **89**:8932–8944.
180. **Provine NM**, **Puryear WB**, **Wu X**, **Overbaugh J**, **Haigwood NL**. 2009. The infectious molecular clone and pseudotyped virus models of human immunodeficiency virus type 1 exhibit significant differences in virion composition with only moderate differences in infectivity and inhibition sensitivity. J Virol **83**:9002–7.
181. **Read AF**, **Baigent SJ**, **Powers C**, **Kgosana LB**, **Blackwell L**, **Smith LP**, **Kennedy DA**, **Walkden-Brown SW**, **Nair VK**. 2015. Imperfect Vaccination Can Enhance the Transmission of Highly Virulent Pathogens. PLoS Biol **13**:e1002198.
182. **Meyerhans A**, **Cheynier R**, **Albert J**, **Seth M**, **Kwok S**, **Sninsky J**, **Morfeldt-Månson L**, **Asjö B**, **Wain-Hobson S**. 1989. Temporal fluctuations in HIV quasispecies in vivo are not reflected by sequential HIV isolations. Cell **58**:901–910.
183. **Kusumi K**, **Conway B**, **Cunningham S**, **Berson A**, **Evans C**, **Iversen AK**, **Colvin D**, **Gallo M V**, **Coutre S**, **Shpaer EG**. 1992. Human immunodeficiency virus type 1 envelope gene structure and diversity in vivo and after cocultivation in vitro. J Virol **66**:875–85.
184. **Aasa-Chapman MMI**, **Aubin K**, **Williams I**, **McKnight Á**. 2006. Primary CCR5 only using HIV-1 isolates does not accurately represent the in vivo replicating quasi-species. Virology **351**:489–496.
185. **Voronin Y**, **Chohan B**, **Emerman M**, **Overbaugh J**. 2007. Primary isolates of human immunodeficiency virus type 1 are usually dominated by the major variants found in blood. J Virol **81**:10232–41.
186. **Dalmau J**, **Codoñer FM**, **Erkizia I**, **Pino M**, **Pou C**, **Paredes R**, **Clotet B**, **Martinez-Picado J**, **Prado JG**. 2012. In–Depth Characterization of Viral Isolates from Plasma and Cells Compared with Plasma Circulating Quasispecies in Early HIV-1 Infection. PLoS One **7**:e32714.

187. **Rosen RK**, **Morrow KM**, **Carballo-Diéguez A**, **Mantell JE**, **Hoffman S**, **Gai F**, **Maslankowski L**, **El-Sadr WM**, **Mayer KH**. 2008. Acceptability of tenofovir gel as a vaginal microbicide among women in a phase I trial: a mixed-methods study. J Womens Health (Larchmt) **17**:383–92.

188. **Sokal DC**, **Abdool Karim QA**, **Sibeko S**, **Yende-Zuma N**, **Mansoor LE**, **Baxter C**, **Grobler A**, **Frolich J**, **Kharsany ABM**, **Miya N**, **Mlisana K**, **Maarshalk S**, **Abdool Karim SS**. 2013. Safety of tenofovir gel, a vaginal microbicide, in South African women: results of the CAPRISA 004 Trial. Antivir Ther **18**:301–310.

189. **Parikh UM**, **Mellors JW**. 2016. Should we fear resistance from tenofovir / emtricitabine preexposure prophylaxis ? Curr Opin HIV AIDS **11**:49–55.

190. **Hurt CB**, **Eron JJ**, **Cohen MS**. 2011. Pre-exposure prophylaxis and antiretroviral resistance: HIV prevention at a cost? Clin Infect Dis **53**:1265–1270.

191. **Parker ZF**, **Iyer SS**, **Wilen CB**, **Parrish NF**, **Chikere KC**, **Lee F-H**, **Didigu C a**, **Berro R**, **Klasse PJ**, **Lee B**, **Moore JP**, **Shaw GM**, **Hahn BH**, **Doms RW**. 2013. Transmitted/Founder and Chronic HIV-1 Envelope Proteins Are Distinguished by Differential Utilization of CCR5. J Virol **87**:2401–2411.

192. **Chenine A-L**, **Wieczorek L**, **Sanders-Buell E**, **Wesberry M**, **Towle T**, **Pillis DM**, **Molnar S**, **McLinden R**, **Edmonds T**, **Hirsch I**, **O'Connell R**, **McCutchan FE**, **Montefiori DC**, **Ochsenbauer C**, **Kappes JC**, **Kim JH**, **Polonis VR**, **Tovanabutra S**. 2013. Impact of HIV-1 backbone on neutralization sensitivity: neutralization profiles of heterologous envelope glycoproteins expressed in native subtype C and CRF01_AE backbone. PLoS One **8**:e76104.

193. **Checkley MA**, **Luttge BG**, **Freed EO**. 2011. HIV-1 Envelope Glycoprotein Biosynthesis, Trafficking, and Incorporation. J Mol Biol **410**:582–608.

194. **Freed E**, **Martin M**. 1996. Domains of the human immunodeficiency virus type 1 matrix and gp41 cytoplasmic tail required for envelope incorporation into virions. J Virol **70**:341–351.

195. **Murakami T**, **Freed EO**. 2000. Genetic Evidence for an Interaction between Human Immunodeficiency Virus Type 1 Matrix and alpha -Helix 2 of the gp41 Cytoplasmic Tail. J Virol **74**:3548–3554.

196. **Sambrook J**, **Russell DW**. 2001. Molecular Cloning: A Laboratory ManualThird Edit. Cold Spring Harbour Laboratory Press, Cold Spring Harbour, New York.

197. **Korber B**, **Gnanakaran S**. 2009. The implications of patterns in HIV diversity for neutralizing antibody induction and susceptibility. Curr Opin HIV AIDS **4**:408–417.

198. **Zhou T**, **Georgiev I**, **Wu X**, **Yang Z-Y**, **Dai K**, **Finzi A**, **Do Kwon Y**, **Scheid JF**, **Shi W**, **Xu L**, **Yang Y**, **Zhu J**, **Nussenzweig MC**, **Sodroski J**, **Shapiro L**, **Nabel GJ**, **Mascola JR**, **Kwong**

PD. 2010. Structural Basis for Broad and Potent Neutralization of HIV-1 by Antibody VRC01. Science **329**:811–817.

199. **Costin JM**, **Rausch JM**, **Garry RF**, **Wimley WC**. 2007. Viroporin potential of the lentivirus lytic peptide (LLP) domains of the HIV-1 gp41 protein. Virol J **4**:123.

200. **Ellerbrok H**, **D'Auriol L**, **Vaquero C**, **Sitbon M**. 1992. Functional tolerance of the human immunodeficiency virus type 1 envelope signal peptide to mutations in the amino-terminal and hydrophobic regions. J Virol **66**:5114–8.

201. **Vogel EP**, **Curtis-Fisk J**, **Young KM**, **Weliky DP**. 2011. Solid-State Nuclear Magnetic Resonance (NMR) Spectroscopy of Human Immunodeficiency Virus gp41 Protein That Includes the Fusion Peptide: NMR Detection of Recombinant Fgp41 in Inclusion Bodies in Whole Bacterial Cells and Structural Characterization of Pur. Biochemistry **50**:10013–10026.